UNIVERSIDADE FEDERAL DE SANTA CATARINA
CENTRO DE CIÊNCIAS DA SAÚDE
PROGRAMA DE PÓS-GRADUAÇÃO EM ODONTOLOGIA
ÁREA DE CONCENTRAÇÃO EM IMPLANTODONTIA

Miguel Alexandre Pereira Pinto Noronha de Oliveira

INTERACTION BETWEEN A FLOWABLE PLATELET-RICH FIBRIN AND PARTICULATE BIOMATERIALS OR ZIRCONIA SURFACES: MORPHOLOGICAL AND TRIBOLOGICAL ASSESSMENT

Florianópolis - SC
2021

Miguel Alexandre Pereira Pinto Noronha de Oliveira

INTERACTION BETWEEN A FLOWABLE PLATELET-RICH FIBRIN AND PARTICULATE BIOMATERIALS OR ZIRCONIA SURFACES: MORPHOLOGICAL AND TRIBOLOGICAL ASSESSMENT

Tese submetida ao Programa de Pós-Graduação em Odontologia da Universidade Federal de Santa Catarina para a obtenção do título de Doutor em Odontologia na área de Concentração de Implantodontia
Orientador: Prof. Dr. Bruno Alexandre Pacheco de Castro Henriques
Coorientador: Prof. Dr. Júlio César Matias de Souza

Florianópolis - SC
2021

Ficha de identificação da obra elaborada pelo autor,
através do Programa de Geração Automática da Biblioteca Universitária da UFSC.

Noronha de Oliveira, Miguel Alexandre Pereira Pinto
Interaction between a flowable Platelet-Rich Fibrin and particulate biomaterials or zirconia surfaces : morphological and tribological assessment / Miguel Alexandre Pereira Pinto Noronha de Oliveira ; orientador, Bruno Alexandre Pacheco de Castro Henriques, coorientador, Júlio César Matias de Souza, 2021.
112 p.

Tese (doutorado) - Universidade Federal de Santa Catarina, Centro de Ciências da Saúde, Programa de Pós Graduação em Odontologia, Florianópolis, 2021.

Inclui referências.

1. Odontologia. 2. Fibrina rica em plaquetas e leucócitos. 3. Cicatrização tecidual. 4. Implantes dentários. 5. Zircônia. I. Henriques, Bruno Alexandre Pacheco de Castro. II. de Souza, Júlio César Matias . III. Universidade Federal de Santa Catarina. Programa de Pós Graduação em Odontologia. IV. Título.

Miguel Alexandre Pereira Pinto Noronha de Oliveira

INTERACTION BETWEEN A FLOWABLE PLATELET-RICH FIBRIN AND PARTICULATE BIOMATERIALS OR ZIRCONIA SURFACES: MORPHOLOGICAL AND TRIBOLOGICAL ASSESSMENT

O presente trabalho em nível de doutorado foi avaliado e aprovado por banca examinadora composta pelos seguintes membros:

Prof. Dr. Bruno Alexandre Pacheco de Castro Henriques
Universidade Federal de Santa Catarina

Prof. Dr. Óscar Samuel Novais Carvalho
Universidade do Minho

Prof. Dr. Dachamir Hotza
Universidade Federal de Santa Catarina

Prof. Dr. César Augusto Magalhães Benfatti
Universidade Federal de Santa Catarina

Certificamos que esta é a versão original e final do trabalho de conclusão que foi julgado adequado para obtenção do título de Doutor em Odontologia, área de concentração de Implantodontia, pelo Programa de Pós-Graduação em Odontologia.

Documento assinado digitalmente
Mariane Cardoso
Data: 28/12/2021 15:28:01-0300
CPF: 888.647.159-91
Verifique as assinaturas em https://v.ufsc.br

_____
Profa. Dra. Mariane Cardoso Carvalho
Coordenação do Programa de Pós-Graduação

Documento assinado digitalmente
Bruno Alexandre Pacheco de Castro Henriques
Data: 28/12/2021 11:43:22-0300
CPF: 704.584.754-83
Verifique as assinaturas em https://v.ufsc.br

_____
Prof. Dr. Bruno Alexandre Pacheco de Castro Henriques
Orientador

Florianópolis, 2021

Dedico este trabalho à minha família, que me apoio incondicionalmente nesta trajetória de Doutorado. A meu pai Osorio, minha mãe Isabel, minha irmã Lelé, minha namorada Valentina, meus avós Helena e Hilário, e a meus tios e primos.

AGRADECIMENTOS

Ao meu pai, **Osório**, por me apoiar incondicionalmente e por sempre me proporcionar o necessário para alcançar o sucesso profissional.

À minha namorada **Valentina**, por todo o amor e apoio nos períodos de maior dificuldade. Obrigado por toda a tua ajuda e por sempre acreditares em mim.

À minha mãe, **Isabel**, sempre presente apesar da sua ausência, por me ter dado apoio sempre no que precisasse, por ter dado amor, a melhor educação, e mostrado que "Sonhar não custa". E por ter demonstrado qual o verdadeiro significado de força e coragem.

À minha irmã, **Lelé**, ausente mas sempre presente, pela Grande lutadora que foi, por ter sido o verdadeiro exemplo de como alcançar a excelência e me ter ajudado mesmo nos momentos mais difíceis.

Aos meus Avós, **Helena** e **Hilário**, obrigado por todos esses anos de carinho dedicados a mim.

Aos meus padrinhos e tios, **Toninho** e **Graça**, e ao meu primo, **António**, pela vossa indescritível ajuda, nos bons e maus momentos, e por hoje sermos uma verdadeira família.

Aos meus **tios** e **primos**, pelo apoio concedido nas piores alturas, e por mostrarem que sempre terei alguém com quem contar.

À **Sandra** e **Júlio**, que fazem agora parte da minha família, por todo o vosso apoio.

Ao **Agustin** e à **Taylor**, que também agora fazem parte da minha família, e que me mesmo à distância me ajudaram na realização deste trabalho.

Ao meu orientador, **Professor Doutor Bruno Henriques**, obrigado por me orientar em todos os momentos que precisei, pela paciência e tempo dispendidos no auxílio a esta pesquisa.

Ao meu co-orientador, **Professor Doutor Júlio Souza**, obrigado por toda a ajuda, pelas oportunidades dadas, por ser um grande exemplo de dedicação profissional e pelo sempre disponível e claro esclarecimento de dúvidas.

Ao **Professor Doutor Óscar Carvalho**, membro externo da banca. Obrigado por sempre se mostrar disponível a ajudar no que fosse preciso. Obrigado pela contribuição na realização desta pesquisa. É uma honra poder contar com a sua participação na minha defesa.

Ao **Professor Doutor César Benfatti**, membro da banca, obrigado pelos conhecimentos transmitidos e oportunidades disponibilizadas durante estes anos de Doutorado.

Ao **Professor Doutor Dachamir Hotza**, membro da banca, fico contente por ter aceite o

meu convite de participar como membro suplente da banca.

Ao **Professor Doutor José Manuel Ramos Gomes**. Fico contente por ter aceite o meu convite de participar como membro suplente da banca e agradecido por ter possibilitado a realização dos testes de Tribologia na Universidade do Minho.

Ao **Sérgio Carvalho**, obrigado pela ajuda e paciência na realização da Tribologia.

À **Elsa Ribeiro**, obrigado pela contribuição na realização da Microscopia.

Ao **Engenheiro João Caramês**, obrigado pelo fornecimento dos enxertos ósseos e pela contribuição na realização da Microscopia para este trabalho.

Obrigado à **Mafalda Costa e Narayan Sahoo**, alunos de Doutoramento da UMINHO, por toda a ajuda disponibilizada, que com certeza me ajudou muito.

Ao Departamento da Engenharia Mecânica da Universidade do Minho, obrigado por me ter permitido realizar a pesquisa.

Ao **Professor Doutor Ricardo Magini,** por todos os ensinamentos e por ter conseguido, de forma bem-sucedida, transmitir a importância do "ensino, pesquisa e extensão".

Ao **Professor Doutor António Carlos Cardoso**, obrigado por ter ajudado a melhorar o meu sentido crítico. Obrigado pelos ensinamentos transmitidos e por me ter dado a oportunidade de crescer no ensino.

Aos Professores **Marco Aurélio Bianchini** e **Claudia Volpato** obrigado pelos conhecimentos transmitidos e oportunidades disponibilizadas durante estes anos de Doutorado.

Ao **Doutor Levy Rau**, "meu pai odontológico", pela imensurável ajuda. Obrigado por todos os ensinamentos transmitidos, oportunidades proporcionadas, e por me ter mostrado que atingir a excelência não é fácil, mas possível.

Aos meus amigos e irmãos, **Daniel** e **Artur**, obrigado pela parceria, pela companhia e por terem tornado mais fácil a minha estadia aqui.

A todos os **amigos do Mestrado e Doutorado**, obrigado pela vossa amizade, compartilha de experiências e torço pelo vosso sucesso.

Obrigado à **Silvane e Melissa** por toda a ajuda disponibilizada no CEPID.

“The brighter the bonfire of enlightenment grows, the more surface area of ignorance becomes more illuminated.”

Terence McKenna

RESUMO

O objetivo deste estudo foi realizar uma caracterização morfológica e tribológica da fibrina rica em plaquetas (PRF) fluida após interação com biomateriais particulados e recobrimento de superfícies de zircônia tetragonal policristalina estabilizada por ítria (YTZP) para implantes. O PRF foi preparado a partir de sangue colhido e imediatamente centrifugado. A microscopia eletrônica de varredura (MEV) foi usada para caracterizar a densidade da rede de fibrina, o diâmetro da fibra de fibrina, as células sanguíneas e a distribuição de partículas de enxerto ósseo embutidas no bloco de PRF. Os testes tribológicos foram realizados em três superfícies de zircônia (YTZP): i) jateada e condicionada por ataque ácido (ZLA); ii) texturizada a laser de forma aleatória (RD); e iii) texturizada a laser com um padrão de 16 linhas e 8 passagens (L16N8). Os coeficientes de atrito (COF) das amostras cobertas ou não com PRF fluido foram avaliados por testes de deslizamento linear recíproco contra osso femoral bovino usando um tribômetro do tipo *pin-on-disc*. O volume de desgaste foi calculado a partir de imagens MEV usando um modelo matemático, bem como medindo a perda de peso das amostras. Imagens obtidas por microscopia SEM revelaram uma rede de fibrina tridimensional com a presença de linfócitos e plaquetas após aglomeração dos materiais de enxerto ósseo particulado e após recobrir superfícies de zircônia. Imagens revelaram o recobrimento das irregularidades da superfície de zircônia pela rede de fibrina tridimensional. Os valores médios de COF para os grupos de teste ZLA e L16N8 (com PRF) foram menores quando comparado aos grupos sem PRF (grupo controle). No grupo RD, foram obtidos valores de COF semelhantes para os grupos teste e controle. Os resultados não mostraram diferenças significativas ($p > 0,05$) nos valores de COF para as amostras ZLA, RD e L16N8, tanto com como sem PRF. Em defeitos ósseos maiores, o PRF deve ser misturado com um biomaterial particulado de enxerto de baixa taxa de reabsorção para manter a estabilidade biológica e mecânica no defeito ósseo. A distribuição de partículas de biomaterial e a viscosidade da mistura entre PRF e biomaterial depende do tamanho, concentração e formato das partículas. Sobre superfícies de zircônia, a rede fibrina foi responsável por uma menor fricção entre zircônia e osso bovino tendo, portanto, um papel lubrificante. Além disso, a textura da zircônia pode melhorar a retenção da rede de fibrina rica em leucócitos e plaquetas para acelerar o processo de osseointegração dos implantes de zircônia.

Palavras-chave: Cicatrização tecidual. Implantes dentários. Fibrina. Fibrina rica em plaquetas e leucócitos. Fibrinogénio. Reparo ósseo. Substitutos ósseos. Tribologia. Zircônia.

RESUMO EXPANDIDO

Introdução

Na implantodontia são usados diferentes tipos de enxertos ósseos para melhorar a consolidação óssea. A formação óssea é dependente da migração de células osteogênicas, angiogênese e taxa de reabsorção do biomaterial. Alguns dos substitutos ósseos usados revelam aspectos morfológicos, propriedades físicas e composição química que levam a uma baixa taxa de migração celular e formação de vasos sanguíneos (angiogênese). Na tentativa de superar tais desvantagens, novos métodos foram desenvolvidos, como o uso de concentrados de sangue conhecido como fibrina rica em plaquetas (PRF). Consiste em uma matriz rica em fibrina que contem diferentes tipos de células que melhoram a cicatrização dos tecidos. O PRF pode ser usado como coágulo ou membrana ou na sua forma fluida. Mais recentemente, o PRF fluido foi usado para o revestimento do implante para acelerar a osseointegração, fornecendo uma fonte de fatores de crescimento, fibrina, leucócitos, plaquetas. No entanto, a literatura sobre a cicatrização após a aplicação de PRF sobre implantes dentários de zircônia é escassa.

Objetivos

O objetivo de este estudo foi avaliar a distribuição e os aspectos morfológicos e tribologicos das partículas e componentes biológicos após a mistura de uma fibrina rica em plaquetas fluida após interação com biomateriais particulados e recobrimento de diferentes tipos de superfícies de zircônia tetragonal policristalina estabilizada por ítria para implantes.

Metodologia

Após aprovação do Comitê de Ética (cód. 2229.085) para estudo clínico e análise de sangue do voluntário o PRF foi preparado a partir de sangue colhido e imediatamente centrifugado a 2700 rpm (408 g), de acordo com o protocolo IntraSpin. A centrifugação foi de 3 minutos para obtenção do PRF fluido e de 12 minutos para obter as membranas de PRF. A microscopia eletrônica de varredura (MEV) foi usada para caracterizar a densidade da rede de fibrina, o diâmetro da fibra de fibrina, as células sanguíneas e a distribuição de partículas de enxerto ósseo embutidas no bloco de PRF. Os testes tribológicos foram realizados em três superfícies de zircônia (YTZP): i) jateada e condicionada por ataque ácido (ZLA); ii) texturizada a laser de forma aleatória (RD); e iii) texturizada a laser com um padrão de 16 linhas e 8 passagens (L16N8). O coeficiente de fricção (COF) dos espécimes foi avaliado em um tribômetro pino-sobre-placa deslizante recíproco com carga normal de 1 N, 1 Hz e comprimento de curso de 2 mm. Ensaios de desgaste deslizante foram realizados contra osso femoral bovino em solução de cloreto de sódio 0,9% à temperatura ambiente (20 ± 2ºC). As superfícies foram então avaliadas por microscopia eletrônica de varredura (MEV). O volume de desgaste foi calculado a partir de imagens MEV usando um modelo matemático, bem como pela medição da perda de peso das amostras.

Resultados e Discussão

Imagens obtidas por microscopia MEV revelaram uma rede de fibrina tridimensional com a presença de linfócitos e plaquetas após aglomeração dos materiais de enxerto ósseo particulado e após recobrir superfícies de zircônia. Imagens revelaram o recobrimento das irregularidades da superfície de zircônia pela rede de fibrina tridimensional. Os valores médios de COF para os grupos de teste (ZLA = 0,35; L16N8 = 0,45) foram menores quando comparados aos grupos controle (ZLA = 0,52; L16N8 = 0,60), com exceção do grupo RD (grupo teste - RD = 0,47; grupo controle - RD = 0,43). Valores médios de COF semelhantes foram registrados para os

grupos de teste e controle dentro do grupo RD. Os resultados não mostraram diferenças significativas ($p > 0,05$) nos valores médios de COF para amostras ZLA, RD e L16N8. A rede tridimensional de fibrina embutida com leucócitos, plaquetas e hemácias foi responsável por menores valores médios de COF nas superfícies jateadas e texturizadas a laser de zircônia, desempenhando assim um papel lubrificante. Além disso, os aspectos topográficos das superfícies de zircônia podem aumentar a adesão da rede de fibrina enriquecida com leucócitos e plaquetas para acelerar o processo de osseointegração de implantes de zircônia.

Considerações Finais

Em defeitos ósseos maiores, o PRF deve ser misturado com um biomaterial particulado de enxerto de baixa taxa de reabsorção para manter a estabilidade biológica e mecânica no defeito ósseo. A distribuição de partículas de biomaterial e a viscosidade da mistura entre PRF e biomaterial depende do tamanho, concentração e formato das partículas. Sobre superfícies de zircônia, a rede fibrina foi responsável por uma menor fricção entre zircônia e osso bovino tendo, portanto, um papel lubrificante. Além disso, a textura da zircônia pode melhorar a retenção da rede de fibrina rica em leucócitos e plaquetas para acelerar o processo de osseointegração dos implantes de zircônia.

Palavras-chave: Cicatrização tecidual. Implantes dentários. Fibrina. Fibrina rica em plaquetas e leucócitos. Fibrinogénio. Reparo ósseo. Substitutos ósseos. Tribologia. Zircônia.

ABSTRACT

The aim of this study was to perform a morphological and tribological characterization of a flowable platelet-rich fibrin (PRF) after interaction with bioactive particulate materials or coating yttria stabilized tetragonal zirconia polycrystals' surfaces for implants. PRF was prepared from collected blood and immediately centrifuged according to the IntraSpin protocol. Scanning electron microscopy (SEM) microscopy was used to characterize the fibrin network density, fibrin fiber diameter, blood cells, and bone graft particle distribution embedded in the PRF block. Tribological tests were performed on three different zirconia surfaces: i) gritblasted and acid-etched (ZLA); ii) laser-textured with a randomly topographic pattern (RD); or iii) with a 16-line and 8-passage pattern (L16N8). The coefficient of friction (COF) of samples covered or not with flowable PRF were assessed after reciprocating sliding wear testing against bovine femoral bone using a pin-on-plate tribometer. The wear volume was calculated from SEM images using a mathematical model as well as by weight loss measurement of the specimens. SEM images revealed a three-dimensional fibrin network that agglomerated particulate graft bioactive materials and lymphocytes, platelets, and red blood cells. On zirconia, the fibrin network covered the micro-scale peaks and valleys of the textured zirconia surfaces. COF mean values recorded for ZLA and L16N8 test groups (with PRF) were lower when compared to the surfaces free of PRF (control groups). Similar COF mean values were recorded for test and control groups within the RD group. Results did not show significant differences ($p > 0.05$) in COF mean values for ZLA, RD, and L16N8 specimens, with or without PRF. On larger bone defects, PRF should be mixed with a low resorption rate graft material to maintain biological and mechanical stability into the bone defect. The distribution of particulate graft biomaterial particles and flowing of the PRF block depends on the size, content, and shape of the graft particles. On zirconia, the fibrin network coating was responsible for a low friction between gritblasted or texturized zirconia surfaces against bovine bone, thus providing a lubricant role. Furthermore, the topographic aspects of the zirconia surfaces can increase the adhesion of the fibrin network enriched with leukocytes and platelets to speed up the osseointegration process of zirconia implants.

Keywords: Bone healing. Bone substitutes. Dental Implants. Fibrin. Fibrinogen. Platelet-Rich Fibrin. Tribology. Wound healing. Zirconia

LIST OF FIGURES

Synergistic benefits on combining injectable platelet-rich fibrin and bone graft porous materials: an integrative review

Figure 1. Flow diagram of the search strategy used in this study. Adapted from the Preferred Reporting Items for Systematic Reviews and Meta-Analyses...……..32

Figure 2. Clinical preparation of a PRF block. ……. 34

Figure 3. Schematic illustration of PRF block and its constituents.....…41

Figure 4. Schematic illustration of the PRF block being applied in a sinus augmentation procedure. ……42

Incorporation of injectable platelet-rich fibrin (i-PRF) for coating and embedment of bone graft materials and implant surfaces: a detailed morphological analysis

Figure 1. (A) Schematic illustration of PRF block and its constituents (chopped PRF membranes, flowable PRF and particulate bone substitute). Bone substitutes presenting different particle size and porosity can be chosen. (B) PRF block containing DBBM with a grain size between 0.125 and 0.800 mm (Biograft®, Ossmed®, Cantanhede, Portugal). (C) PRF block containing a synthetic microcrystalline non-ceramic hydroxyapatite with a grain size between 0.300 and 0.400 mm (Osteogen®, IntraLock™, Boca Raton, FL, USA). ……....50

Figure 2. (A) Flowable PRF and PRF block samples on titanium disks. (B) PRF block with DBBM after gold sputtering and ready to be analyzed on the SEM. …….……....55

Figure 3. Scanning electron microscope (SEM) image showing the morphological aspects of flowable PRF, PRF block with the synthetic hydroxyapatite, and PRF block composed with a DBBM. ……57

Figure 4. Scanning electron microscope (SEM) images of flowable PRF and DBBM particles……..……...58

Figure 5. SEM images of a porous zirconia block with fibrin. ……...59

Figure 6. SEM images of a laser textured zirconia surface covered with fibrin…….....60

Figure 7. Schematic illustration of the PRF block being applied in a sinus augmentation procedure. …….....66

Tribological behavior of flowable platelet-rich fibrin placed over zirconia implant surfaces for biomimetic functionalization: In Vitro Study

Figure 1. Schematics of dental implant placement with flowable PRF for biomimetic surface functionalization. ...…….....71

Figure 2. Representative morphologies of the tested surfaces.…….....74

Figure 3. A) Bruker-UMT-2 reciprocating pin-on-plate tribometer. (B) Schematic representation the reciprocating pin-on-plate tribometer……...…….75

Figure 4. (A) IntraSpin® centrifuge (Intralock™, Boca Ranton, FL, USA). (B) Plastic tubes containing the flowable PRF (yellow liquid phase). (C) L16N8 Zirconia disk. (D) Bone specimen. (E) Flowable PRF being injected over a zirconia disk with a plastic disposable transfer pipette. (F) Bone and zirconia disk with PRF ready for friction test.….....76

Figure 5. SEM images of the inside of the wear track…….....79

Figure 6. Fibrin distribution over the L16N8 laser zirconia surface during the friction test ..80

Figure 7. (A) Fibrin displacement over the RD zirconia surface during the friction test. (B) High magnification SEM micrograph of the correspondent counterpart bone specimen with fibrin retained on its surface after the sliding test. ….....81

Figure 8. SEM images of the outside of the wear track (2000x magnification)….....81

Figure 9. Evolution of the coefficient of friction (COF) with time for ZLA samples with and without PRF against bone in 0.9% sodium chloride solution (F_N = 1 N, stroke length 2 mm, 1 Hz, 300 s of sliding)..... 83

Figure 10. Evolution of the coefficient of friction (COF) with time for RD samples with and without PRF against bone in 0.9% sodium chloride solution (F_N = 1 N, stroke length 2 mm, 1 Hz, 300 s of sliding)..... 83

Figure 11. Evolution of the coefficient of friction (COF) with time for L16N8 samples with and without PRF against bone in 0.9% sodium chloride solution (F_N = 1 N, stroke length 2 mm, 1 Hz, 300 s of sliding)..... 84

Figure 12. Mean values of the coefficient of friction (COF) for each subgroup....…….86

LIST OF TABLES

Incorporation of injectable platelet rich fibrin (i-PRF) for coating and embedment of bone graft materials and implant surfaces: a detailed morphological analysis.

Table 1. Details on the particulate bone graft materials…….....50

Table 2. Properties of the zirconia and titanium specimens.…….……...…..52

LIST OF ABREVIATIONS AND ACRONYMS

ADTM – Autologous Demineralized Tooth Matrix

AFB – Autologous Fibrin Binder

A-PRF – Advanced Platelet-Rich Fibrin

AuPd – Gold Palladium Alloy

BSE – Backscattered Electrons

ß-TCP – Beta-Tricalcium Phosphate

CEPSHUFSC – Comitê de Ética em Pesquisa com Seres Humanos da Universidade Federal de Santa Catarina

COF – Coefficient of Friction

cp Ti – Commercially Pure Titanium

DBBM – Demineralized Bovine Bone Mineral

DBMA – Demineralized Bone Matrix Allograft

EDS – Energy-Dispersive Spectrometer

EMC – Department of Mechanical Engineering

FDBA – Freeze-dried Bone Allograft

FEG-SEM – Field Emission Gun Scanning Electron Microscopy

Hap – Hydroxyapatite

IPA – Isopropyl Alcohol

i-PRF – Injectable Platelet-Rich Fibrin

L-PRF – Leukocyte and Platelet-Rich Fibrin

L16N8 – Laser-textured with 16-line and 8-passage pattern

Nd:YAG – Neodymium-doped Yttrium Aluminium Garnet

nHap – Nanostructured Hydroxyapatite Microspheres

PBS – Phosphate Buffered Saline

PDGF – Platelet-Derived Growth Factor

PPP – Platelet-Poor Plasma

PRF – Platelet-Rich Fibrin

PRP – Platelet-Rich Plasma

SE – Secondary Electrons

RD – Laser-textured with a randomly topographic pattern

RPM – Rotations Per Minute

SEM – Scanning Electron Microscopy

TGF-B 1 – Transforming Growth Factor Beta 1

UFSC – Universidade Federal de Santa Catarina

VEGF – Vascular Endothelial Growth Factor

YTZP – Yttria stabilized tetragonal zirconia polycrystals

ZLA – Gritblasted and acid-etched zirconia surf

TABLE OF CONTENTS

SCOPE AND STRUCTURE OF THE THESIS 19

CHAPTER 1 - INTRODUCTION AND OBJECTIVES 21

CHAPTER II - SYNERGISTIC BENEFITS ON COMBINING INJECTABLE PLATELET-RICH FIBRIN AND BONE GRAFT POROUS MATERIALS: AN INTEGRATIVE REVIEW 25

ABSTRACT 25
INTRODUCTION 27
METHOD 29
RESULTS 31
DISCUSSION 32
CONCLUSIONS 45

CHAPTER III- INTERACTION BETWEEN AN INJECTABLE PLATELET-RICH FIBRIN (I-PRF) AND BONE GRAFT MATERIALS OR IMPLANT SURFACES: A DETAILED MORPHOLOGICAL ANALYSIS 47

ABSTRACT 47
INTRODUCTION 48
MATERIALS AND METHODS 49
RESULTS 55
DISCUSSION 60
CONCLUSIONS 66

CHAPTER IV - TRIBOLOGICAL BEHAVIOR OF FLOWABLE PLATELET-RICH FIBRIN PLACED OVER ZIRCONIA IMPLANT SURFACES FOR BIOMIMETIC FUNCTIONALIZATION: IN VITRO STUDY 68

ABSTRACT 68
INTRODUCTION 70
MATERIALS AND METHODS 71
RESULTS AND DISCUSSION 77
CONCLUSIONS 86

GENERAL CONCLUSIONS 88

BIBLIOGRAPHY 89

CHAPTER I 89
CHAPTER II 92
CHAPTER III 96
CHAPTER IV 100

APPENDIX A –UFSC ETHICS COMMITTEE 104

APPENDIX B –BLOOD TEST OF THE TRIBOLOGY STUDY VOLUNTEER 107

ANNEX A – SCIENTIFIC PRODUCTION DURING THE DOCTORAL PROGRAM 109

SCOPE AND STRUCTURE OF THE THESIS

The purpose of this thesis is to clarify the distribution and morphological aspects of particles and biological components after mixing a flowable platelet-rich fibrin (PRF) and particulate bioactive ceramics. Also, the flowable PRF can cover zirconia surfaces to enhance the bioactivity of implants and to speed up the osseointegration process. In this way, studies on sliding wear and friction become key methods to understand the stability of the PRF coatings on implant surfaces. Relevant recommendations can be drawn for clinical use of a flowable (injectable) PRF in the field of implant dentistry regarding morphological and tribological assessment.

This thesis is comprised into four chapters. The first chapter involves an introduction on the use of PRF in dentistry. The second chapter deals with an integrative review on the combination of flowable PRF and bone graft porous materials is presented. An integrative review is a specific review method that presents the state of the science, thus helping the reviewer to identify possible gaps in current research, and identifying the need for future research and bridging between related areas of work. A bibliographic search was performed on different science databases using the following search items: (“PRF” OR “L-PRF” OR “platelet-rich fibrin” OR “fibrin”) AND (“bone substitutes” OR “bone graft” OR “hydroxyapatite” OR “DBBM” OR “deproteinized bovine bone mineral”) AND (“wound healing” OR “bone healing” OR “bone repair” OR “bone regeneration” OR “bone augmentation” OR “bone defect”).

Chapter 3 includes a detailed morphological characterization of PRF combined with bioactive graft materials by scanning electron microscopy. Blood samples were harvested from one volunteer. Fibrin network density, fibrin fiber diameter, blood cells, and bone graft particle distribution embedded in the PRF block were assessed. The experiments were performed at

the Department of Mechanical Engineering (EMC) at the Federal University of Santa Catarina (UFSC), Brazil.

At last, Chapter 4 focuses on the tribological characterization of flowable PRF covering zirconia surfaces with different patterns to enhance the osseointegration. For tribological assays, reciprocating sliding wear was performed followed by volume loss evaluation and scanning electron microscopy. It should be highlighted this study provides novel approaches on the development of implants surfaces by laser-assisted methods as well as on the clinical application of a flowable PRF to speed the osseointegration process. The tribological assays were carried out at the department of mechanical engineering (DEM) at the University of Minho, Portugal.

The Ethics Committee approval (cod. 2229.085) for clinical study and the blood analysis of the volunteer participant can be seen in the annexes. Also, the scientific output is described in the annexes. One book chapter on PRF and one on image analysis were published. Two articles, an integrative review on PRF, and an *in vitro* study evaluating the tribological behavior of PEEK-matrix composites were also published. Also, an integrative review on flowable PRF and a tribological assay on PRF/Zirconia were submitted.

CHAPTER 1 - INTRODUCTION AND OBJECTIVES

Different types of bone substitutes are used to enhance bone healing in implant dentistry (URBAN et al., 2011; HANNINK et al., 2011; PRADEEP et al., 2017; DEGIDI et al., 2013; CÖMERT KILIÇ et al., 2017; LIU et al., 2019). The enhancement of bone reparation is dependent on the osteogenic cell migration, angiogenesis, and biomaterial resorption rate. Some of the bone substitutes used reveal morphological aspects, physical properties, and chemical composition that leads to a low rate of cell migration and blood vessel formation (angiogenesis). Therefore, novel bone graft materials have been developed in an attempt to overcome such disadvantages (KIRCHHOFF et al., 2006; BEST et al. 2008; NORONHA OLIVEIRA et al., 2017).

Regarding the earliest reports on the use of fibrin gel, blood concentrates gained notoriety with the discovery of Platelet-Rich Plasma (PRP) over a period of 30 years (MARX et al, 1998; XU et al. 2020). However, one of the drawbacks when using PRP was related to the use of bovine thrombin to minimize the rapid diffusion of growth factors into the surgical site (EPPLEY et al., 2006; CARTER et al., 2011). In 2001, a second-generation of platelet concentrate emerged known as the Platelet-Rich Fibrin (PRF). It consists of a fibrin-rich matrix embedding leukocytes, platelets, cytokines, growth factors, and stem cells (CHOUKROUN et al., 2001, DOHAN et al., 2006; YOON et al., 2014; SCHÄR et al., 2015; DOHAN EHRENFEST et al., 2018; VARELA et al. 2018). PRF has shown to enhance tissue healing in different fields of medicine and dentistry (PINTO et al., 2018; CASTRO et al., 2019; NACOPOULOS et al., 2019). PRF can be used as a clot or as a membrane, and reveals a dense and extremely viscous-elastic fibrin network with nano-scale fibers that act as scaffold for cell proliferation, migration, and differentiation (MOSESSON et al., 2006; GUTHOLD et al., 2007; DOHAN EHRENFEST et al., 2010).

Different protocols have been created to obtain the PRF (DOHAN EHRENFEST et al., 2018). A recent protocol allows to produce a flowable PRF known as i-PRF, by reducing centrifugation time and using plastic tubes (CHOUKROUN et al., 2014). In fact, i-PRF comprises fibrin monomers and fibrinogen which form the fibrin network in the coagulation cascade. Such flowable PRF is rich in platelets and leukocytes as reported in previous studies (MIRON et al., 2017; VARELA et al., 2018). The flowable PRF can be injected by using syringes or in combination with particulate bone substitutes (MIRON et al., 2017). The cross-linking process takes places due to the conversion of the fibrin monomers into the fibrin network. It also allows an agglomeration of particulate biomaterials regarding the cross-linking process into a viscous fibrin network, thus acting as an autologous fibrin binder (AFB) (CASTRO et al., 2019).

A bioactive composite block can be produced by combining chopped PRF membranes, i-PRF, and particulate graft materials (CORTELLINI et al., 2018). The PRF block can overcome the clinical limitations of particulate bone grafts regarding their clinical handling, bioactivity, and fitting in surgical sites. Graft instability of particulate biomaterials is one of the main reasons for failure during bone healing (MIR-MARI et al., 2016). The graft stability can be achieved due to the cross-linking polymerization of the PRF fibrin and then the PRF is gradually absorbed during the tissue healing process. The patient experiences less morbidity since no secondary harvesting surgical site is needed. Thus, a combined application of PRF with bone graft materials enhances the tissue healing in large bone defects (TANAKA et al., 2015; NIZAM et al., 2018; PICHOTANO et al., 2019). Nonetheless, studies regarding the morphologic characterization of flowable PRF and PRF block containing different particulate biomaterials are scarce.

More recently, flowable PRF has been used for implant coating to speed up the osseointegration by providing a source of growth factors, fibrin, leukocytes, platelets (LOLLOBRIGIDA et al., 2018; ANDRADE et al., 2021). A crucial event in the healing process at the bone-implant

interface is the formation of a stable fibrin network clot (DAVIES, 2003). That provisional fibrin network scaffold is essential for the migration and differentiation of osteogenic cells (VILLAR et al., 2011; WEISEL et al., 2013). The morphological aspects of the implant surface have an influence on the adhesion of the fibrin clot (TING et al., 2017; WANG et al., 2017). Thus, literature regarding the effects of the implant surface on the adhesion of fibrin or the use of PRF for implant coating is scarce and therefore further studies should focus on such challenge to improve clinical outcomes (STRAUSS et al., 2018).

Recently, the use of zirconia dental implants has been growing. However, literature on the healing after PRF application over zirconia dental implants is scarce. This could be especially important in patients where healing is affected. Thus, future *in vitro* studies should focus on the effect of PRF on osseointegration. Also, split-mouth clinical trials comparing implants with and without PRF are needed.

The purpose of this thesis was to evaluate the morphological aspects of the mixture between a flowable platelet-rich fibrin (PRF) and particulate bioactive ceramics or zirconia surfaces. Also, the tribological behavior of the PRF-based coating was assessed on different zirconia surfaces for implants.

- Preparing an integrative review regarding recent studies on the combined use of flowable platelet-rich fibrin (PRF) and bone graft porous materials.
- Performing a morphological inspection of two hydroxyapatite-based bone grafts mixed with a flowable PRF.
- Comparing the adhesion of fibrin over different types of zirconia for implant surfaces covered.
- Assessing the tribological behavior of PRF-coated zirconia against bovine bone when immersed in saline solution.

- The first hypothesis is that the flowable PRF would agglomerate the particulate biomaterials providing a PRF block with a homogenous distribution of particles, leukocytes, platelets, and fibrin network. The second hypothesis is based on the coating of laser-texturized zirconia surfaces to increase the i-PRF retention and therefore providing a source of fibrin network to enhance the osseointegration.

CHAPTER II - SYNERGISTIC BENEFITS ON COMBINING INJECTABLE PLATELET-RICH FIBRIN AND BONE GRAFT POROUS MATERIALS: AN INTEGRATIVE REVIEW

ABSTRACT

Objectives: The main aim of this study was to perform an integrative review on the enhanced bone healing by combining a flowable (injectable) platelet-rich fibrin (PRF) and bone graft porous materials. **Method:** A search was carried out on the PubMed MEDLINE, Embase, Cochrane, Scopus, and Web of science databases up to January 13, 2021. The following search terms were used: ("PRF" OR "L-PRF" OR "platelet-rich fibrin" OR "fibrin") AND ("bone substitute" OR "bone graft" OR "hydroxyapatite" OR "DBBM" OR "deproteinized bovine bone mineral") AND ("wound healing" OR "bone healing" OR "bone repair" OR "bone regeneration" OR "bone augmentation" OR "bone defect"). The chemical, biologic, and physical properties of flowable platelet-rich fibrin combined with bone graft biomaterials were discussed in this review. **Results:** The repair of different bone defects were reported such as alveolar cleft reconstruction, sinus floor elevation, socket preservation, jaw defects, and impacted teeth in one study. Regarding studies evaluating alveolar cleft defects, results showed potential benefits of PRF to enhance bone formation when mixed with autogenous bone graft. Two studies on socket preservation found enhanced bone growth on the addition of PRF to bone substitutes, although one study found similar results with or without bone substitutes. Also, the addition of PRF to demineralized bovine bone mineral improved the bone healing in the repair of jaw defects. No synergistic effect was reported in bone formation when PRF was associated to particulate bone graft in sinus floor elevation. **Conclusions:** The combination of PRF and bone graft materials revealed significant outcomes when compared to solely use of

bone graft materials in alveolar cleft and jaw defects. In socket preservation, bone healing was improved when PRF and bone graft materials were applied in comparison to the solely use of PRF. The addition of PRF to particulate bone substitutes did not enhance bone formation in sinus lift procedures. **Clinical relevance:** On the reconstruction of larger bone defects, PRF should be mixed with a low resorption rate graft material to maintain biological and mechanical stability into the bone defect. Flowable PRF provides better handling of bone substitutes in larger bone defects such as alveolar clefts and maxillary sinus. In fact, PRF and particulate graft materials appear to exhibit a synergistic effect during bone tissue healing.

Keywords: Bone healing; bone substitutes; fibrin; fibrinogen; platelet rich fibrin; wound healing.

INTRODUCTION

Remodeling of bone tissue following tooth extraction or extensive cranio-maxillofacial defects results in bone loss that can negatively affect the rehabilitation with endosseous implants [1–5]. Nowadays, several bone substitutes are used to enhance bone healing including autogenous, xenogenous, allogenous, and synthetic or aloplastic graft materials [6–11]. Although autogenous bone is often selected as the first choice, some disadvantages are reported such as deficient bone graft volume, morbidity, and surgical complications [12–15]. Xenografts (e.g. bovine bone graft) are then chosen when a high stability of bone tissue is desired although they provide low bone resorption rates [16–19]. Additionally, some of these bone substitutes reveal morphological aspects, physical properties, and chemical composition that lead to a low rate of cell migration and blood vessel formation (angiogenesis) [6–11].

Platelet-rich fibrin (PRF), an autologous leukocyte- and platelet-rich fibrin matrix has shown evidences to enhance human tissue healing in different applications [20–25]. Platelet-rich fibrin clot is formed by a natural cross-linking polymerization process during centrifugation of blood in the presence of a physiological amount of fibrinogen and thrombin [22,25,26]. In fact, PRF consists of an autologous fibrin matrix, embedding leukocytes, platelets, cytokines, growth factors, and stem cells [24,27–30]. PRF also offers a proper mechanical behavior and elasticity due to the formation of a three-dimensional fibrin network [22,31,32]. However, the high rate of resorption of solely PRF may not sustain long-term volume stability. Considering PRF is completely resorbed during tissue healing, a combined application with bone graft materials is recommended to repair large bone defects [16–18,25,33,34]. Clinical attention has been taken when choosing the bone graft substitute for mixing with PRF, since data on resorption rate of such mixture are lacking.

A combination of bone graft and implants is often used for large bone defects that involve high strength biocompatible and bio-absorbable particulate materials [35–39]. However, clinical

limitations are reported in handling particulate bone grafts and on placement in surgical sites [19,40–42]. The preparation of low-viscosity absorbable and bioactive biomaterials involving particulate bone graft is useful for clinical application. For instance, an injectable PRF (i-PRF) is slowly transformed in a viscous fibrin network depending on the centrifugation method and equipment [31,43,44]. Therefore, injectable PRF can be used to agglomerate particulate bone graft materials acting as an Autologous Fibrin Binder (AFB) [25,34,43,45]. Thus, the injectable PRF is a low-viscosity or flowable biologic material that can be clinically handled by using centrifugation and syringes [31,43]. The flowable PRF can be produced at an early time point at low centrifugation speed by modifying the spin centrifugation forces, and using non-glass centrifugation tubes [31,34,43]. The flowable i-PRF is also rich in platelets, fibrinogen, fibrin monomer, leukocytes, and growth factors as previously reported in literature [25,31]. The combination of chopped PRF membranes, injectable PRF, and particulate graft materials results in manufacturing a bioactive composite block properly designed for bone augmentation [25,31,34,43]. Increased mechanical properties can be achieved by involving particulate or blocks composed of bioactive ceramics [25,46]. Particulate graft materials can act as scaffolds and mineralization nuclei for cell migration and angiogenesis. Such bioactive composite block can be produced by using a simple technique and therefore the association between PRF with other biomaterials may reduce treatment costs as less bone graft is needed to fill the bone defect [34,43]. To the best of our knowledge, there is no report on the selection of nanostructured bone graft materials for mixture with flowable PRF. Also, previous systematic reviews and *in vivo* studies failed to report conclusive results.

The main aim of this study was to perform an integrative review on the combination of flowable (injectable) PRF and grafting porous materials to enhance the bone healing in implant dentistry. It was hypothesized that the selection of novel nanostructured porous bone substitutes can enhance the wound healing of bioactive composite blocks involving a flowable PRF. The

present integrative review was accomplished concerning the scientific knowledge gaps, variation in methods, and unclear concepts on combining injectable platelet-rich fibrin and bone graft materials.

METHOD

Information sources and search strategy

A bibliographic search was performed on PubMed MEDLINE, Embase, Cochrane, Scopus, and Web of science databases using the following search items: ("PRF" OR "L-PRF" OR "platelet-rich fibrin" OR "fibrin") AND ("bone substitutes" OR "bone graft" OR "hydroxyapatite" OR "DBBM" OR "deproteinized bovine bone mineral") AND ("wound healing" OR "bone healing" OR "bone repair" OR "bone regeneration" OR "bone augmentation" OR "bone defect"). Also, a hand-search was performed on the reference lists of all primary sources and eligible studies of this integrative review for additional relevant publications.

The inclusion criteria comprised articles published in the English language up to January 13, 2021, on the synergistic benefits of bone graft porous materials and an injectable platelet-rich fibrin to enhance the bone healing. The eligibility inclusion criteria used for article searches also involved, randomized controlled trials, animal assays, and prospective cohort studies. No follow-up limitation was applied. Only bone defects were included and did not encompass periodontal defects. Studies comparing the solely use of PRF or bone graft materials with the combination of PRF and bone substitutes were included. The exclusion criteria were the following: papers without abstract; articles assessing the solely effect of PRF or bone graft materials. Studies based on publication date were not restricted during the search process.

Study selection and data collection process

The articles retrieved by the search process were evaluated in three steps. At first, studies were scanned for relevance by title, and the abstracts of those that were not excluded at this stage were assessed. Two of the authors (JCMS, MNO) independently analyzed the titles and abstracts of potentially relevant articles. A third author (WT) intervened in cases of disagreement. The total of identified articles was compiled for each combination of key terms and therefore the duplicates were removed using Mendeley citation managers software program (Ed. Elsevier). A preliminary evaluation of the abstracts was carried out to establish whether the articles met the purpose of the study. The second step comprised the evaluation of the abstracts and non-excluded articles, according to the eligibility criteria on the abstract review. Selected articles were individually read and evaluated concerning the purpose of this study. At last, the eligible articles received a study nomenclature label, combining first author names and year of publication. The following factors were retrieved for this review: author names, journal, publication year, purpose, study design, type of bone defect, PRF and surgical protocols, chemical composition and porosity data on the ceramic graft materials, main outcomes. For each study, the centrifuge, the tubes, the g-force (or RPM when g-force not available), the time, and clot/volume of PRF were reported. PICO question was adjusted to the issue where "P" was related to the patients or specimens while "I" referred to the methods of analyses, "C" for comparison of results, and "O" for the main outcomes. Data of the reports were harvested directly into a specific data-collection form to avoid multiple data recording regarding multiple reports within the same study (e.g., reports with different set-ups). This evaluation was individually carried out by two researchers, followed by a joint discussion to select the relevant studies. The present method was performed in accordance with the search strategy applied in previous studies on integrative or systematic reviews [47–49].

RESULTS

A total of 1678 articles were identified on PubMed, as shown in Fig.1. After removing duplicates and reading the titles & abstracts, 787 articles were excluded because they did not meet the inclusion criteria. Then, 34 articles were selected for full reading although 23 articles were removed due to the lack of information considering the purpose of the present review. At last, 11 articles were selected for this review study. Regarding the type of bone defect, 3 studies (27.27%) focused on alveolar cleft reconstruction while 4 studies (36.36%) reported findings on sinus floor elevation. Three studies (27.27%) reported findings on socket preservation while only one reported the bone healing on jaw defects and impacted teeth.

Data on the type of bone defect, PRF preparation, surgical protocol, and main outcomes of relevant studies are described in Table 1. Scientific findings were related to the benefits of mixing PRF and bone substitutes, as follows:

- The selected studies have reported potential synergistic mechanism between PRF and bone graft materials on bone healing in socket preservation [50-52];
- The use of PRF is advantageous for alveolar cleft reconstruction since it increased the density and volume of bone formation and allows to easily handle bone substitutes [18,53,54]. However, the addition of PRF did not enhance bone density [18];
- On impacted teeth case, excision of jaw tumors, and a traumatic jaw defect, the addition of PRF to DBBM promoted significantly higher bone formation and density compared to the solely use of DBBM [55];
- No advantages in bone repair could be showed when mixing PRF to bone substitutes for sinus floor augmentation. PRF improved the amount of newly formed bone, but not significantly [56,57]. Equivalent new bone formation was found in the presence or absence of PRF in the other 2 studies [19,58];

- The addition of flowable PRF to bone graft materials showed to be valuable when used in larger defects such as alveolar cleft reconstruction and sinus floor augmentation [54,58]. Adequate handling of the bone substitutes was reported when it was associated with injectable PRF, optimizing the time of the surgical procedure and reducing the material waste.

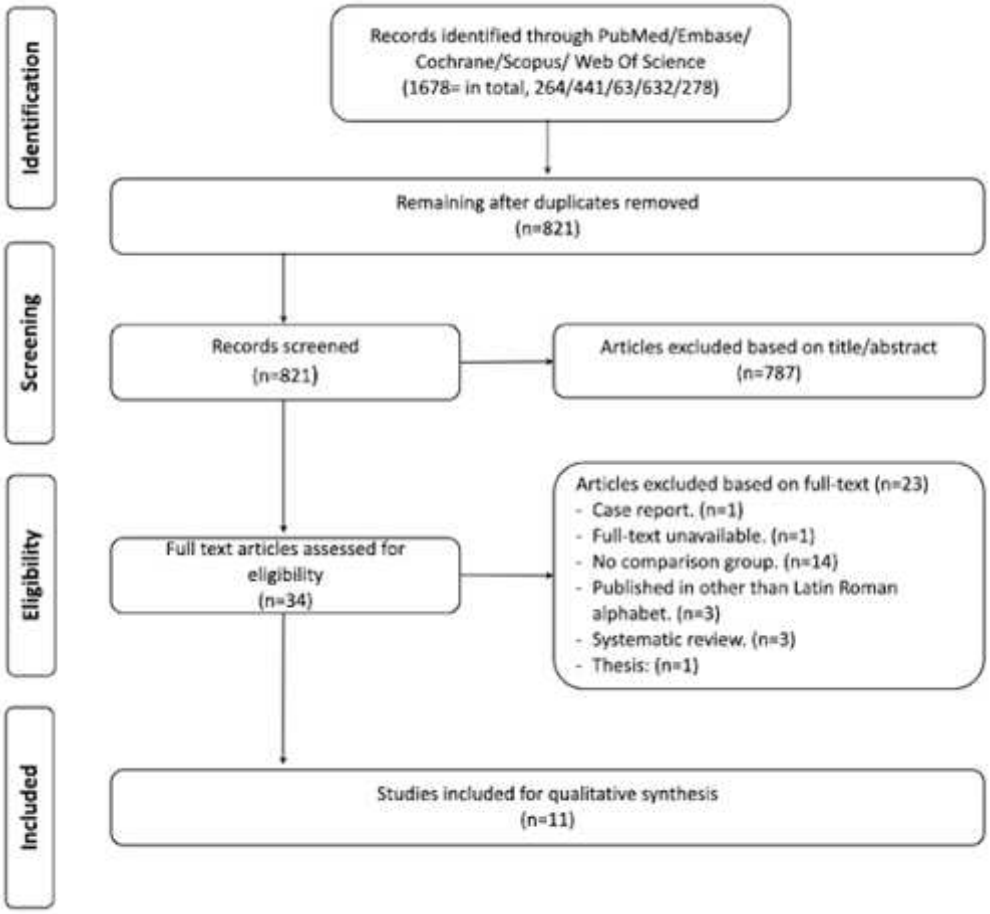

Figure 1. Flow diagram of the search strategy used in this study. Adapted from the Preferred Reporting Items for Systematic Reviews and Meta-Analyses.

DISCUSSION

Considering the available data, the combined use of PRF and bone substitutes play an important role the bone repair since the bone graft maintain the long-term bone volume and the PRF

enhances the biological events of tissue healing. Thus, the working hypothesis was confirmed in this review study. Furthermore, the synergistic effects of combining PRF and bone substitutes can also be clinically noticed considering handling and placement in the surgical site. The type of bone graft material should be discussed since the chemical composition and interconnected pores' network affect the migration and differentiation of osteogenic cells, angiogenesis, and new bone formation. Significant findings of the biomaterials, PRF methods, and bone defects are detailed discussed as follow.

Preparation of platelet-rich fibrin at different physical states

Different protocols have been proposed to obtain PRF like a membrane or block for different clinical cases. PRF, known as L-PRF, can be produced by harvesting approximately 9 mL blood from a patient to specific glass-coated plastic tubes free of anticoagulant. Due to recent shortage of plain glass blood-collection tubes, alternative silica-containing plastic tubes have been used [59]. When in contact with the glass surface or silica particles, coagulation factor XII existing in the plasma can be activated, consequently producing a fibrin-based clot through the activation of the intrinsic coagulation cascade [60]. This reaction may also occur between ceramic bone substitutes and the injectable PRF, thus their mixing is beneficial. Also, one hypothesis is that the use of porous bone substitutes would increase this reaction due to their higher surface area.

On the PRF preparation, the blood is immediately centrifuged using a high-quality table centrifuge at 2700 rpm (~400 g force) for 12 min, as seen in Figure 2. After the centrifugation process of the blood three layers can be noted: red blood corpuscles at the bottom of the tube,

platelet-poor plasma (PPP) on the top, and an intermediate layer called “buffy coat” (yellow layer) where most leucocytes and platelets are concentrated (Figure 2).

Figure 2. Clinical preparation of a PRF block. (A) Centrifugation process. (B) Harvesting L-PRF clot. (C) Mixture of chopped L-PRF membranes with bone substitute in Ti-based recipient. (D) Harvesting the injectable PRF. (E) Injectable PRF is sprayed over the mixture and encapsulation of bioactive graft particles, resulting in clotting after a few seconds, thus leading to a formation of a compact block. (F) PRF block ready to be used in the bone defect.

Fibrin-based clots should be removed from the tubes using tweezers and the red blood cells can be separated from the fibrin-based clot by using surgical instruments such as a periosteal elevator [61]. Red blood corpuscles and PPP are discarded and then a yellow L-PRF clot can be collected from the middle of each tube. The L-PRF clot can be used directly to fill a tissue defect or compressed to a membrane or a fibrin block using the adequate equipment to avoid any damage to the clot. According to the same original protocol, an injectable low-viscosity (flowable) PRF can be produced at 2700 rpm in plastic tubes by reducing the time of centrifugation down to 3 min.

L-PRF membranes can be fragmented into small pieces and added to particulate graft materials. Then, the flowable or moldable PRF is used to agglomerate the particulate graft material to

form a PRF block and therefore to act like a “biological matrix” that promotes the osteoprogenitor cell migration, growth factor delivery, and neoangiogenesis. Thus, the flowable PRF, namely i-PRF, is injected over the fragmented L-PRF and bone graft to allow the molding of the PRF block into the surgical site (Figure 2). The clotting of the PRF block starts slowly after mixing due to the polymerization of the i-PRF [34,46,48]. The inorganic particulate graft materials improve strength and space-maintaining of the biomaterial-PRF assembly into the bone defect.

Several protocols and centrifuges are available for manufacturing the platelet-rich fibrin at different viscosity or physical sates. A variation of factors related to the centrifuge has been reported in literature such as radius inclination and vibration amplitude of the tube holders [33]. Vibration of the tube holders result in an increase of temperature, which negatively affect the biological and morphological integrity of the platelet-rich fibrin. Different centrifugation forces can be adopted for producing the PRF [33]. Variations in protocols and experimental designs lead to differences in morphological, cell content, and physiological aspects of PRF. Therefore, results from a certain protocol may not be compared or extrapolated to other protocols 33]. In the included studies, different types of centrifuges and protocols were used (Table1).

Morphological and biological aspects of platelet-rich fibrin

Leucocyte- and platelet-rich fibrin (L-PRF) contains most of the platelets (95% initial blood) and approximately half of the leukocytes (majority of lymphocytes) present in the initial blood harvest [35,62]. The activated blood platelets release a high amount of transforming growth factor beta-1 (TGF-β 1), platelet-derived growth factor (PDGF), vascular endothelial growth factor (VEGF), and thrombospondin-1 growth factors that stimulate the migration and maturation of mesenchymal and epithelial cells [63]. Growth factors are responsible for

stimulating biological functions, such as chemotaxis, angiogenesis, as well as proliferation and differentiation of osteogenic cells [64,65]. PRF membranes reveals a high elasticity due to the three-dimensional cross-linked fibrin monomer units. The morphologic aspect and mechanical behavior of PRF depend on the proportion of harvested fibrinogen and thrombin. A wide cell population and content of mediators (particularly platelet growth factors) are embedded in the 3D fibrin matrix. Fibrin contains binding sites for integrins, growth factors, and other extracellular matrix components including fibronectin, that provides molecular signals to direct cell function [66]. The efficacy of PRF in tissue healing depends on the 3D morphological aspect and density of the fibrin network, cell content, and presence of growth factors [29].

Varela et al. performed a cellular, morphological, and protein characterization of an injectable platelet-rich fibrin (i-PRF, obtained at 700 rpm for 3 min) [34]. That study revealed a higher density of the 3-dimensional fibrin network for i-PRF than that for the peripheral blood clot. Also, a higher density of blood platelets was reported for i-PRF (˜4000 $x10^2$ μl^{-1}) than that for the blood clot (˜3500 $x10^2$ μl^{-1}) as well as on leukocytes (˜8000 μl^{-1} in i-PRF and 6000 μl^{-1} in peripheral blood). Miron et al., reported the capability of i-PRF to release higher content of various growth factors (e.g. PDGF, TGF-β) and type I collagen and therefore to stimulate higher fibroblast migration when compared to platelet-rich plasma (PRP) [46]. Some studies have found in traces of BMP-2 released from L-PRF [67,68]. BMP-2 is an important osteoinductive molecule belonging to the TGF-β superfamily of proteins and playing particularly an important function in bone development. Thus, the *in vitro* biological characterization of L-PRF and i-PRF leads to a better understanding of its clinical effects. That can support the development of further effective clinical guidelines for several applications. Nanostructured porous bone graft materials when in association with PRF could retain proteins and growth factors in its interior and gradually release them, improving bone healing.

Combination of PRF and commercially available bone graft materials

The beneficial effects of platelet-rich fibrin on tissue healing have already been reported in previous studies [24,31,62,66]. Animal studies frequently fail to confirm the L-PRF-mediated human bone healing. Considering the protocol for L-PRF preparation was mainly developed for human tissue healing, translation to other species should be further studied [67].

Studies using solely PRF for bone regeneration have achieved good results for smaller bone defects such as intra-bony defects and extraction sockets [9,60,68-70]. Some studies reported that the addition of PRF into bone defects resulted in an accelerated rate and degree of bone formation [20,58,71]. Alam et al. used PRF after third molar extraction, however the addition of DBBM showed to be beneficial in terms of soft and tissue healing and postoperative discomfort, demonstrating some synergism between PRF and DBBM [47]. The other two included studies on socket preservation found the use of autologous demineralized tooth matrix with PRF to increase bone formation capacity and preserving bone ridge width [48,49]. In other randomized clinical trial, the combination of PRF and DFDBA revealed significant results in preserving bone ridge width for 180 days when compared to DFDBA [72]. Other study found no significant differences in ridge width reduction when A-PRF was used alone or with freeze-dried bone allograft (FDBA). However, significantly more vital bone was present in the A-PRF group (46% ± 18%) compared to the FDBA group (29% ± 14%) [73]. New randomized controlled clinical trials using a combination of PRF and other bone graft materials would be interesting to compare the efficacy of those materials when mixed with PRF in well-contained sockets.

Regarding alveolar cleft reconstruction, Shawky et al. observed that PRF in combination with iliac crest graft allowed statistically significant increase in bone formation (mean 82.6% ± 3.9%) in comparison to the solely use of autogenous bone (mean 68.38% ± 6.67%) ($p \leq .05$) [15]. However, the mean bone density (quality) of the newly formed bone was lower in the PRF

group, but the difference was not statistically significant ($p > .05$) [15]. Also, Desai et al. found increased new bone regeneration and better wound healing when autogenous bone was mixed to PRF [50]. These authors also found that patients with wider clefts treated with PRF had lesser resorption when compared with the patients with wider cleft where PRF was not used [50]. Dayashankara et al. also found higher percentage of bone volume and lesser chances of bone resorption when mixing i-PRF and A-PRF with iliac bone graft. However, from the included studies on alveolar cleft reconstruction, this study was the only one using i-PRF [51]. In other study, the combination of chin symphysis bone, allograft, and PRF proved to be a proper combination for bone regeneration in alveolar cleft defects with a small to moderate volume range [74]. The use of PRF allows to obtain a more stable graft, without particle spreading, easy to handle, allowing the total closure of the oronasal fistulae [75].

Concerning maxillary sinus floor elevation (SFE), Zhang et al. found no qualitative difference in histological analyses among the DBBM and PRF+DBBM groups after 6 months ($p = 0.138$) [53]. Also, Nizam et al. observed no improvements in bone gain after 6 months when adding PRF to DBBM [16]. This comes in accordance with the study of Cömert Kılıç et al that did not stated conclusive outcomes on adding PRF to beta-tricalcium phosphate (ß-TCP) over a tissue healing period of 6 months [11]. Mourão et al. used nanostructured carbonated hydroxyapatite (cHap) microspheres and observed equivalent new bone formation with or without PRF in bilateral SFE after 6 months [55]. In a recent study, Adali et al. found higher percentages of bone formation when CGF was mixed with allograft, however, not statistically significant ($p = 0.285$) [54]. Literature is not consensual, as some studies report advantages in adding PRF to bone substitutes for SFE. Tatullo et al. found histologically faster bone formation by adding PRF to inorganic particulate graft materials and therefore acceptable primary stability of endosseous implants was achieved for 106 days [76]. Also, Pichotano et al. found the addition of L-PRF to DBBM into the maxillary sinus allowed early implant placement (4 months) with

increased new bone formation than DBBM alone after 8 months of healing [17]. Higher percentages of newly bone by the DBBM/PRF mixture than those by DBBM could also be found in other study [18]. However, other study found that both combinations can be successfully used for sinus augmentation [77]. A meta-analysis of randomized controlled trials concluded that there were no statistical differences in survival rate, new bone formation, contact between newly formed bone and bone substitute, percentage of residual bone graft (BSV/TV), and soft-tissue area between the non-PRF and PRF groups [9]. The authors concluded that current evidence supporting the necessity of adding PRF to bone graft in sinus augmentation is still limited [9]. Nevertheless, the addition of PRF to the mixture by itself constitutes an advantage, as less bone substitute is necessary, leading to a reduction of costs for the patient. PRF can be used as a sole filling material in sinus floor elevation only on immediate implant placement once implant raise the sinus membrane [71,78-80].

Concerning PRF is eventually completely resorbed, the mixing of PRF with a bone substitute is crucial to reconstruct critical-size bone defects. No RCTs evaluating horizontal or vertical bone reconstructions could be found and included in this article. In a proof-of-concept study, Cortellini et al. used a combination of flowable PRF and DBBM (L-PRF Block) to horizontally augment deficient alveolar ridges [34]. Superimposition of pre-operative and post-healing CBCT scans showed an average linear horizontal bone gain of 4.6 ±2.3 mm, 5.3 ±1.2 mm, and 4.4 ±2.3 mm, measured at 2, 6, and 10 mm away from the alveolar crest, respectively. Also, the volumetric bone gain was at 1.05 ±0.7 cm^3 for 5-8 months. The resorption rate of the graft material was at 15.6 ±6.7 vol.%, which allowed implant placement in all cases. According to these authors, the combination of flowable PRF and a bone substitute is a suitable technique to enhance bone healing in deficient alveolar ridges. Nevertheless, randomized controlled clinical trials and histological analysis are necessary to validate those results. Histologic assessment

could bring additional information regarding the resorption of the flowable PRF and the bone healing process.

The impact of type and size of bone substitutes to mix with PRF

The reconstruction of large bone defects can be performed using guided bone healing. Guided bone healing relies on a space-maintaining scaffold and a matrix, which allows cell recruitment, neovascularization, and delivery of morphogenetic, regulatory, and growth factors [81]. The advantages of adding PRF membranes, clots or flowable PRF to bone substitutes include less morbidity to the patient since no secondary harvesting surgical site is needed, reduction of expenses with expensive commercial graft materials, and faster tissue healing. Also, the graft instability of particulate biomaterials can be avoided due to the cross-linking polymerization of the PRF (Figure 3) that decreases the failure risks during bone healing [34,82]. The type of bone graft material used in combination with the flowable PRF plays a key role on the clinical outcomes. Inorganic bone substitutes act as a space maintainer and mineralization nuclei and the PRF will enhance cell migration, differentiation, and neoangiogenesis. Thus, attention should be taken when choosing the bone graft substitute to be agglomerated into the PRF matrix. The RCTs included in this article compared the solely use of PRF or bone graft materials with the combination of PRF and bone substitutes. The list of bone substitutes used in the selected studies included autologous demineralized tooth matrix (ADTM) demineralized bovine bone mineral (DBBM), demineralized bone matrix allograft (DBMA), hydroxyapatite (Hap) and nanostructured hydroxyapatite microspheres (nHap), as seen in Table 1.

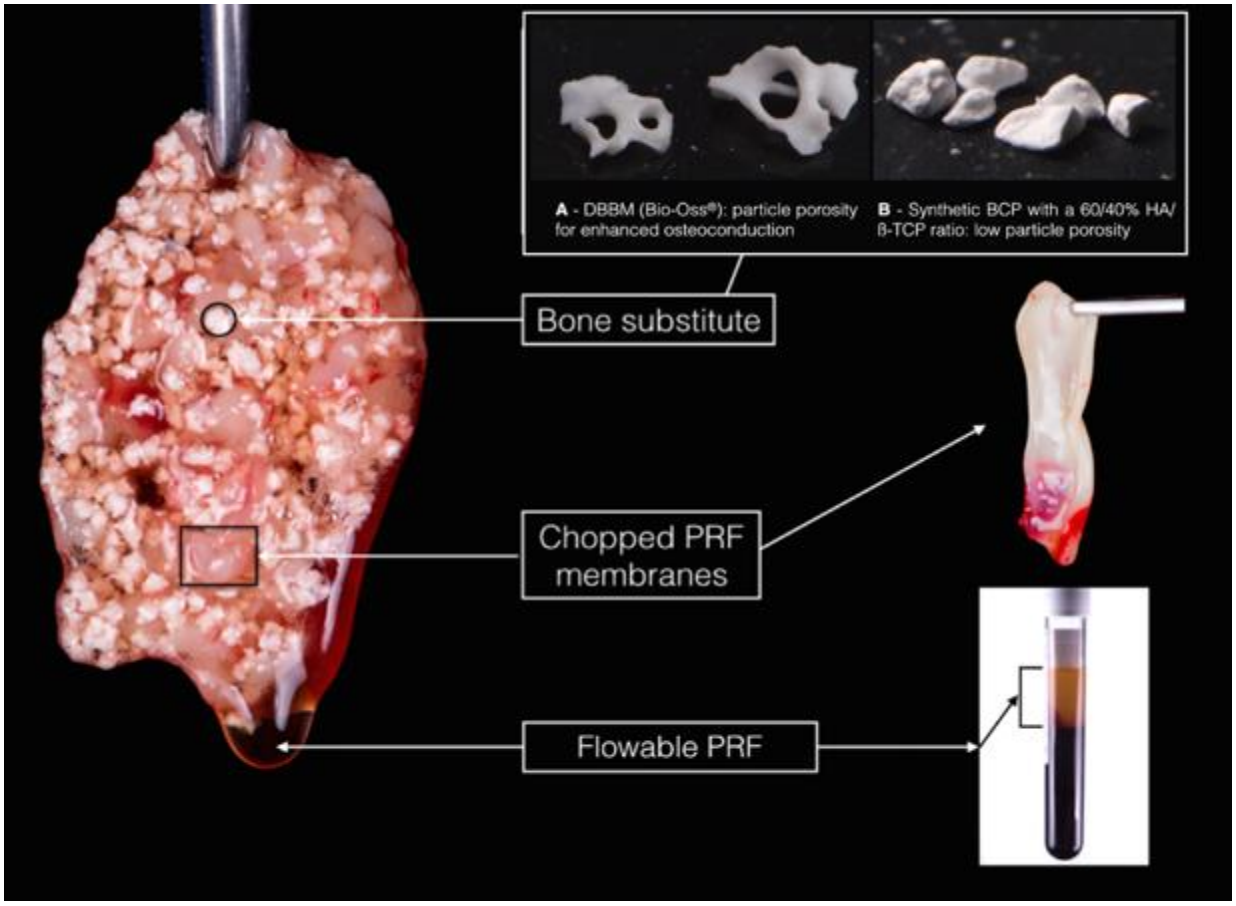

Figure 3. Schematic illustration of PRF block and its constituents: chopped PRF membranes, injectable PRF, and particulate bone substitute. Bone substitutes revealing different particle size and porosity can be chosen.

The particle size and porosity of bone graft materials also influence the bone formation, as seen in Figures 3 and 4 [25,46]. Human bone has a porous structure ranging from 20 to 400 μm that is necessary for penetration, adhesion, growth, and proliferation of osteogenic cells [83-85]. Particle size distribution of ordinary bone graft materials is reported in literature ranging from 250 μm to 2 mm (Table 2) [1,19,86]. Smaller granules present higher material volumes and surface areas than the larger granules [85]. Granules with a 100–300 μm size have shown higher osteoconductive potential when compared with 1–2 mm particles (Table 2) [87].

Despite being considered the first choice, autogenous bone presents some disadvantages such as donor-site morbidity and limited sources. Also, the high rate of resorption of autogenous bone graft may not sustain long-term volume stability [88]. Biomaterials with a low resorption rate such as xenogenous or ceramics can provide a higher volume stability when compared with autogenous bone grafts. A clinical study on 20 patients evaluated 11 years after sinus floor augmentation and found unchanged DBBM particles that were integrated with the regenerated bone [89].

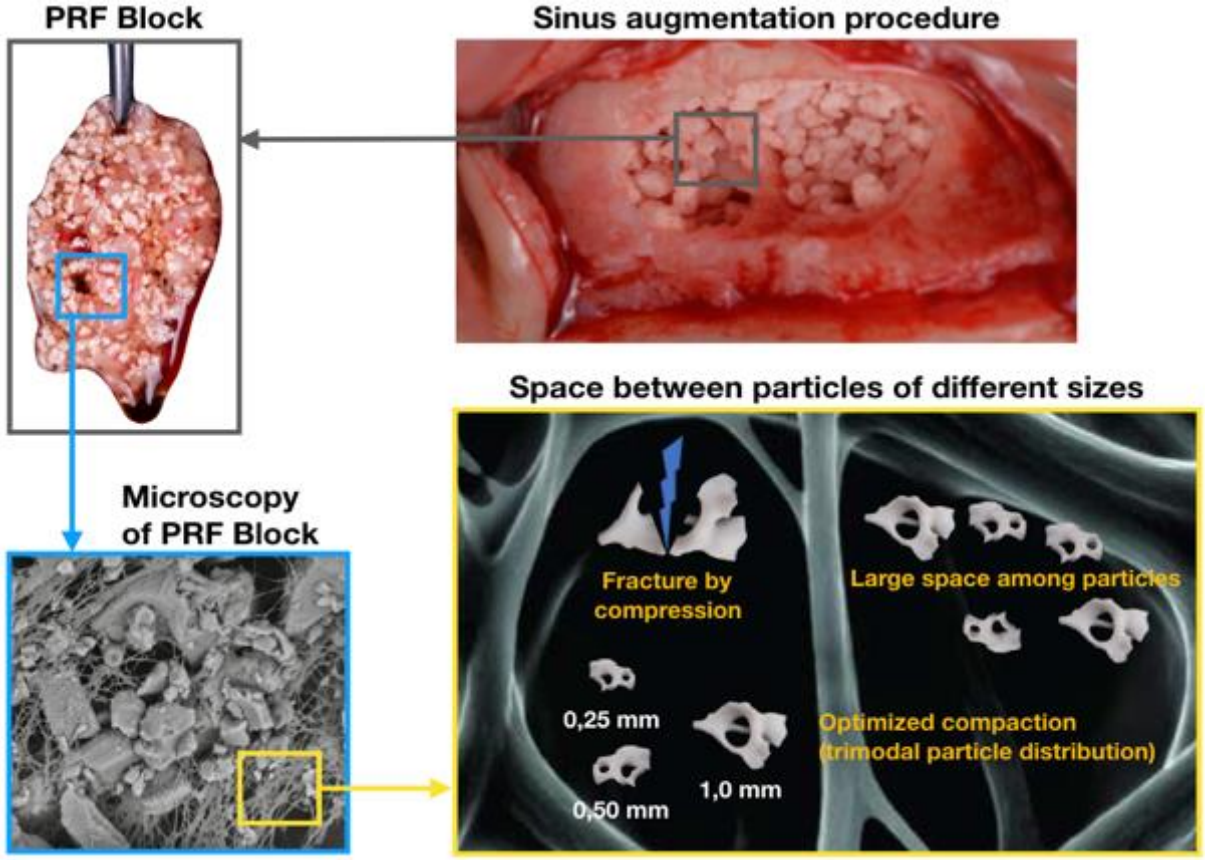

Figure 4. Schematic illustration of the PRF block being applied in a sinus augmentation procedure. Bone substitutes revealing different particle size and porosity can be chosen. Some particle fracture can occur during the handling of bone substitutes. Large spaces between particles of different sizes can be occupied by fibrin fibers and blood cells rich in growth factors.

DBBM is essentially considered a ceramic hydroxyapatite after the removal of its organic components. The size of its particles normally varies between 250 µm and 2 mm [86]. Fujoka-

Kobayashi et al. investigated the influence of bone substitute size on macrophage and osteoblast behaviors in vitro [90]. The authors found that cells cultured on DBBM small size granules exhibited lower cell viability, higher osteopromotive ability, and no noticeable macrophage polarization changes. Thus, the use of DBBM with a smaller granule size might be advantageous due to higher bone healing potential [90]. However, Chackartchi et al. observed no differences in clinical outcome between two DBBM sizes (small and large) for sinus floor augmentation procedures at 6 to 9 months [91]. Nonetheless, Testori et al., found better results in favour of DBBM large size granules (26.77% ± 9.63%) comparing with DBBM small size ones (18.77% ± 4.74%) [92]. DBBM reveals a proper resorption rate and its combination with particulate autogenous bone showed good results in large bone defects [6].

Allografts, derived from a cadaveric donor, can be used in a mineralized or demineralized form [54]. They can be supplied from tissue banks in which they are stored in sterile conditions, in ample quantities and at an affordable price [93]. Allografts are better adapted to human bone tissue than xenografts or synthetic materials and contain bone morphogenic proteins and growth factors, which stimulate osteoinduction. However, allograft graft materials have shown a more rapid resorption and replacement by new bone when compared with xenogenous graft materials [94]. Thus, they are often mixed with other allograft bones, synthetic graft materials, or platelet concentrate products [95].

Autogenous tooth bone graft has been developed and used clinically for bone substitution [49,96]. ADTM is biocompatible, bioresorbable, and facilitates new bone formation as shown radiologically and histologically [97]. ADTM has shown its potential as a bone substitute that can help fasten bone remodeling. As the tooth is autogenous, immunogenicity is reduced, medical waste is recycled, and expense is reduced for the patient [48]. However, there are a limited number of studies evaluating the effect of ADTM graft on bone formation in the literature.

Granule porosity may play a decisive role in the bone healing process [85]. Pores with a diameter of less than 1 μm play a role in bioactivity and protein interaction. Pores with diameters between 1 and 20 μm will determine cell behavior and the type of cells that will adhere. The pores between 100 and 1000 μm are responsible for cell growth, blood circulation and mechanical resistance. However, pores larger than 1000 μm will determine the shape of the material and its functionality [98]. Thus, the materials used must have a diameter between 2 nm and 1000 μm and a coexisting macro-, micro- and nano-porosity [98]. A study carried out in dogs by Carvalho et al. showed that DBBM particles with an increased porosity, up to 10 μm, appeared to benefit the osteoconduction process [86]. Ghanaati et al. showed that size, shape, and porosity of β-TCP granules had an influence on material integration, multinucleated giant cell formation, and angiogenesis in a rat subcutaneous implant model [83]. Hap nano-scale porosity leads to a very large surface area, thus improving cell migration and absorption of growth factors [50]. The porosity of Hap granules has been recorded at 60 and 80% [100], with pore sizes ranging between 10 and 20 nm [101]. Nanostructured Hap reveals a high osteoconductivity and bioresorbablity, due to the higher contact area when compared to the ordinary Hap particles [99]. The new ceramic materials have been extensively studied in terms of their particle size, chemical composition, porosity, pore size and resorption rate [1,55,86,90,102,103].

There must be a minimum space of 100 μm between particles, essential to allow neovascularization and bone formation [104,105]. Larger particles (1-2 mm) are commonly used for sinus floor elevation due to the defect size [11,16]. The combination of PRF and large bone graft particles or scaffolds become a good alternative for enhanced tissue healing at large bone defect sites (Figure 4). However, reports showing the effects of bone substitute granule size on biocompatibility and osteopromotive potential are scarce.

The benefits of platelet-rich fibrin in wound healing are widely described in literature [43,59]. In this review, the selected studies have reported potential benefits and a synergistic mechanism between PRF and bone graft materials in socket preservation [47-48,52] and alveolar cleft reconstruction [15,50,51]. The majority of studies on sinus floor augmentation reported no improvements in bone repair when adding PRF to bone substitutes [16,53,55], with only one study reporting better results when mixing PRF to bone substitutes [54]. Thus, the addition of PRF seems to be more beneficial for bone repair in smaller size bone defects. However, the use of PRF clots, membranes and flowable PRF by itself will help to better handle bone substitutes in larger bone defects such as alveolar clefts and maxillary sinus. Articles that used flowable PRF showed that its use seems to be valuable [51,55]. Nevertheless, literature on this topic is still scarce and further animal and human studies on combining flowable PRF and different biomaterials are required for several clinical situations. This study presents some limitations: some of the studies included have a small sample, various protocols for PRF production were used, and no long-term follow-up was adopted.

CONCLUSIONS

Within the limitations of the selected studies, the following concluding remarks can be drawn as follow:

- The selected studies have reported potential synergistic effects when mixing PRF and bone graft materials in socket preservation;
- On alveolar cleft reconstruction, previous findings are consensual considering benefits of adding PRF to bone substitute since that enhances the density and volume of new bone. Also, the handling of the PRF-based mixture become effective for placement in the surgical site taking into consideration large bone defects;

- Regarding sinus floor augmentation, previous findings did not reveal significant gains on mixing PRF to bone substitutes in comparison to the solely use of PRF or bone substitutes. However, the clinical handling of bone substitutes when mixed with PRF and the decrease of the bone graft amount required for the surgical site comprises a noteworthy clinical reward.

CHAPTER III- INTERACTION BETWEEN AN INJECTABLE PLATELET-RICH FIBRIN (I-PRF) AND BONE GRAFT MATERIALS OR IMPLANT SURFACES: A DETAILED MORPHOLOGICAL ANALYSIS

ABSTRACT

Objectives: The aim of the present study was to perform a morphological inspection of two hydroxyapatite-based bone grafts mixed with platelet-rich fibrin (PRF). **Materials and Methods:** Blood samples were harvested from one volunteer to prepare the flowable PRF and the PRF samples containing bone grafts. Scanning electron microscopy (SEM) was used to characterize the fibrin network density, fibrin fiber diameter, blood cells, and bone graft particle distribution embedded in the PRF block. **Results:** SEM images revealed a noticeable fibrin networking in both flowable PRF and PRF block samples. Flowable PRF was converted into a viscous three-dimensional fibrin network that agglomerated particulate bone graft materials. The cross-linking between the fibrin fibers stabilized the architecture of the hybrid PRF-bone graft structure. **Conclusions:** The flowing and viscosity of an injectable platelet-rich fibrin allowed the agglomeration of synthetic or xenogeneic particulate ceramic graft materials. The fibrin bundles also comprised clusters of platelets and some leukocytes which seemed to hold the graft materials assembled. **Clinical relevance:** Platelet-rich fibrin mixed with bone graft materials can enhance clinical attachment level gain and decrease the pocket depth in intra-bony defects. On the reconstruction of larger bone defects, platelet rich fibrin should be mixed with a low resorption rate graft material to maintain biological and mechanical stability into the bone defect.

Keywords: Bone healing, bone substitutes, morphology, platelet-rich fibrin.

INTRODUCTION

Different types of bone substitutes can be used to enhance bone healing such as autogenous, xenogeneic, allogeneic, and synthetic, or alloplastic graft materials [1]. Some of those bone substitutes reveal morphological aspects, physical properties, and chemical composition that lead to a low rate of cell migration and blood vessel formation (angiogenesis) [1-3]. Many efforts have been carried out to develop novel bone graft materials that can enhance the wound healing [4-6]. Advanced ceramic materials have been studied considering particle size, chemical composition, porosity, pore size, and absorption rate into the bone [7-10]. Thus, the enhancement of bone reparation is strongly dependent on the osteogenic cell migration, angiogenesis, and biomaterial resorption rate.

Platelet-rich fibrin (PRF) is an autologous biomaterial that contains a high amount of growth factors, platelets, fibrin monomer, fibrinogen, and blood platelets and therefore it has been shown to enhance tissue healing in different fields of medicine and dentistry [11,12]. PRF reveals a dense fibrin network with nano-scale fibers that can act as scaffold for cell proliferation, migration, and differentiation. Also, PRF acts like a drug delivery system of growth factors leading to an enhancement of neoangiogenesis [12,13]. The cross-linking of fibrin fibers mechanically stabilizes the architecture of the PRF-based scaffold and therefore such intricate fibrin nanostructure shows extraordinarily viscous-elastic behavior for agglomeration of other materials and surgical application [14,15].

PRF can be obtained like a membrane or a liquid phase substance by varying methods of centrifugation [12,16] . The liquid phase of PRF can be achieved at an early time point at low centrifugation speed and using non-glass centrifugation tubes. Such flowable PRF can be injectable by using syringes or agglomerated with particulate biomaterials [17,19]. Flowable

PRF is slowly converted into a viscous fibrin network that agglomerates particulate bone graft materials acting as an Autologous Fibrin Binder (AFB) [19].

The use of PRF can overcome the clinical limitations of particulate bone grafts regarding its handling, bioactivity, and fitting in surgical sites. The combination of chopped PRF membranes, flowable PRF, and particulate graft materials results in manufacturing a bioactive composite block properly designed for bone augmentation [19]. Also, the graft instability of particulate biomaterials can be avoided due to the cross-linking polymerization of the PRF that decreases the failure risks during bone healing [20]. Particulate graft materials can act as scaffolds and mineralization nuclei for cell migration and angiogenesis [21,22]. Such bioactive composite block can be produced by using a simple technique and therefore the association between PRF with other biomaterials may reduce treatment costs as less bone graft material is needed to fill the bone defect [19,23]. Also, the patient experiences less morbidity since no secondary harvesting surgical site is needed accompanied by a faster tissue healing.

However, studies regarding the morphologic characterization of flowable PRF and PRF block containing different particulate biomaterials are scarce. The present study aimed to evaluate the morphological aspects of flowable PRF containing two different types of hydroxyapatite-based graft materials. It was hypothesized that the combination of bone graft materials revealed morphological and chemical aspects for bone healing maintaining the biological potential of the platelet-rich fibrin.

MATERIALS AND METHODS

Particulate bone graft materials

Two different types of particulate hydroxyapatite (HAp) derivatives were used to produce PRF-based blocks (putty state): deproteinized bovine bone mineral (DBBM) and a synthetic HAp

(Fig. 1b,c). Particulate DBBM had a grain size ranging from 125 up to 800 μm (Biograft®, Ossmed®, Cantanhede, Portugal) while the synthetic HAp had a grain size ranging from 300 up to 400 μm (Osteogen®, IntraLock™, Boca Raton, FL, USA).

Table 1. Details on the particulate bone graft materials.

Properties	Synthetic HAp	DBBM
Chemical composition	$Ca_5(PO_4)_3(OH)$	$Ca_{10}(PO_4)_6(OH)_2$
Size grain (μm)	300-400	125-800

.

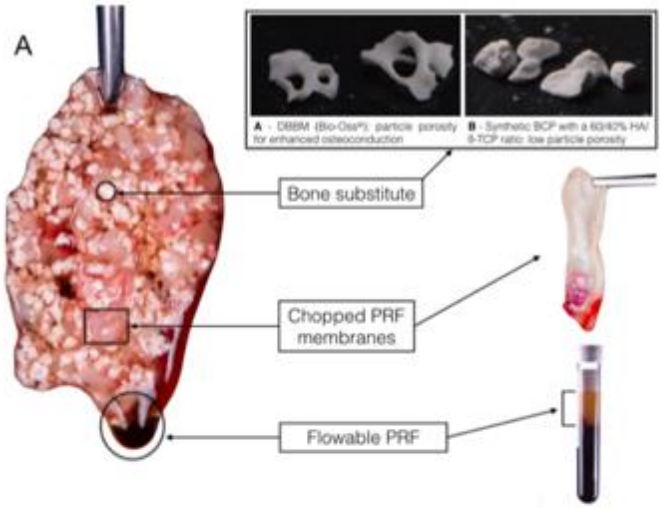

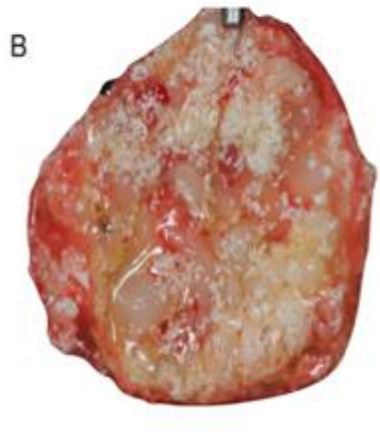

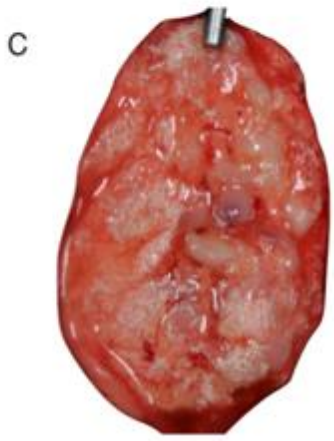

Figure 1. (A) Schematic illustration of PRF block and its constituents (chopped PRF membranes, flowable PRF and particulate bone substitute). Bone substitutes presenting different particle size and porosity can be chosen. (B) PRF block containing DBBM with a grain size between 0.125 and 0.800 mm (Biograft®, Ossmed®, Cantanhede, Portugal). (C) PRF block containing a synthetic microcrystalline non-ceramic hydroxyapatite with a grain size between 0.300 and 0.400 mm (Osteogen®, IntraLock™, Boca Raton, FL, USA).

Preparation of zirconia porous structures

Yttria-stabilized zirconia spray-dried powder (TZ-3YSB-E, TOSOH Co., Tokyo, Japan) with high purity (99% Y-TZP) was used in this study. The specifications of the material are shown in Table 2. According to the supplier, the powder had a maximum particle size of 120 μm and spherical agglomerates with an average size of 60 μm.

A zirconia suspension was prepared according to the method described in previous studies [24,25]. Suspensions thus contained 60 wt% of yttria-stabilized zirconia powder and 1 wt% Duramax D3005, a dispersant used to adjust the pseudoplastic and thixotropic rheological behavior. The suspension was produced by adding 20 ml of distilled water to 30 g zirconia powder and then milled in a planetary ball mill (PM100, Retsch) at 400 rpm for 80 min. That step provides a powder deagglomeration and slurry homogenization. Afterward, the dispersant Duramax was added to achieve the desired rheological behavior. For the development of the optimal processing route, porous specimens were produced using PU sponges of 60 ppi (10 mm x 10 mm x 10 mm) as temporary templates. The PU sponges were manually impregnated with the ceramic suspension without clogging the pores and kept in a stove at 100°C for 20 min. A heat treatment with the usual parameters for sintering this material (5°C/min up to 1500°C for 120 min) was performed in a conventional high-temperature furnace to eliminate PU and consolidate the porous structures. At the end of the thermal treatment, fully sintered monolithic Y-TZP porous structures were produced.

Table 2. Properties of the zirconia and titanium specimens.

Properties	Cp Ti	Zirconia
Chemical composition	Ti	3Y-TZP
Density (g/cm^3)	4.5	6.05
Bending strength (MPa)	560-620	1100
Young's modulus	115	240
Micro-hardness (HV)	180	1250
Fracture toughness ($MPa*m^{1/2}$)	55-60	5

Preparation of zirconia and titanium implant surfaces

Zirconia discs were obtained by cold pressing and texturized according to the method described in a previous study [26]. The compaction of the 3 mol% yttria-stabilized zirconia spray-dried powder (TZ-3YSB- E, Tosoh Corporation, Japan) was performed on a steel cylindrical mold with an internal diameter of 8 mm and 30 mm of height, with a pressure of 200 MPa for 30 s. After that, the pressure was released evenly and green zirconia compacts with a mean of 8 mm of diameter and 5 mm of thickness were obtained. The texture of zirconia discs was performed with Nd:YAG laser (OEM Plus, SISMA, Italy), using an output power of 6W, a spot size of 3 μm and a pulse width of approximately 35 ns. A focusing unit containing a fused quartz lens with a nominal focal length of 160 mm, a fundamental wavelength of 1.064 μm and a maximum pulse energy of 0.3 mJ/pulse was used. Surface texturing was carried out in normal air under atmospheric pressure and a jet of air braided was used to remove any debris produced during laser processing. Two strategies regarding line design (8 and 16 lines design) and different laser parameters (laser power and number of laser passages) were adopted to assess their influence on geometry and depth of created textures. This design was defined in a computer-aided design system and then it was engraved on the zirconia surfaces.

Also, Ti grade 2 specimens with 8 mm diameter and 5 mm thickness were cut and laser textured using a Nd:YAG laser (OEM Plus, Italy), as previously described in previous studies (Faria et

al. 2017). As in the zirconia disks, a focusing unit containing a fused quartz lens with a nominal focal length of 160 mm, a fundamental wavelength of 1.064 μm and a maximum pulse energy of 0.3 mJ/pulse was used. The duration of scanning process was about 6 min in each experiment. Different laser parameters were tested to produce the above-mentioned textured lines, always using an argon atmosphere. Specimens were then cleaned with acetone in ultrasound to remove any debris generated during Nd:YAG laser texturing.

Preparation of flowable PRF and PRF block

Peripheral venous blood was collected from one healthy, nonsmoker, man volunteer (age 32 years). A total of 78 mL blood was collected in 8 tubes within 9 mL in 2 plastic tubes without anticoagulants or silica coating (VACUETTE®, Greiner Bio-one GmbH, Kremsmünster, Austria) while 10 mL blood was harvested in 6 silica-coated tubes (BD Vacutainer Serum Becton Dickinson, Franklin Lakes, NJ, USA). Blood retrieval was performed by a nurse at the Center for Education and Research on Dental Implants (CEPID), Dept. of Dentistry, Federal University of Santa Catarina (UFSC). The use of human blood was approved by the Human Research Ethics Committee at the Federal University of Santa Catarina (CEPSHUFSC), cod. 2229.085, that is in accordance with the Helsinki declaration of 1964. The volunteer signed the informed consent prior to inclusion in the study the study since the purpose of the study was described.

The harvested blood was immediately centrifuged by using a high-quality table centrifuge at 2700 rpm (408 g) and at room temperature for 3 min, according to the IntraSpin protocol (IntraSpin®, IntraLock™, Boca Raton, FL, USA). After centrifugation, 2 plastic tubes were removed from the centrifuge while 6 silica-coated tubes remained under centrifugation for 9 min over a period of 12 min centrifugation [18,19].

After the 12 minutes centrifugation in silica-coated tubes, three phases can be noted: red blood corpuscles at the bottom of the tube, platelet-poor plasma (PPP) on the top, and an intermediate layer called “buffy coat” (yellow layer) where most leucocytes and platelets are concentrated [27]. Immediately after centrifugation, the flowable PRF (upper yellow liquid phase) was harvested from the plastic tubes. Fibrin-based clots were harvested from the tubes using tweezers and the red blood cells were separated from the fibrin-based clot by using a periosteal elevator. Red blood corpuscles and PPP were discarded and then a yellow PRF clot was harvested from the middle of each tube. PRF clot was then compressed into a membrane using a proper apparatus (Xpress kit, IntraLock™, Boca Raton, FL, USA) to avoid any damage to the cells. The PRF membranes were fragmented into small pieces from 2 membranes and added to 0.5 g particulate graft materials at a 50:50 ratio. Then, the flowable PRF was added and stirred gently for ± 10 s while shaping it to the desired PRF block form regarding particulate or porous structures as well as PRF coating onto cp Ti or zirconia surfaces.

Scanning Electron Microscopy (SEM)

For SEM analysis in triplicate, three drops of the flowable PRF (each one within 40 μL) onto each titanium or zirconia surface specimen ($n = 9$). In the case of the PRF blocks, samples ($n = 9$) were placed onto titanium-based stubs for coupling to the SEM chamber (Fig. 2a). The SEM preparation protocol was adapted from the study of Varela et al. (2018) [19]. Samples were exposed to titanium for 20 min for the achievement of the fibrin fibers’ cross-linking followed by washing three times in distilled water for 5 min. Then, samples were fixed in a solution containing *2.5% glutaraldehyd*e and 2.5% *paraformaldehyde* for 30 min and therefore they were washed 3 more times in PBS for 5 min. The dehydration of samples was achieved by immersing in a gradually series (25%, 50%, 75%, 95%, and 100%) of ethanol solutions. At last,

samples were air-dried at room temperature for 5 min and then placed in a vacuum oven at 37ºC for 2h.

Specimens embedded with PRF were sputtered with AuPd thin films and analyzed using a scanning electron microscope (SEM, vega 3, TESCAN, Brno, Czech Republic) equipped with energy-dispersive spectrometer (EDS) (Fig. 2b). The morphological analysis of the fibrin fiber's network and the bioactive block or coating was performed by SEM on secondary (SE) or backscattered electrons (BSE) mode at an accelerated voltage of 15 *kV*. SEM images were recorded at magnification ranging from x2,000 up to x20,000 at three different areas for each sample (n = 9). The chemical composition of the bone substitute particles was evaluated by EDS. The particle size distribution, density, and area of the bone graft materials were analyzed using the ImageJ 1.51 software (NIH, Bethesda, Maryland, USA).

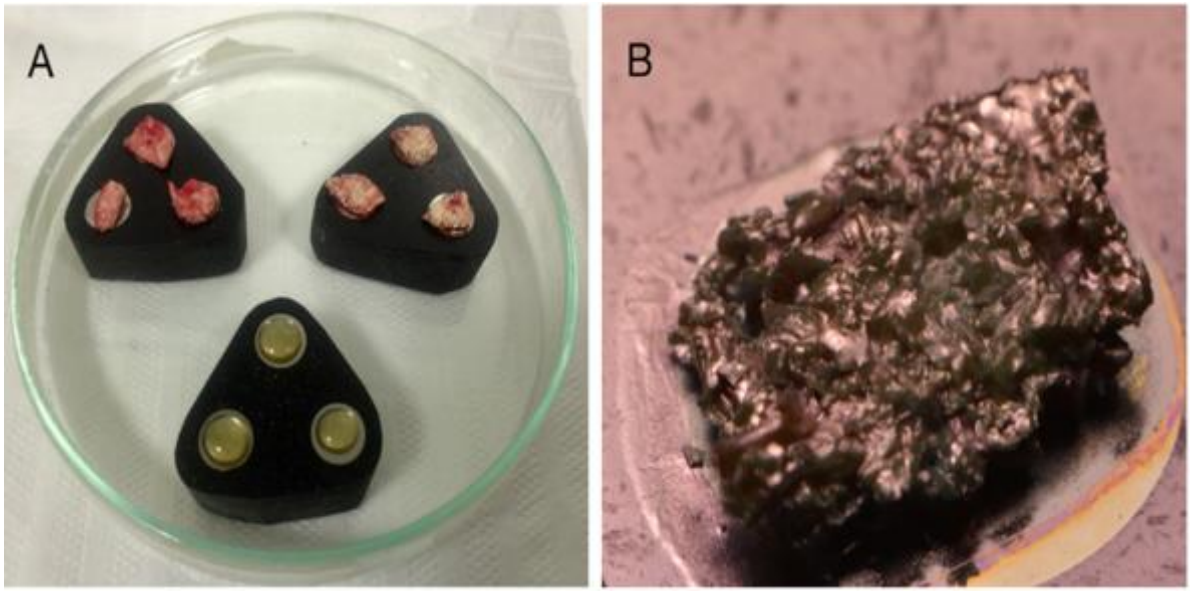

Figure 2. (A) Flowable PRF and PRF block samples on titanium disks. (B) PRF block with DBBM after gold sputtering and ready to be analyzed on the SEM.

RESULTS

SEM analysis

The SEM images from the surface of the flowable PRF showed a dense fibrin network, as seen in Figure 3a. The same pattern of fibrin fibers was noticed in the PRF blocks (Figure 3b-e). SEM cross-sectional images from the surface of the PRF blocks revealed a dense fibrin mesh covering the whole surface of bone substitute particles and connecting different particles. These bundles contained clusters of platelets, red blood cells, and some leukocytes which seemed to keep the components of the block assembled (Fig. 3d).

Energy dispersive X-ray spectroscopy (EDX) showed the following weight percentage of elements in the flowable PRF sample were the following: 50.6% C, 15.6% O, 1.5% S, 1.0% Ti, and 0.8% Na. The sample containing the PRF Block with the synthetic non-ceramic hydroxyapatite showed a weight percentage of 23.6% Ca and 12.3% P. Therefore, the weight percentage of elements in the sample containing the PRF Block with the DBBM were 8.1% Ca and 3.3% P (Table 1).

The mean thickness of the fibrin clusters was recorded at 389 nm, as seen in Fig. 4a, while the area occupied by fibers was measured at 49.55% flowable PRF (Fig. 4b) (x20,000 magnification). A DBBM particle exhibiting a macro pore with a diameter of 110 μm can be seen in Fig. 4c (x500 magnification). The mean pore diameter of a DBBM particle was 477 nm, with a maximum of 667 nm maximum and 335 nm minimum pore size (Fig. 4d) (x20,000 magnification).

SEM images of porous Y-TZP blocks at different magnifications showed a dense fibrin mesh covering the entire surface and pores (Fig. 5). Fibrin fibers ran mostly parallel to the zirconia block surface (Fig. 5c,d). A lymphocyte trapped inside of the fibrin filaments covering the surface of the zirconia could be noticed (Fig. 5d).

A thick and dense uniform fibrin layer with cells trapped inside could be noticed covering the surface of laser textured zirconia disks, both in peaks and valleys (Fig.6). SEM images showed a substantial number of large diameter fibrin fibers inserted and interconnected with the

microroughness on the surface and blood cells (Fig.6 b,c,d). Fibers can be seen running both parallel and perpendicularly to the surface.

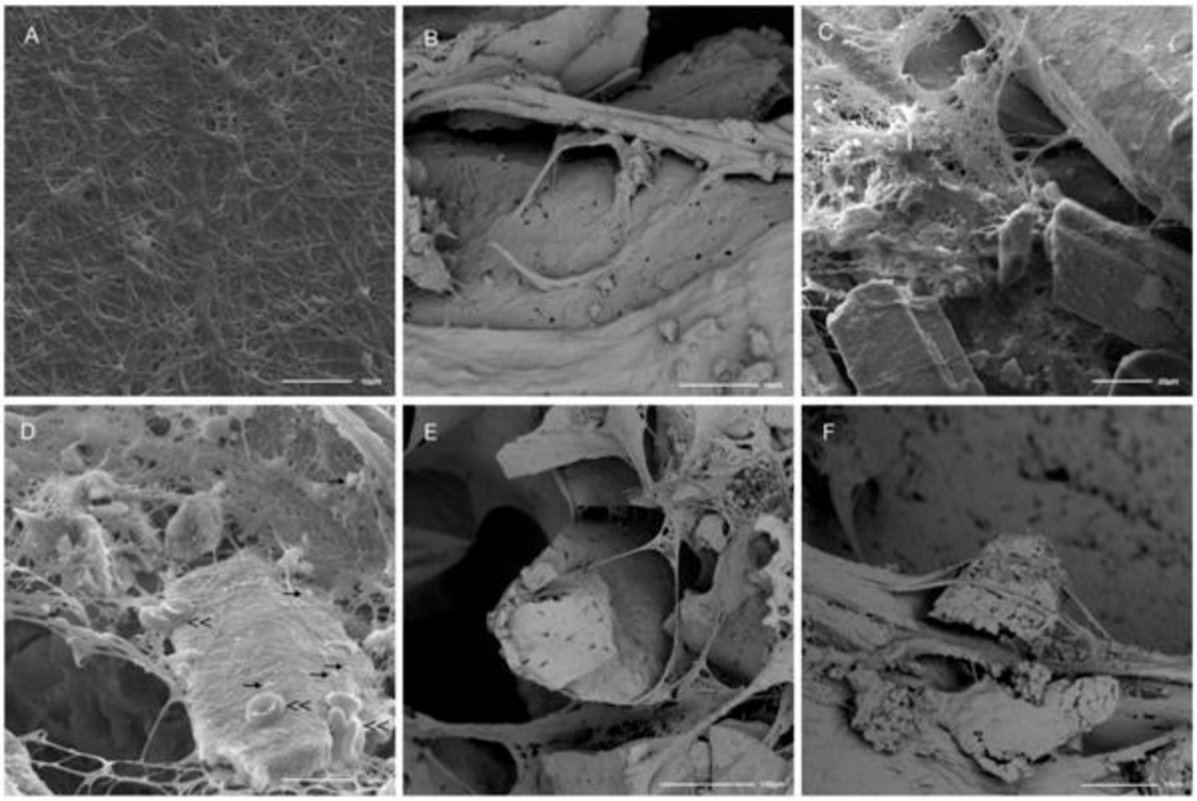

Figure 3. Scanning electron microscope (SEM) images showing the morphological aspects of flowable PRF, PRF block with the synthetic hydroxyapatite, and PRF block composed with a DBBM. (A) A dense fibrin network with embedded cells at x5,000 magnification. (B) Fibrin fibers penetrating into the pores of a DBBM particle (x5,500 magnification). (C) Fibrin filaments with trapped blood cells covering the surface of bone particles (x2,000x original magnification). (D) Dense fibrin and blood cells cover the surface of bone particles (x5,000x magnification). (* - leukocytes; << - red blood cells; ⟶ - platelets) (E) Fibrin filaments embedding a bone particle (x650 magnification). (F) Bone graft particles embedded by the fibrin network (x5,200 magnification).

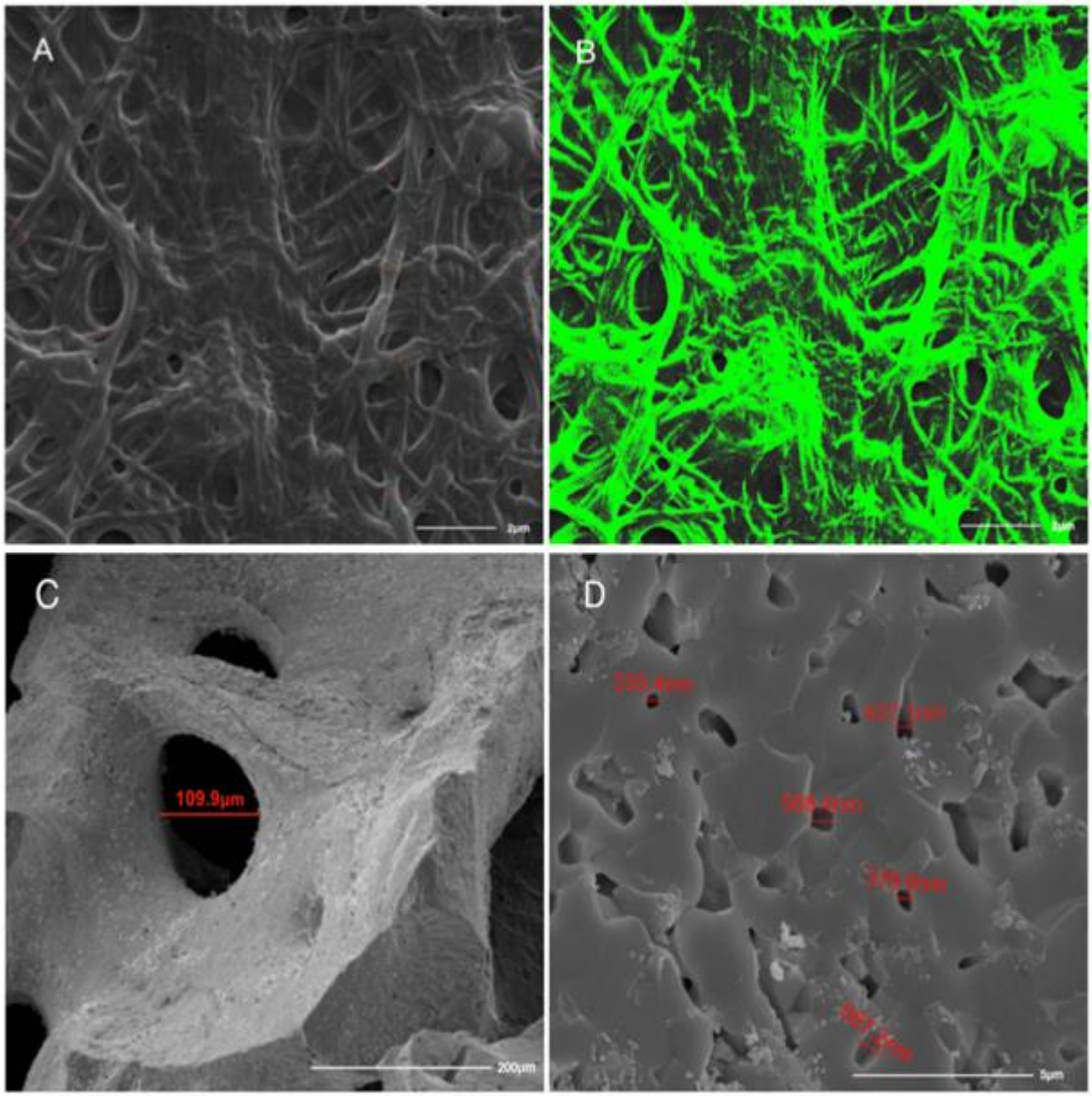

Figure 4. Scanning electron microscope (SEM) images of flowable PRF and DBBM particles.

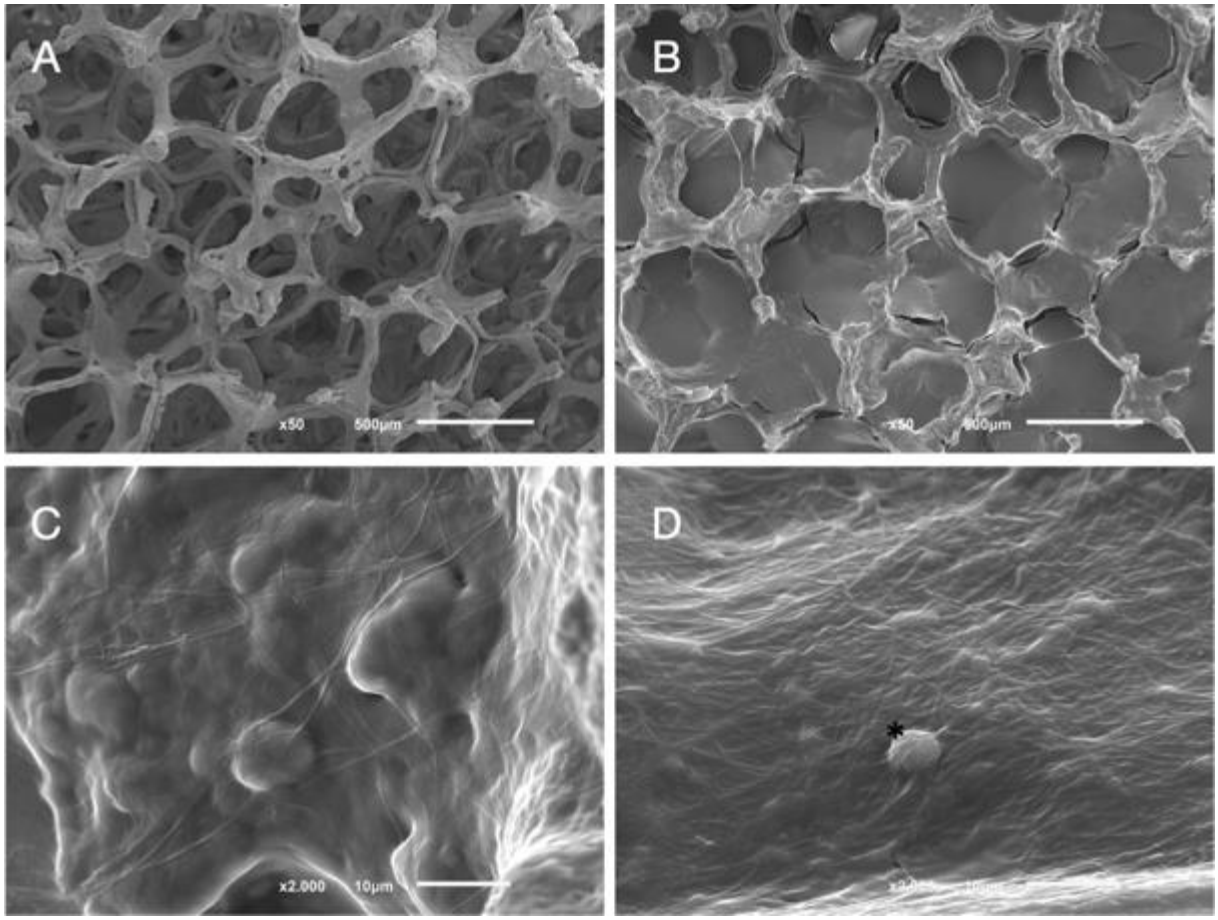

Figure 5. SEM images of a porous zirconia block involved by a flowable injectable PRF (i-PRF). A) Zirconia block with porous to improve osteoconductive properties (x50 magnification). (B) Porous zirconia block embedded with a flowable PRF (x50 magnification). (C) Fibrin filaments covering the surface of the zirconia (x2,000 magnification) and (D) a lymphocyte covered by i-PRF (x2,000 magnification). (* - lymphocyte)

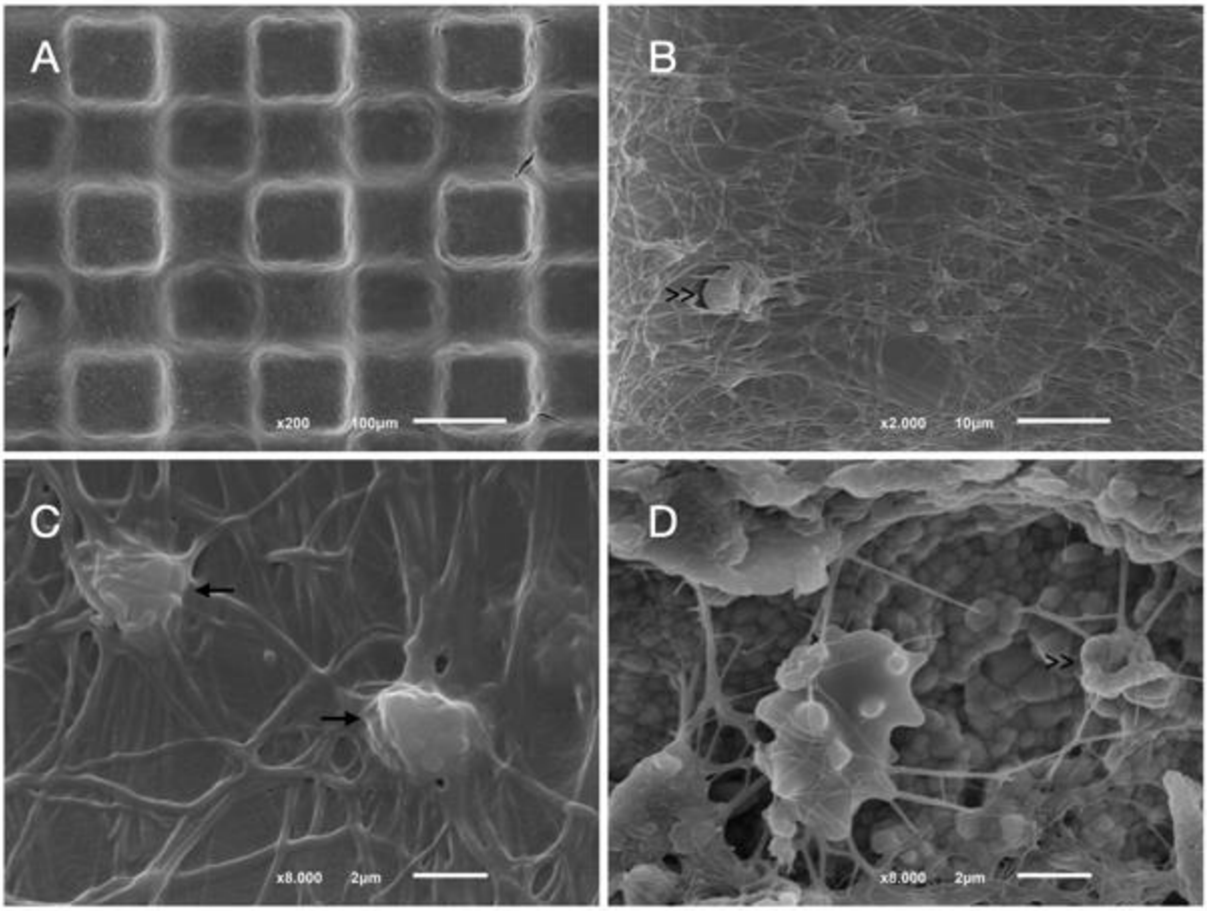

Figure 6. SEM images of a laser textured zirconia surface covered with a flowable injectable PRF (i-PRF. (A) Fibrin can be seen covering both the micro-scale ridges and valleys of the zirconia surface (x200 magnification) and (B) red blood cells entrapped in fibrin (x2,000 original magnification). (<< - red blood cells) (C) Platelets can be detected in the dense fibrin network. (x8,000 original magnification). (→ - platelets) (D) Fibrin fibers embedding and connecting the laser textured zirconia and red blood cells. (x8,000 original magnification). (<< - red blood cells)

DISCUSSION

This study described the morphology of an innovative bioactive composite block composed by bone substitutes and a flowable platelet-rich fibrin. The combination of particulate bone substitutes and PRF showed morphological and chemical aspects that allow to validate the hypothesis that this mixture can be used for bone augmentation procedures.

Flowable PRF revealed a dense fibrin network with nanometric fibers that can act as a scaffold for cell proliferation, migration, and differentiation and for delivery of growth factors, leading

to an enhancement of neoangiogenesis [21,22]. Particulate graft materials serve as a space maintainer for the regenerative volume. Biomaterial embedding PRF supports the nucleation and accumulation of the newly formed bone matrix, thus giving the biomechanical strength necessary during the first steps of healing.

In the present study, a low content of red blood cells, leukocytes and platelets was still present in the flowable PRF samples. However, this was observed in SEM images and a cell counting analysis would be needed to determine the exact number of blood cells contained in the flowable PRF samples. Thus, the yellow liquid was harvested from the resultant liquid phase (region) above the red blood cells phase once the harvesting handle method can vary depending on the clinical operator. In previous studies, a higher number of red blood cells, leukocytes, and platelets were recorded because the yellow liquid was harvested as near as possible to the blood cell region [18,28]. Varela et al. (2019) reported a higher concentration of platelets and leukocytes in flowable PRF compared to those in peripheral blood samples [18]. However, Castro et al. (2019) noted that around 88% of platelets and 70% of leukocytes in the initial blood sample were still present in the flowable PRF [28]. Despite the different results, both studies cannot be compared as different protocols for preparation of flowable PRF were adopted, thus different final products were obtained.

A porous fibrin structure in PRF has shown to enable rapid vascularization and host cell penetration, while a dense fibrin structure is rather resistant to host cell penetration and vascularization [29]. Bai et al. (2018) performed a histological analysis of PRF sections and found that porosity of PRF clots is inversely related to fibrin diameter [30]. The same authors observed an uneven porosity of the PRF network, a clear gradient of porosity across the PRF clot (from the red blood cell end to the plasma end of a clot), exhibiting a decrease in compactness and an increase in porosity. This gradient of porosity across the PRF clot was seen in all young and middle-aged individuals but not in older individuals. Thus, authors could

conclude that porosity of fibrin-based clots is influenced by sex and age [30]. These results confirm the ones obtained in the present study where thinner fibrin fibers, thus a less porous fibrin mesh, was observed. This could be attributable to the region of collection adopted, the liquid phase (region) above the red blood cell phase. Changes in fibrin network pattern are also dependent on the choice of the centrifugation protocol. Mamajiwala et al. (2019) found denser fibrin network patterns in PRF membranes obtained at 3500 rpm for 15 min compared to the ones obtained at 1400 rpm for 8 min, meaning that lowering speed and time leads to a less dense fibrin network pattern [31]. The same authors also revealed that a highest platelet concentration, antimicrobial activity, and dense fibrin network were obtained in 20–34 years age group [31].

In the present study, flowable PRF showed to have fibrin clusters with a mean thickness of 389 nm (min: 179 nm; max: 563 nm) (Fig. 4a). Varela et al. (2018) studied the fibrin network of flowable PRF by field emission gun scanning electron microscopy (FEG-SEM). These authors observed fibrin fibers with a thickness ranging from 20 up to 200 nm with an average diameter of 90 nm [18]. On the fibrin network, the fibrinogen was polymerized into fibrin (by the activated platelets of the chopped membranes) within a few minutes and trapped the biomaterial into a fibrin mesh containing platelets and leukocyte, forming the PRF Block (Fig. 1). The cross-linking between the fibrin fibers mechanically stabilizes the architecture of the fibrin-based scaffold. That avoids the graft instability of particulate biomaterials, thus decreasing the risk for failure during bone healing [20]. That intricate nanostructured fibrin network shows extraordinarily elastic mechanical and biological behavior [14,15,32].

The synthetic non-ceramic hydroxyapatite used in this study is a biocompatible, osteoconductive material that conducts bone ingrowth much like high-temperature particulate hydroxyapatite [33]. Mostly, HAp ceramics that are formed at high temperatures, such as the DBBM used in the present study (above 1200ºC), are more stable than those formed at lower temperatures, like the one synthetic non-ceramic hydroxyapatite used (60º to 80ºC). This

phenomenon is related to the effect of temperature on the size of the crystals being formed and, in turn, on the effect of crystal size on solubility (Table 1) [33]. The synthetic non-ceramic hydroxyapatite presents a slow dissolution, contrary to the DBBM which is relatively stable, and thus considered permanent in nature [34-36].

DBBM used in the present study had a grain size between 0.125 and 0.8 mm (Biograft®, Ossmed®, Cantanhede, Portugal) and the synthetic one had a grain size between 0.3 and 0.4 mm (Osteogen®, IntraLock™, Boca Raton, FL, USA). Granules with a 100–300 μm size have shown higher osteoconductive potential when compared with 1–2 mm granules [37]. Particle size distribution of ordinary bone graft materials is reported in literature ranging from 250 μm to 2 mm [1,9,10]. Regarding the selection of particulate bone graft materials, attention should be paid to its morphologic characteristics such as the size and porosity of granules and resorption time. By mixing bone substitutes with PRF, spaces among granules can be occupied by fibrin fibers and blood cells rich in growth factors that will enhance bone healing (Fig. 5).

DBBM used in this study presented a nano-scale porosity with a mean pore size of 0.608 μm (min: 0.265 μm; max: 0.905 μm). DBBM can be classified as a nanostructured HAp after organic removal that still results in a proper cell migration and absorption of growth factors. DBBM is often used when bone volume stability is desired due to its slow resorption and delayed healing. Residual particles could be detected after several years following bone augmentation procedures [34,35]. Commercially DBBM has shown a pore size at micro-scale up to 10 μm [8]. After adequate thermal treatment, DBBM does not lose its natural ceramic state [$Ca_5(PO_4)_3(OH)$] maintaining physicochemical properties similar to human trabecular bone [38]. A previous study reported that increased porosity of DBBM seemed to benefit the osteoconduction process in dogs [38]. Nanostructured HA reveals a high osteoconductivity and bioresorbablity, due to the higher contact area when compared to the ordinary HAp particles and has been used with success for different treatment approaches such as bone loss by peri-

implantitis [9,39]. Bone tissue possesses a porous structure ranging from 20 to 400 μm that is necessary for migration, adhesion, growth, and proliferation of osteogenic cells [9,40]. Previous studies reported that the porosity of HAp granules ranges between 60 and 80% [4,41]. The hydroxyapatite nano-scale porosity leads to a very large surface area, thus improves cell migration and absorption of growth factors [42].

The synthetic non-ceramic hydroxyapatite granules used in the present study did not possess a porosity such that found in the DBBM (Fig. 3c,d and 4c). Osteogen® crystals present an ultrathin nanocrystalline fluorapatite coating, that provides a bioactive and bacteriostatic barrier leading. That bacteriostatic state can prevent the accumulation of pathogenic species responsible for inflammatory reactions and bone loss. Osteogen® crystals have shown to promote osteoblast cell differentiation, migration, and proliferation, which are expected to accelerate bone growth [43]. Clinical studies have shown that bioactive glass granules possess morphological aspects that provide proper space among particles, as seen in Figure 5. Inter-spaces among granules facilitate cellular and tissue proliferation into the grafted material, thus enhancing osseointegration.

Bone substitutes scaffolds used for bone regeneration can be emerged in flowable PRF and thus improve its osteoinductive properties. (Fig. 5). Flowable PRF can also be used to cover laser-modified implant surfaces and provide bioactive properties (Fig. 6). Zirconia (3Y-TZP) has been increasingly used as a metal substitute for biomedical applications including implants and some strategies have been studied regarding surface modification by improving roughness and producing different patterns [44-46].

Laser technology has emerged as a promising processing technique to create complex microstructures at micro-nano scale (regarding surface texture design) due to its versatility and ability to remove material quickly, with low waste and without surface contamination since there is no contact between the biomaterial and laser (energy transfer from the laser to the

zirconia occurs through the irradiation) [47-49]. Some studies have reported that this technique changes the way as biological fluids interact with the biomaterial and also enhances zirconia surface wettability improving, therefore, the bone-implant interface [50-52]. Faria et al. (2020) explored two strategies regarding line design and different laser parameters (laser power and number of laser passages) to assess their influence on geometry and depth of created textures [53]. It was possible to produce well-defined textured surfaces with regular geometric features (cavities or pillars) that were evaluated regarding surface wettability, friction performance (static and dynamic coefficient of friction evolution) against bone, aging resistance and flexural strength. These new surface designs enhanced surface wettability and improved the fixation at the initial moment of the implantation, and did not significantly compromise the resistance to aging and the mechanical performance of zirconia [53].

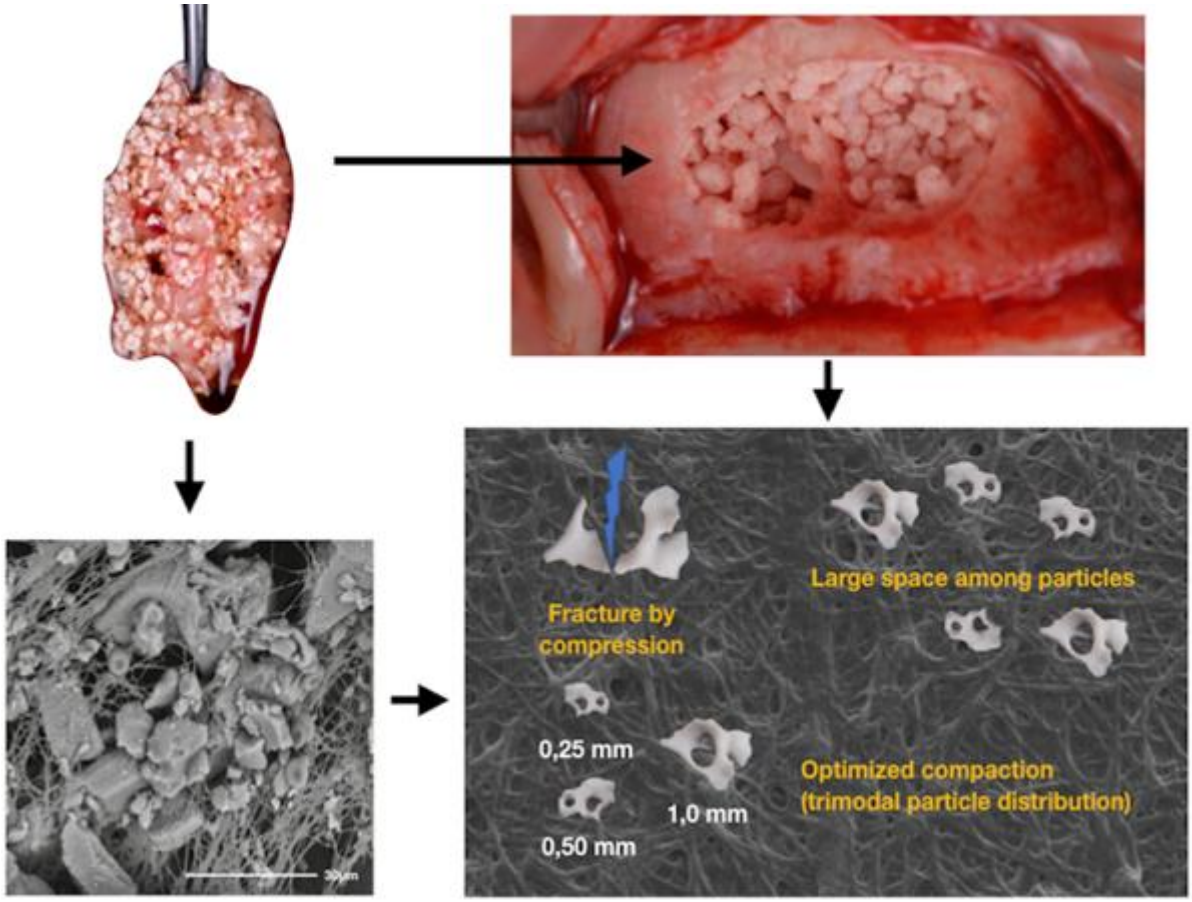

Figure 7. Schematic illustration of the PRF block being applied in a sinus augmentation procedure. Bone substitutes presenting different particle size and porosity can be chosen. Some particle fracture can occur during the clinical handling of bone substitutes. By using PRF, large spaces between particles of different sizes can be occupied by fibrin fibers and blood cells rich in growth factors that can enhance bone healing.

CONCLUSIONS

- The use of PRF improves handling, bioactivity, and fitting of particulate graft materials in surgical sites. The bioactive composite block obtained by combining chopped PRF membranes, flowable PRF, and particulate graft materials is appropriate for bone augmentation.
- Different protocols for preparation of PRF are available. There is a need for standardization of protocols for preparation, as different protocols originate different products of PRF that cannot be compared.

- SEM images of the flowable PRF showed a dense fibrin network, and in the PRF blocks this dense fibrin mesh was covering the whole surface of bone substitute particles and connecting different particles. The fibrin bundles contained clusters of platelets, red blood cells, and some leukocytes which seemed to keep the block components assembled.
- Bone substitutes act as a space maintainer and mineralization nuclei and the PRF will enhance cell migration, differentiation, and neoangiogenesis. Clinical data on the resorption of such mixture are lacking, thus attention should be taken when choosing the bone graft substitute for mixing with PRF. Future studies should compare the effectiveness of different materials to be mixed with PRF and evaluate the healing in the long term after using the bioactive composite block.
- On zirconia, a dense fibrin network filled porous Y-TZP blocks as well as i-PRF also covered micro-scale peaks and valleys of laser textured zirconia surfaces.

CHAPTER IV - TRIBOLOGICAL BEHAVIOR OF FLOWABLE PLATELET-RICH FIBRIN PLACED OVER ZIRCONIA IMPLANT SURFACES FOR BIOMIMETIC FUNCTIONALIZATION: IN VITRO STUDY

ABSTRACT

The present *in vitro* study aimed to evaluate the tribological behavior of gritblasted or laser-texturized zirconia surfaces after coating with a flowable injectable platelet-rich fibrin (i-PRF). Three zirconia surfaces were compared: (i) gritblasted with 250 μm spherical alumina particles and acid-etched with hydrofluoric acid (20%) (ZLA); (ii) laser-textured with a randomly topographic pattern (RD); or (iii) with a 16-line and 8-passage pattern (L16N8). The coefficient of friction (COF) of the specimens was assessed on a reciprocating sliding pin-on-plate tribometer at 1 N normal load, 1 Hz, and stroke length of 2 mm. Sliding wear tests were carried out against bovine femoral bone in 0.9% sodium chloride solution at room temperature (20 ±2ºC). Surfaces were then assessed by scanning electron microscopy (SEM). The wear volume was calculated from SEM images using a mathematical model as well as by weight loss measurement of the specimens.

COF mean values for test groups (ZLA=0.35; L16N8=0.45) were lower when compared to the control groups (ZLA=0.52; L16N8=0.60), with the exception of the RD group (test group - RD=0.47; control group - RD=0.43). Similar COF mean values were recorded for test and control groups within the RD group. Results did not show significant differences ($p > 0.05$) in COF mean values for ZLA, RD, and L16N8 specimens. The tridimensional fibrin network embedded with leukocytes, platelets, and red blood cells was responsible for lower mean values of COF on the gritblasted and laser-texturized zirconia surfaces, thus providing a lubricant role. Furthermore, the topographic aspects of the zirconia surfaces can increase the adhesion of the

fibrin network enriched with leukocytes and platelets to speed up the osseointegration process of zirconia implants.

Keywords: Coefficient of friction, Dental implants, Laser surface texturing, Platelet-Rich Fibrin, Zirconia

INTRODUCTION

The placement of dental implants has increased in the last years although limitations are still reported in literature considering aesthetic and biological factors [1]. Regarding biological factors, the early osteointegration process depends on several factors including patients' health conditions, materials, implant-to-bone interface integrity, materials, and implant design [2-10]. Recently, dental implants composed of yttria-stabilized tetragonal zirconia polycrystals (Y-TZP) known as zirconia has gathered attention since their optical properties and high chemical stability provide a high rate of aesthetic and biological success for the patients [11-14]. However, such high chemical stability decreases the interactions between zirconia surfaces and osteogenic cells during the first stage of the osseointegration [15]. Then, the migration and differentiation of osteogenic cells is dependent on the roughness and morphological aspects of the zirconia implants [2-7]. Also, the formation of a stable fibrin clot in contact with the moderately rough implant surfaces is key step in the healing process, as it provides a provisional scaffold for the migration of differentiating osteogenic cells towards the bone-implant interface [3,16-19].

Implant surfaces can be biofunctionalized by adding inorganic or organic bioactive materials such found in previous studies [20,21]. However, many approaches are not clinically used considering the lack of *in vitro* and *in vivo* studies to validate the findings. Injectable PRF can be obtained by reducing centrifugation time, and by using plastic tubes [22]. Castro et al. noted that around 88% of platelets and 70% of leukocytes in the initial blood sample were still present in the flowable PRF [23]. These growth factors released by leukocytes and platelets present in PRF allow to reduced bacteria on contaminated implant surfaces [24,25]. PRF plugs have shown to clinically improve primary stability of implants [26,27]. Several studies have reported the use the i-PRF suitable for mixing with bone substitutes although only a few studies have reported its use for implant coating [29-31,35]. It was hypothesized that the flowable i-PRF

used as implant coating can provide a dense fibrin-based clot on micro- and nano-scale features on implant surfaces [33]. Thus, further studies are required to validate the use of i-PRF for implant coating regarding the types of surface, material, and design for dental implants [32]. However, it can also be hypothesized that the i-PRF coating or some components (leukocytes, platelets) can flow away from the implant-to-bone interface during implant placement [35]. The removal of the coating and its components can occur on friction of roughness implant surfaces and bone tissue since the placement should performed on a torque monitoring to achieve a primary stability.

In this way, the main aim of the present *in vitro* study was to evaluate the tribological behavior of gritblasted or laser-texturized zirconia surfaces after coating with a flowable injectable platelet-rich fibrin. The tribological assessment involved a well-designed reciprocating sliding wear testing of the specimens against a bovine bone in a saline solution.

MATERIALS AND METHODS

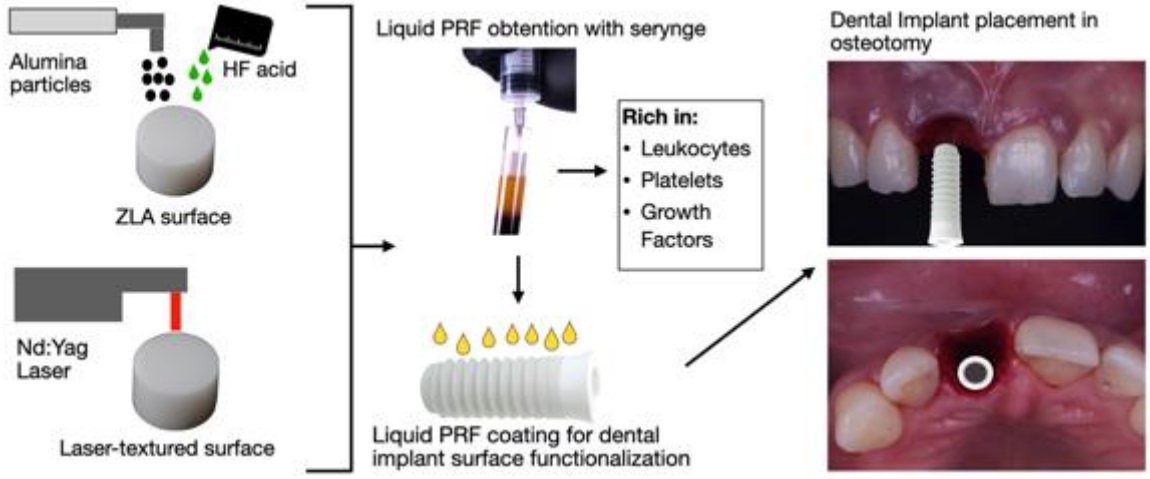

Fig. 1. Schematics of dental implant placement with liquid PRF for biomimetic surface functionalization. Note: The zirconia dental implant figure was retrieved from Straumann website, from https://www.straumann.com/pt/pt/profissionais-de-odontologia/produtos-e-solucoes/implantes-dentarios/implantes-de-ceramica.html

Preparation of the zirconia surfaces

Implant specimens were prepared using a 3 mol% yttria-stabilized zirconia spray-dried powder (TZ-3YSB-E, Tosoh Corporation, Japan), with high purity (99%) and theoretical density of 6.05 g/cm3 was used. At first, the zirconia powder was poured into a steel cylindrical mold having diameter of 10 mm and a height of 30 mm and then a compression of 200 MPa was applied at room temperature for 30s. Green zirconia compact disks produced had a dimension of 8 mm in diameter and a thickness of 5 mm.

A group of sintered zirconia surfaces were grit-blasted with 250 μm spherical alumina (Al_2O_3) particles at a constant pressure of 6 bar, a distance of 50 mm away from the blasting nozzle, and at an impact angle of 90° for 30 s. Specimens were ultrasonically cleaned in isopropyl alcohol for 5 min. Zirconia disks were then immersed in 20% hydrofluoric acid (HF) for 1 min and then ultrasonically cleaned in an isopropyl alcohol for 5 min. The grit-blasting and acid etching surface treatment was adapted from the method previously described by Faria et al. [36]. After all the surface modification, all the samples were cleaned ultrasonically in isopropyl alcohol for 10 min and then in distilled water for 10 min to avoid any contamination on the specimens' surface (Fig. 2A-C).

The other groups of zirconia discs were laser-texturized on Nd:YAG laser (OEM Plus, SISMA, Italy) at 6W through a spot size of 3 μm and a pulse width of approximately 35 ns. A focusing unit containing fused quartz lens was used with a nominal focal length of 160 mm, a wavelength of 1.064 μm, and a maximum pulse energy of 0.3 mJ/pulse. No surface pattern was designed in one of the groups (RD) and the laser-texture was randomly performed (Fig. 2D-F). Another group of specimens (L16N8) was subjected to a laser-texturizing with a 16-line and 8-passage, as seen in figure 2J-L. The surface pattern was designed by computer-aided design (CAD). Surface texturing was carried out at room air and atmospheric pressure. A jet of air braided was used to remove debris produced during laser processing. The sintering of zirconia discs was

carried out using a high temperature furnace (Zirkonofen 700, Zirkonzahn, Italy) at 1500 °C, a heating and cooling rate of 8 °C/min, and 2 h of holding time.

Preparation of the flowable platelet-rich fibrin

Peripheral venous blood was collected from one healthy, nonsmoker, man donor (age 32 years). For the sliding wear tests, a total of 54 mL blood was harvested in 6 tubes from one volunteer within 9 mL in plastic tubes without anticoagulants or silica coating (VACUETTE™, Greiner Bio-one GmbH, Austria). The use of human blood was approved by the Human Research Ethics Committee at the Federal University of Santa Catarina (CEPSHUFSC), cod. 2229.085, that is in accordance with the Helsinki declaration of 1964. The volunteer signed the informed consent prior to inclusion in the study since the purpose of the study was described. The harvested blood was immediately centrifuged by using a high-quality table centrifuge at 2700 rpm (408 g) and at room temperature for 3 min, according to the IntraSpin™ protocol (IntraSpin™, IntraLock, USA). After centrifugation, the plastic tubes were removed from the centrifuge.

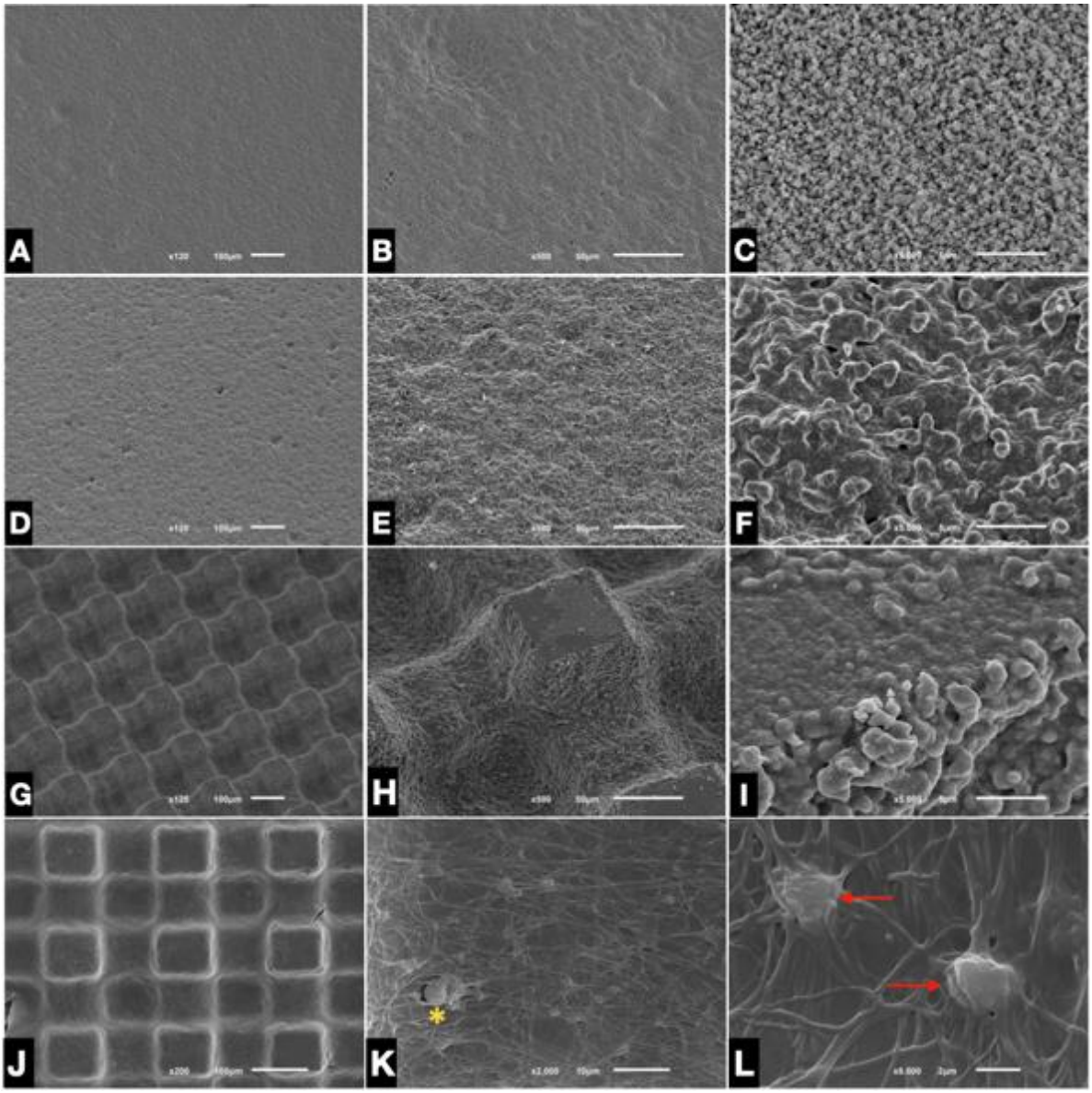

Fig. 2. Representative morphologies of the tested surfaces. (A-C) Sandblasted and acid-etched sample (ZLA); (D-F) Laser textured sample with no adopted design (RD); (G-I) Laser textured sample with a 16-line and 8-passage design (L16N8). (J-L) L16N8 surface covered with fibrin. * Red blood cells. ⟶ Platelets.

Tribological tests

The flowable PRF (upper yellow liquid phase) was aspirated from the plastic tubes with a plastic disposable transfer pipette (avoiding red blood cells) and then injected over the zirconia surfaces until completely coating. After 5 min, sliding wear started since the fibrin fibers' cross-linking was achieved. One tube of flowable PRF was used for 3 independent specimens.

The tribological tests were performed on the zirconia specimens to evaluate the dynamic coefficient of friction evolution and the structural integrity of the surface patterns against bovine

bone tissue in an environment mimicking the placement of a dental implant. The tests were carried out on a reciprocating sliding pin-on-plate tribometer (Bruker-UMT-2, USA) (Fig. 3). Bone cylindrical specimens with 4.2 mm of diameter and 12mm in length were cut from a fresh femoral part of a young bovine and washed 3 times in 0.9% sodium chloride solution (NaCl) to remove debris. Specimens were positioned in the upper site of the apparatus and zirconia specimens were attached to an oscillating table at the bottom as seen in Figure 4.

Reciprocating sliding wear tests were performed at 1 N loading (nominal), at 1 Hz, and over a stroke length of 2mm at room temperature (20 ±2 ^{o}C) for 5 min. The tests were carried out in 0.9% NaCl solution (B. Braun Medical Inc., Irvine, CA). Tests were performed in triplicate for each test condition. After each test, two random specimens of each group were washed 3 times in 0.9% NaCl solution to remove any wear debris. One random specimen from each group was not cleaned for inspections of bone remnants with SEM.

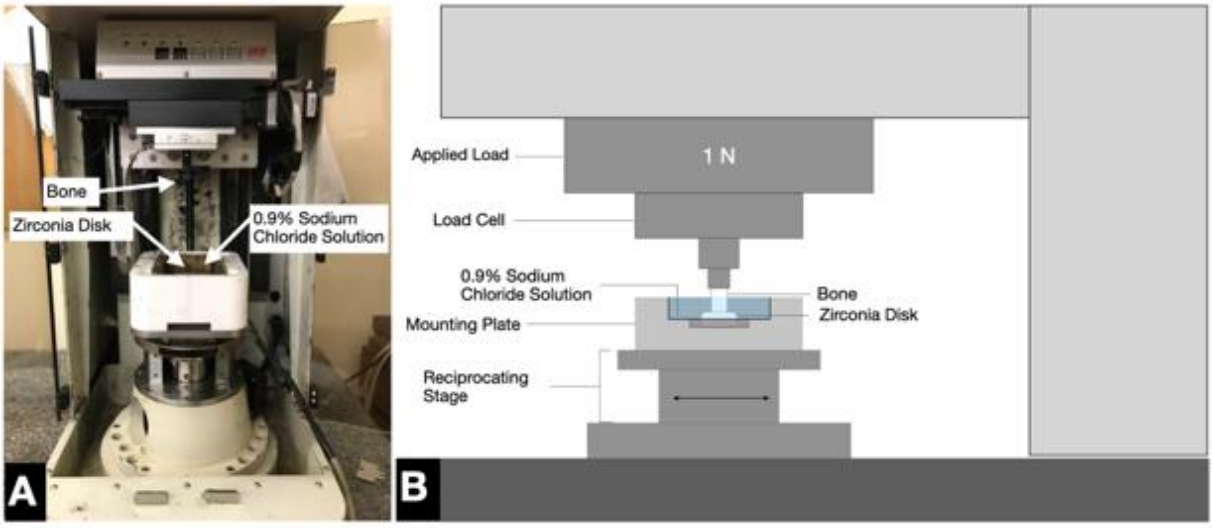

Fig. 3 (A) Bruker-UMT-2 reciprocating pin-on-plate tribometer. (B) Schematic representation of the reciprocating pin-on-plate tribometer.

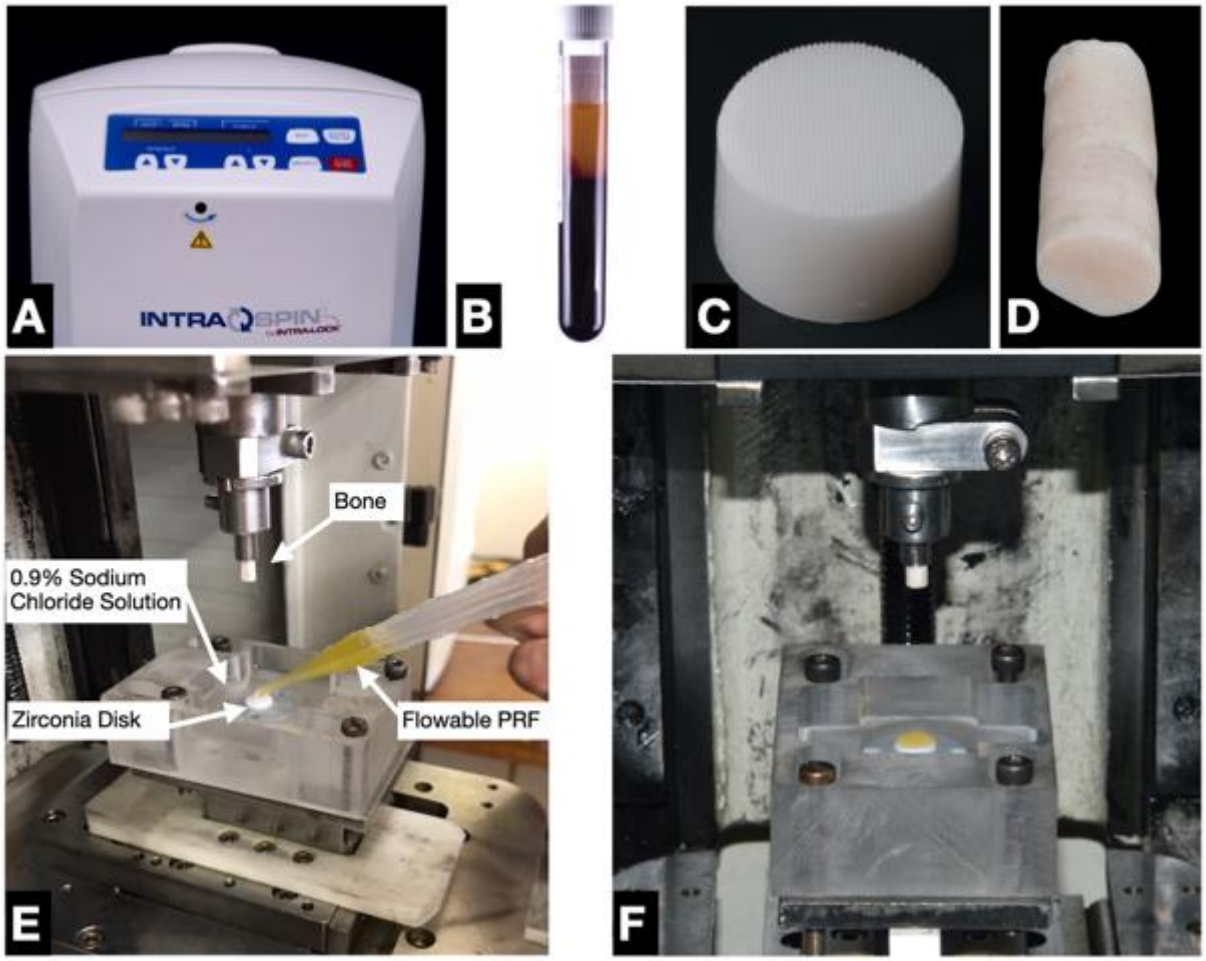

Fig. 4. (A) IntraSpin® centrifuge (Intralock™, Boca Ranton, FL, USA). (B) Plastic tubes containing the flowable PRF (yellow liquid phase). (C) L16N8 Zirconia disk. (D) Bone specimen. (E) Flowable PRF being injected over a zirconia disk with a plastic disposable transfer pipette. (F) Bone and zirconia disk with PRF ready for friction test.

Scanning electron microscopy (SEM)

SEM preparation was adapted from the study of Varela et al. (2018) [28]. Specimens coated with i-PRF or not were placed in a 12-well culture plate and then fixed in a solution containing 2.5% glutaraldehyde for 10 min and then washed in distilled water. The dehydration of specimens was achieved by immersing in a gradually series (25, 50, 75, 95, and 100%) of ethanol solutions for 5 min. Specimens were sputter-coated with AuPd thin films and analyzed using a scanning electron microscope (SEM, JSM-6010 LV, JEOL, Japan) equipped with an energy-dispersive spectrometer (EDS). An elemental chemical analysis was performed by EDS to inspect the transference of material after the sliding wear tests. The morphological analyses

of the flowable PRF coating, zirconia, and the bovine bone surfaces were performed by SEM on secondary (SE) and backscattered electrons (BSE) mode at an accelerated voltage of 5-10 kV. SEM images were recorded at magnification ranging from x30 up to x8,000 at three different areas for each specimen (n = 9).

Statistical analysis

A two-way ANOVA and multiple comparison tests were used. At first, Kolmogorov–Smirnov was applied to test the assumption of normality. P-values lower than 0.05 were considered statistically significant ($\alpha = 0.05$). The t student test was used to compare the COF results for surfaces coated with i-PRF or not. The power analysis performed by t student test or ANOVA, to determine the number of specimens for each group (n), revealed a test power of 100% in the present study. Statistical analyses were carried out using Origin Lab™ statistical software (Origin Lab, Northampton, MA, USA).

RESULTS AND DISCUSSION

Morphological characterization

Differences in the fibrin network coatings were noticed between and within groups. Laser-textured surfaces showed more zones covered by a dense fibrin network when compared to the gritblasted and acid-etched surfaces (ZLA group). The morphological aspects of the laser-structured surfaces provide a high retention of the fibrin network enriched with platelets, leukocytes, and growth factors. The flowable PRF coating covered both peaks and valleys of the laser-textured zirconia surfaces (Fig. 2J-L). Blood cells can also be seen trapped into the fibrin network on the laser-textured surfaces (Fig. 2K). Even though the ZLA surfaces revealed a lower roughness, the flowable PRF was detected on some regions of the surfaces that is also a promising outcome for commercial implant surfaces. Results validate the first hypothesis

considering the morphological improvement of zirconia surfaces can increase the retention of the flowable platelet-rich fibrin.

After the tribological assays, retention of bone fragments and cells entrapped in the fibrin network could be detected on laser-textured surfaces (Fig. 5,6). Also, the majority of previous studies only reported the morphological aspects of PRF on titanium implant surfaces. In this study, the use of reciprocating sliding tests aimed to simulate an implant placement procedure and the remnant i-PRF coating and bone fragments on zirconia surfaces. The reciprocating sliding direction is indicated on the SEM images. The absence of aligned abrasion groves can be explained by the low load (1N) applied and the presence of i-PRF. An axial load up to 200 N is reported in finite element analysis studies evaluating the stress distribution of dental implants and surrounding bone [37,38]. Thus, in order to avoid bone surface destruction, a low load (1N) was adopted in this study [39]. The existence of cracks and adherent thin tribo-layers were only detected at the edges of the wear track on the ZLA surfaces (Fig. 5C). The absence of these cracks on the laser-textured surfaces can occur due to the high PRF retention on their surface. A high amount of bone tissue (dark regions) was transferred to the laser-textured zirconia surfaces (RD and L16N8) (Fig 5 D-G). Bone fragments entrapped in the fibrin network covering the L16N8 surface can be noted in Figure 6. The transference of bone tissue leads to a stronger and effective contact between implant and bone, thus promoting a higher primary implant stability.

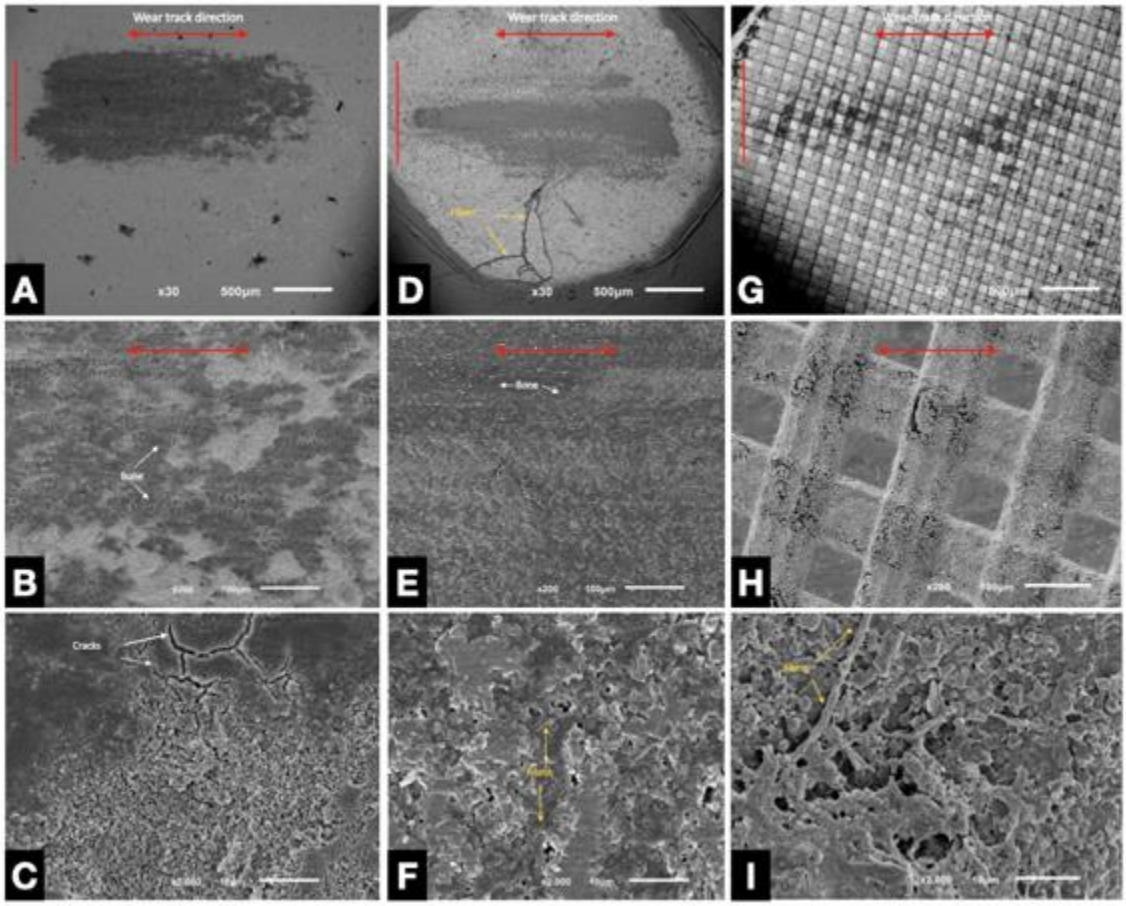

Fig. 5. SEM images on wear track. (A-C) Grit-blasted and etched zirconia surface (ZLA group). Less quantity of fibrin can be seen on the ZLA surface. (D-F) Non-textured zirconia surface (RD group). Fibrin is well distributed throughout the surface. (G-I) Laser-textured zirconia surface (L16N8 group). Fibrin was also detected on the peaks of the L16N8 surfaces.

To date, no studies assessing the behavior of i-PRF on zirconia implant surfaces are available. However, the effects of L-PRF clots around immediately placed titanium implant surfaces was studied in dogs [40]. Significantly increased bone formation was achieved on the micro- and nano-scale structured surfaces. However, the use of a flowable fibrin-based gel could be advantageous since the fibrin cross-linking occurs in direct contact with the implant surface. A previous study compared the behavior of different implant titanium surfaces when in contact with three different flowable PRF products: a fibrinogen concentrate, a fluid harvested from L-PRF clots, and a combined approach with fibrinogen and L-PRF fluid [33]. Previous findings revealed an overall increased retention of the fibrin network, leading to a dense coating over

rougher surfaces. Similar results can be noticed in our study regarding the laser-textured surfaces. Another previous study evaluated the interaction between five different titanium dental implant surfaces and liquid fibrinogen, and reported that the initial contact between an implant surface and the fibrin network differs significantly among commercial brands [34]. Thicker fibrin fibers were noted in contact with gritblasted/etched or 3D printed implant surfaces.

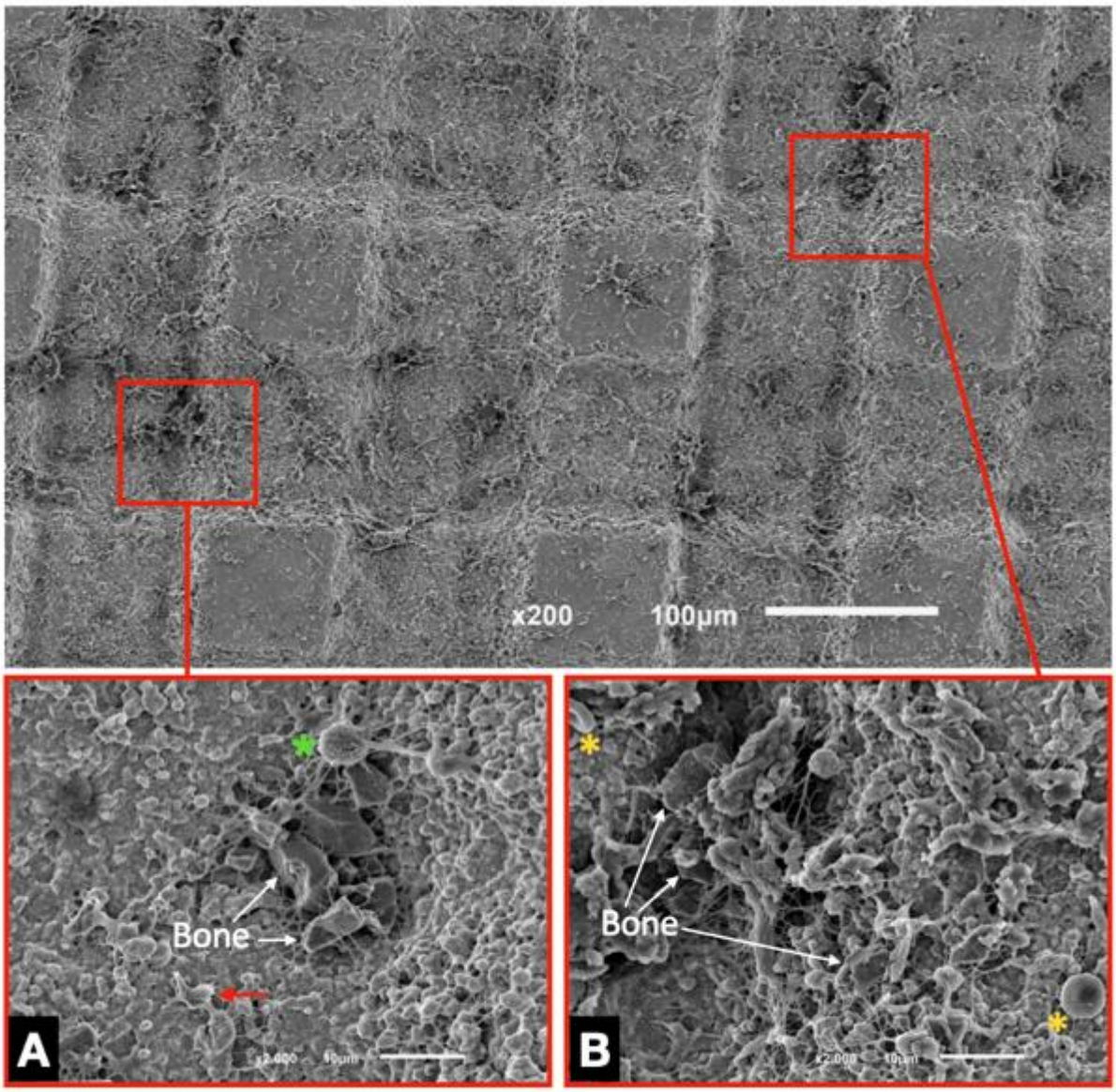

Fig. 6. Fibrin distribution over the L16N8 laser-textured zirconia surface (L16N8) after reciprocating sliding wear test. (A,B) Bone fragments entrapped in the fibrin network covering the surface can be observed. * Red blood. ≫T Lymphocyte cell. ⟶Platelet.

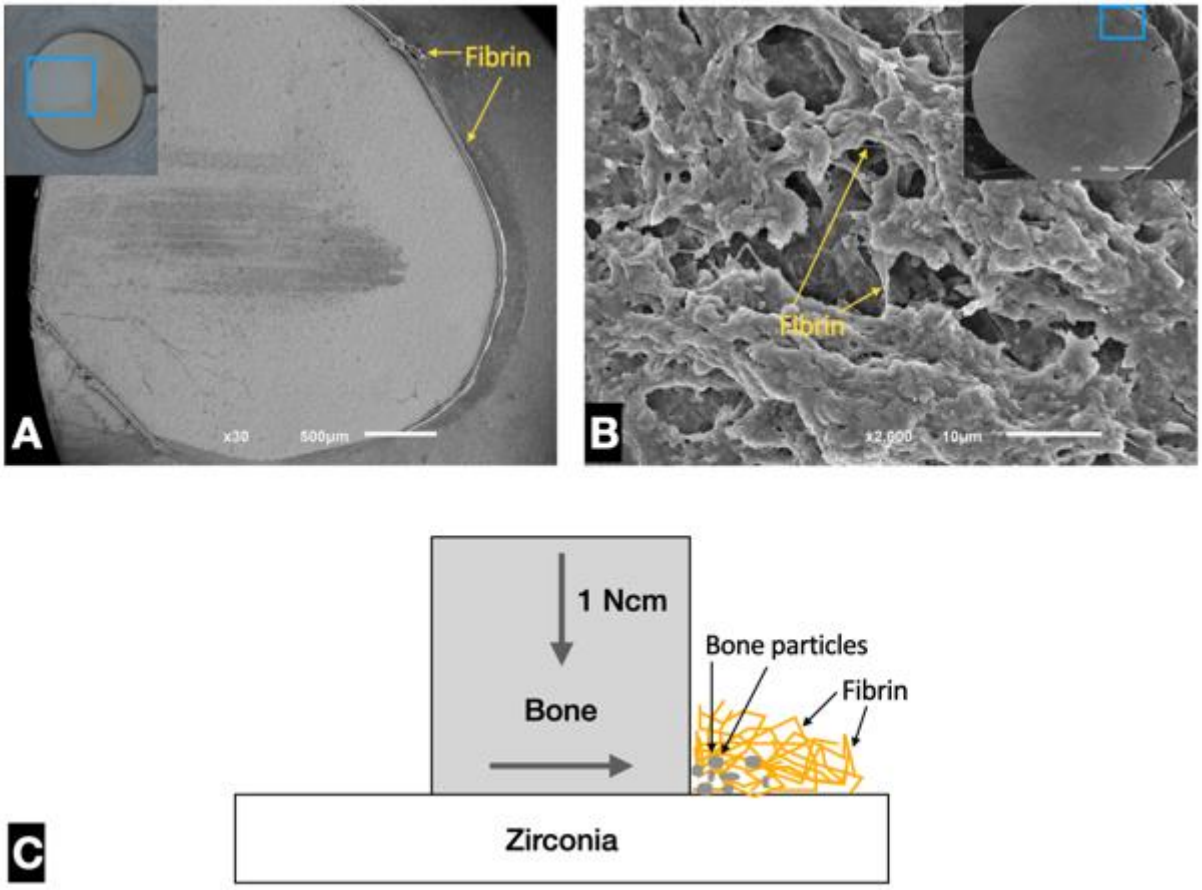

Fig. 7. (A) Fibrin displacement over the RD zirconia surface during the friction test. (B) High magnification SEM micrograph of the correspondent counterpart bone specimen with fibrin retained on its surface after the sliding test. (C) Schematics of the frictional behavior of fibrin during sliding tests.

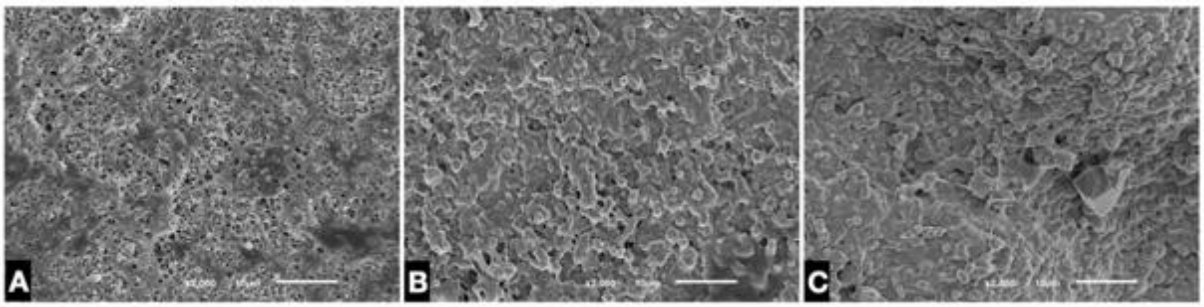

Fig. 8. SEM images of the outside of the wear track (2000x magnification). (A) ZLA. (B) RD. (C) L16N8. Fibrin can be seen covering the surface of zirconia samples.

Coefficient of friction

The evolution of the coefficient of friction (COF) recorded for gritblasted/etched or laser-textured zirconia-based specimens against bone in a 0.9% NaCl solution is shown in Figures 9, 10, and 11.

Initial COF values on zirconia free of PRF (control group) ranged from 0.42 to 0.90 and on zirconia coated with flowable PRF (test groups) ranged from 0.53 to 0.94. Regarding the COF evolution for the ZLA surfaces free of i-PRF, an initial running down period took place and was followed by a progressive increase in the COF values (Fig 9). On the COF evolution for the L16N8 surfaces free of i-PRF, different plots were noted although a relative steady-state regime with some oscillations in COF was representative for all specimens.

Mean values of COF for ZLA and L16N8 coated with flowable PRF were lower (ZLA=0.35; L16N8=0.45) when compared to ZLA and L16N8 surfaces free of flowable PRF (ZLA=0.52; L16N8=0.60), although not statistically significant (ZLA: $p = 0.21$; L16N8: $p = 0.85$) (Fig. 12). A decrease in the COF values suggest a lubricant effect of the flowable platelet-rich fibrin. On L16N8 zirconia surfaces, a significant decrease in COF values from around 0.6 down to 0.4 validate the lubricant effect of the injectable PRF coating. Also, oscillations in the COF evolution showed low values at around 0.1 and 0.2 (Fig. 9B) that indicate an ultra-low friction on some zirconia spots due to the fibrin network coating effect. The lubricating effect of PRF was maintained over test durations (Fig. 9,10,11), probably because fibrin covered the zirconia providing a smoother surface, as seen by SEM (Fig. 7 and 8). Also, fibrin itself and the debris resulting from test materials can lead to third viscous-elastic body effect and may have contributed to the small COF oscillations [41-43]. Retention of PRF occurred due to high strength and elasticity of fibrin fibers, thus resisting to the reciprocating sliding movement on friction. Thus, the use of flowable PRF may bring benefits, by decreasing the implant surface degradation by wear against bone. As a result, less particles from the implant surfaces are

released to the peri-implant tissues. This could be especially important in patients where healing is affected such as the ones with severe periodontal disease [8], irradiated patients [9], and individuals receiving bisphosphonates [10]. In these patients, the success rate is significantly lower.

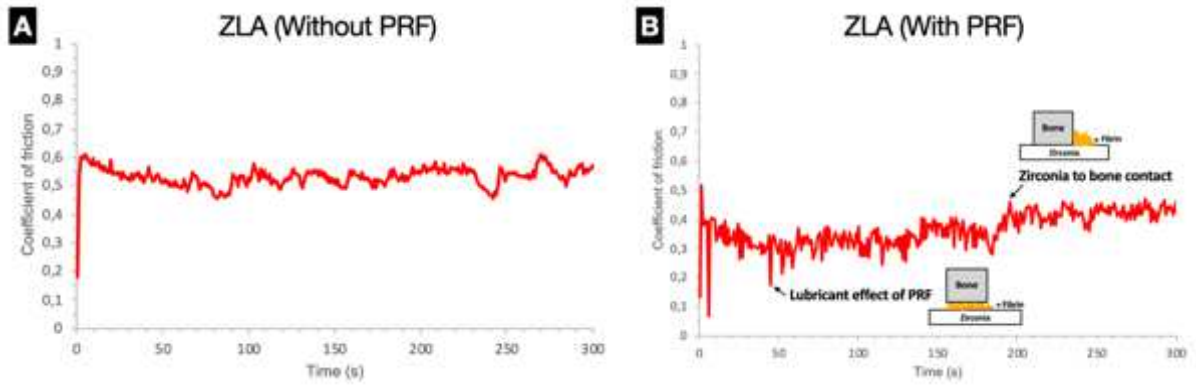

Fig. 9. Evolution of the coefficient of friction (COF) with time for ZLA surfaces coated or not with i-PRF against bone in 0.9% sodium chloride solution (F_N = 1 N, stroke length 2 mm, 1 Hz, 300 s of sliding).

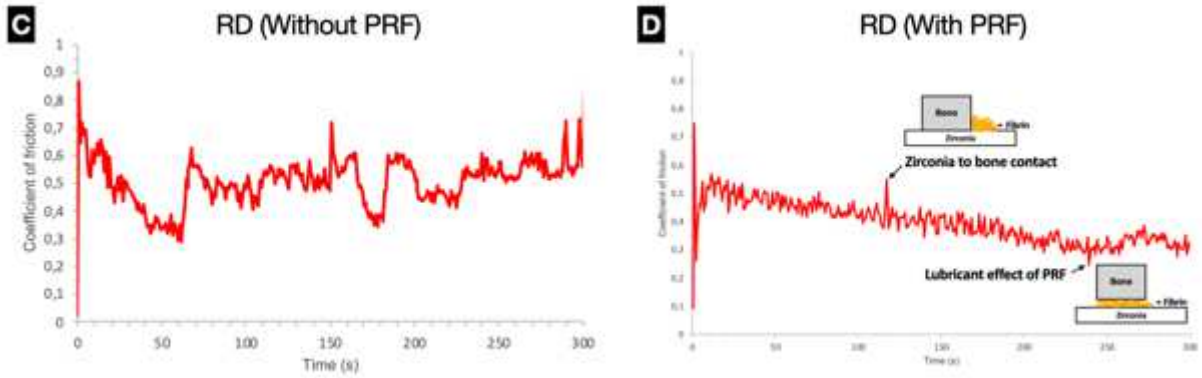

Fig. 10. Evolution of the coefficient of friction (COF) with time for RD surfaces coated or not with i-PRF against bone in 0.9% sodium chloride solution (F_N = 1 N, stroke length 2 mm, 1 Hz, 300 s of sliding).

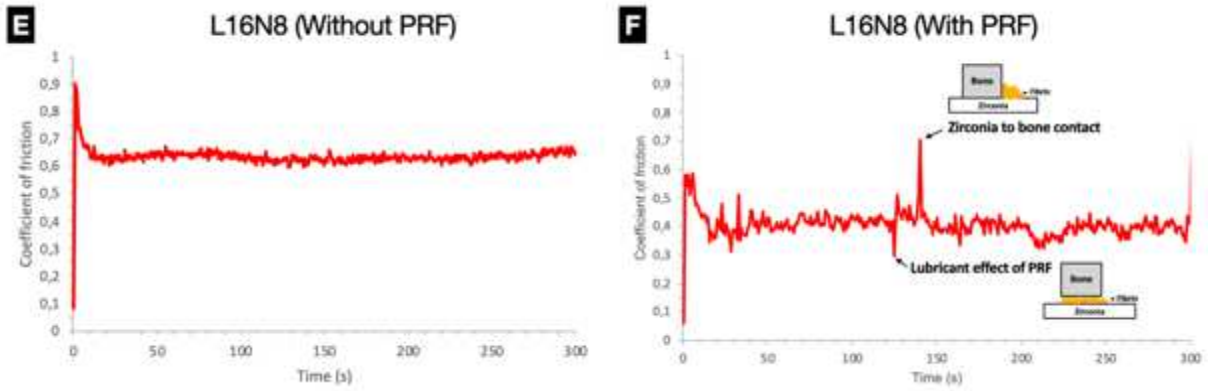

Fig. 11. Evolution of the coefficient of friction (COF) with time for L16N8 surfaces coated or not with i-PRF against bone in 0.9% sodium chloride solution (F_N = 1 N, stroke length 2 mm, 1 Hz, 300 s of sliding).

On the randomly laser-textured zirconia surfaces (RD group), the evolution of COF was not linear on the surfaces free of PRF (Figure 10A) and the COF mean values ranged from 0.3 up to 0.7 at a few spots. The mean COF value for the RD surfaces free of flowable PRF coating was lower (0.43) than those recorded for RD surfaces coated with flowable PRF (0.47) (p = 0.56) (Fig. 12).

There were differences in the reciprocating sliding wear behavior between the test groups, but not significant (p = 0.82). The lowest mean values of COF were recorded for the surfaces coated with flowable PRF that ranged from 0.35 up to 0.47. An extensive running down period characterized by a progressive decrease in the COF values up to 300 s. Similar mean values of COF for zirconia surfaces free of flowable PRF were quite similar to those values reported in previous studies [36,42,43].

The formation of discontinuous bone layers over the laser-textured surfaces can also explain the highest values of COF recorded in the reciprocating sliding wear tests. Laser-textured zirconia surface with a well-designed pattern (ie., L16N8) could be a good choice for increasing friction between implant and bone as well as retaining the flowable PRF layer in the micro-scale regions at the valleys on the surface profile. In this study, SEM images and COF values obtained for laser-textured surfaces showed that these surfaces retain more fibrin on its surface

and from a clinical point of view this could play a role in primary stability during immediate implant placement [26,27,44]. Also, textured surfaces maintained their mechanical integrity after friction tests. By combining the suitable laser parameters, the primary stability of the dental implants can be improved and consequently speeding up the osseointegration early stage. A favorable bone-to-implant contact (BIC) is essential to prevent implant micro-mobility and for maximizing the implant survival rate [45]. An improvement of the osseointegration process decreases the risk of early failures concerning the variation in loading and microbiota in the oral cavity.

Andrade et al. evaluated the interaction of different implant surfaces with a flowable L-PRF product and found some implant surfaces to be more suitable for a biomimetic functionalization with platelet concentrates [34].

In our study, the interaction time of PRF over the zirconia surfaces differed between specimens. However, time did not show to have a significant influence on COF values within groups. In previous studies, different times for fibrin cross-linking were assessed. A previous study reported the interaction between implant surfaces and flowable PRF for 10 minutes [33], while another study reported such interaction for 60 minutes [34].

In a recent study, macro-scale texturization of zirconia surfaces by using Nd:YAG laser did not show a higher percentage of osteoblast viability and differentiation when compared to grit-blasted/etched surfaces [46]. Another study reported an improvement on osteoblast proliferation and mineralization after application of i-PRF on machined commercially pure titanium [21]. Traini et al. found significantly lower blood clot extension on grit-blasted/etched zirconia surfaces when compared to titanium surfaces modified by grit-blasting and etching procedures [47]. Although 5-year clinical data exist for different zirconia implants, no analysis has yet been performed focusing on how the surface topography of the implant affects clinical parameters [15]. Studies evaluating the COF of yttria-stabilized zirconia for prosthetic [48-50]

and dental implant purposes can be found in literature [36,41-43]. However, no studies regarding the application of PRF on zirconia surfaces could be found in the literature. The present study is the first evaluating the behavior of a flowable PRF on laser-textured zirconia surfaces for dental implants. Further studies on novel surfaces could provide new data to be used for clinical purposes.

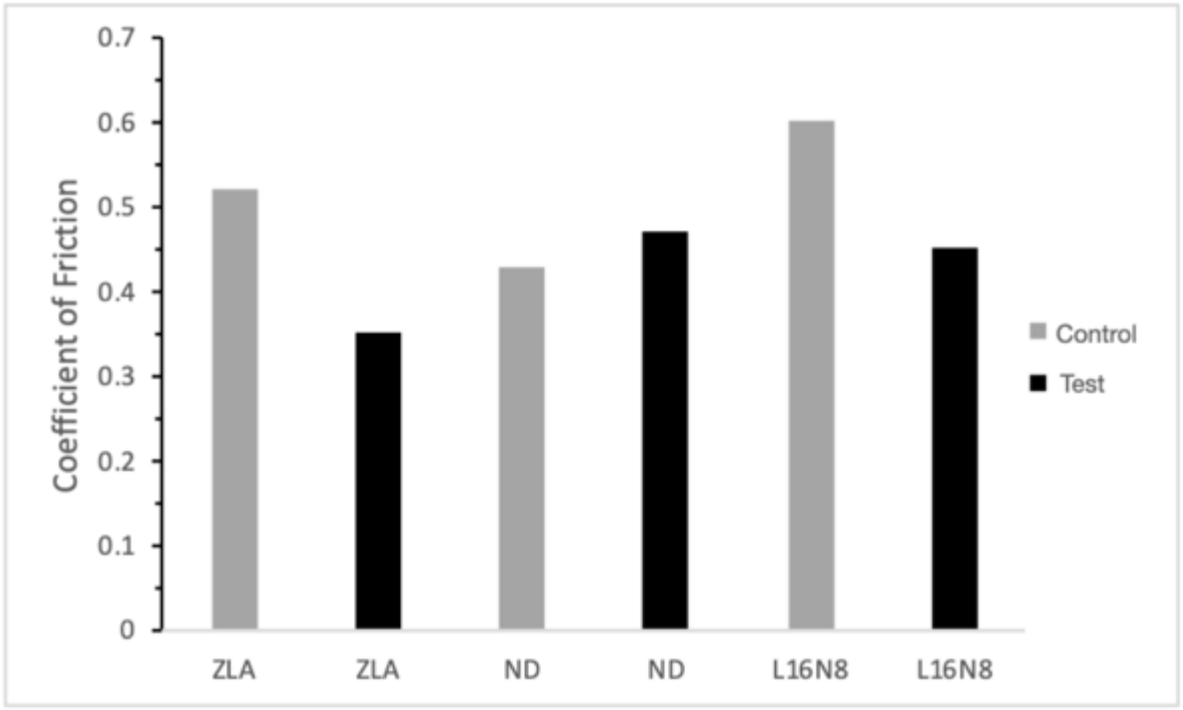

Figure 12. Mean values of the coefficient of friction (COF) for each subgroup.

CONCLUSIONS

Within the limitations of this *in vitro* study, the following conclusions can be drawn:

- Laser-textured zirconia surfaces revealed a higher number of regions covered by a dense fibrin network layer including platelets and leukocytes when compared to zirconia surfaces modified by grit-blasting and etching procedures. The morphological aspects and roughness increased the retention of the flowable platelet-rich fibrin;

- A decrease in the friction between zirconia surfaces and bone tissue was achieved when the zirconia surfaces were coated with flowable platelet-rich fibrin layer. Such COF was lower for ZLA and L16N8 groups after flowable PRF was applied.
- Similar COF values were observed for RD group with and without PRF.
- Fibrin may have played a lubricant role and reduce the friction between the zirconia and bone surfaces.
- The time of usage after obtaining PRF does not seem to have an influence on the fibrin adhesion to zirconia surfaces.
- Further studies are necessary to explore the clinical impact of these observations.

GENERAL CONCLUSIONS

Literature reported potential synergistic effects when mixing PRF and bone graft materials in smaller bone defects, while there is no consensus for larger defects. However, by using the PRF improved handling, bioactivity, and fitting of particulate graft materials in surgical sites can be achieved. The microscopic analysis performed showed a dense fibrin network covering the whole surface of bone substitute particles and connecting different particles. The fibrin bundles contained clusters of platelets, red blood cells, and some leukocytes which seemed to keep the block components assembled. Flowable PRF can also be applied over implant surfaces for biomimetic functionalization. Tribological tests were performed on zirconia surfaces with different textures. Laser-textured zirconia surfaces revealed a higher number of regions covered by a dense fibrin network layer including platelets and leukocytes when compared to zirconia surfaces modified by grit-blasting and etching procedures. Fibrin may have played a lubricant role and reduce the friction between the zirconia and bone surfaces. Further studies comparing the effectiveness of different materials to be mixed with PRF and evaluate the healing in the long term after using the bioactive composite block are necessary. Also, functionalization with PRF of other implant surfaces with a bigger volunteer sample should be studied.

BIBLIOGRAPHY

CHAPTER I

1. Urban IA, Nagursky H, Lozada JL (2011) Horizontal ridge augmentation with a resorbable membrane and particulated autogenous bone with or without anorganic bovine bone-derived mineral: a prospective case series in 22 patients. Int J Oral Maxillofac Implants 26:404–414.
2. Hannink G, Arts JJC (2011) Bioresorbability, porosity and mechanical strength of bone substitutes: what is optimal for bone regeneration? Injury 42 Suppl 2:S22-5. https://doi.org/10.1016/j.injury.2011.06.008
3. Pradeep AR, Bajaj P, Rao NS, et al (2017) Platelet-Rich Fibrin Combined With a Porous Hydroxyapatite Graft for the Treatment of 3-Wall Intrabony Defects in Chronic Periodontitis: A Randomized Controlled Clinical Trial. J Periodontol 88:1288–1296. https://doi.org/10.1902/jop.2012.110722
4. Degidi M, Perrotti V, Piattelli A, Iezzi G (2013) Eight-year results of site retention of anorganic bovine bone and anorganic bovine matrix. J Oral Implantol 39:727–732. https://doi.org/10.1563/AAID-JOI-D-11-00091
5. Comert Kilic S, Gungormus M, Parlak SN (2017) Histologic and histomorphometric assessment of sinus-floor augmentation with beta-tricalcium phosphate alone or in combination with pure-platelet-rich plasma or platelet-rich fibrin: A randomized clinical trial. Clin Implant Dent Relat Res 19:959–967. https://doi.org/10.1111/cid.12522
6. Liu R, Yan M, Chen S, et al (2019) Effectiveness of Platelet-Rich Fibrin as an Adjunctive Material to Bone Graft in Maxillary Sinus Augmentation: A Meta-Analysis of Randomized Controlled Trails. Biomed Res Int 2019:7267062. https://doi.org/10.1155/2019/7267062
7. Kirchhoff M, Bienengräber V, Lenz S, Gerber T, Henkel KO. A new synthetic bone replacement material with osteoinductive properties–in vivo investigations. BIOmaterialien. 2006;7:78–96.
8. Best SM, Porter AE, Thian ES, Huang J. Bioceramics: Past, present and for the future. J Eur Ceram Soc. 2008;28:1319–27.
9. Noronha Oliveira M, Schunemann WVH, Mathew MT, et al (2018) Can degradation products released from dental implants affect peri-implant tissues? J Periodontal Res 53:. https://doi.org/10.1111/jre.12479
10. Marx RE, Carlson ER, Eichstaedt RM, Schimmele SR, Strauss JE, Georgeff KR. Platelet- rich plasma: growth factor enhancement for bone grafts. Oral Surg, Oral Med, Oral Pathol, Oral Radiol Endod. 1998;85:638–646.
11. Eppley BL, Pietrzak WS, Blanton M. Platelet-rich plasma: a review of biology and applications in plastic surgery. Plast Reconstr Surg 2006;118(6):147e–59e. https://doi. org/10.1097/01.prs.0000239606.92676.cf.
12. Carter MJ, Fylling CP, Parnell LKS. Use of platelet rich plasma gel on wound heal- ing: a systematic review and meta-analysis. Eplasty 2011;11:e38. papers3://publication/ uuid/1EA2CFAD-571B-40C9-AE35-5A7D3DE3C6B0.
13. Choukroun J, Adda F, Schoeffler C, Vervelle A. Une opportunité en paro-implantologie: Le PRF. Implantodon-tie. 2001;42:55-62.
14. Dohan DM, Choukroun J, Diss A, et al (2006) Platelet-rich fibrin (PRF): A second-generation platelet concentrate. Part I: Technological concepts and evolution. Oral

Surgery, Oral Med Oral Pathol Oral Radiol Endodontology 101:. https://doi.org/10.1016/j.tripleo.2005.07.008.
15. Yoon J-S, Lee S-H, Yoon H-J (2014) The influence of platelet-rich fibrin on angiogenesis in guided bone regeneration using xenogenic bone substitutes: a study of rabbit cranial defects. J Craniomaxillofac Surg 42:1071–1077. https://doi.org/10.1016/j.jcms.2014.01.034
16. Schär MO, Diaz-Romero J, Kohl S, et al (2015) Platelet-rich concentrates differentially release growth factors and induce cell migration in vitro. Clin Orthop Relat Res 473:1635–1643. https://doi.org/10.1007/s11999-015-4192-2
17. Pinto NR, Ubilla M, Zamora Y, et al (2018) Leucocyte- and platelet-rich fibrin (L-PRF) as a regenerative medicine strategy for the treatment of refractory leg ulcers: a prospective cohort study. Platelets 29:468–475. https://doi.org/10.1080/09537104.2017.1327654
18. Castro AB, Meschi N, Temmerman A, Pinto N, Lambrechts P, Teughels W, Quirynen M. Regenerative potential of leucocyte- and platelet-rich fibrin. Part B: sinus floor elevation, alveolar ridge preservation and implant therapy. A systematic review. J Clin Periodontol. 2017;44:225–34.
19. Nacopoulos C, Gkouskou K, Karypidis D, et al. Telomere length and genetic variations affecting telomere length as biomarkers for facial regeneration with platelet-rich fibrin based on the low-speed centrifugation concept. J Cosmet Dermatol. 2019;18(1):408-413.
20. Mosesson MW, Siebenlist KR, Meh DA. The Structure and Biological Features of Fibrinogen and Fibrin. Ann N Y Acad Sci. 2006;936:11–30.
21. Guthold M, Liu W, Sparks EA, Jawerth LM, Peng L, Falvo M, Superfine R, Hantgan RR, Lord ST. A comparison of the mechanical and structural properties of fibrin fibers with other protein fibers. Cell Biochem Biophys. 2007.
22. Dohan Ehrenfest DM, Del Corso M, Diss A, et al (2010) Three-Dimensional Architecture and Cell Composition of a Choukroun's Platelet-Rich Fibrin Clot and Membrane. J Periodontol 81:546–555. https://doi.org/10.1902/jop.2009.090531
23. Dohan Ehrenfest DM, Pinto NR, Pereda A, et al (2018) The impact of the centrifuge characteristics and centrifugation protocols on the cells, growth factors, and fibrin architecture of a leukocyte- and platelet-rich fibrin (L-PRF) clot and membrane. Platelets 29:171–184. https://doi.org/10.1080/09537104.2017.1293812
24. Choukroun J (2014) Advanced PRF, &i-PRF: platelet concentrates or blood concentrates. J Periodont Med Clin Pract 1:3
25. Miron RJ, Fujioka-Kobayashi M, Hernandez M, et al (2017) Injectable platelet rich fibrin (i-PRF): opportunities in regenerative dentistry? Clin. Oral Investig. 1–9
26. Varela HA, Souza JCM, Nascimento RM, et al (2019) Injectable platelet rich fibrin: cell content, morphological, and protein characterization. Clin Oral Investig 23:1309–1318. https://doi.org/10.1007/s00784-018-2555-2
27. Castro A, Cortellini S, Temmerman A, et al (2019) Characterization of the Leukocyte- and Platelet-Rich Fibrin Block: Release of Growth Factors, Cellular Content, and Structure. Int J Oral Maxillofac Implants. https://doi.org/10.11607/jomi.7275
28. Cortellini S, Castro AB, Temmerman A, et al (2018) Leucocyte- and platelet-rich fibrin block for bone augmentation procedure: A proof-of-concept study. J Clin Periodontol 45:624–634. https://doi.org/10.1111/jcpe.12877
29. Mir-Mari J, Wui H, Jung RE, Hammerle CHF, Benic GI. Influence of blinded wound closure on the volume stability of different GBR materials: an in vitro cone-beam computed tomographic examination. Clin Oral Implants Res. Denmark; 2016;27:258–65.

30. Tanaka H, Toyoshima T, Atsuta I, et al (2015) Additional Effects of Platelet-Rich Fibrin on Bone Regeneration in Sinus Augmentation With Deproteinized Bovine Bone Mineral: Preliminary Results. Implant Dent 24:669–674. https://doi.org/10.1097/ID.0000000000000306
31. Nizam N, Eren G, Akcali A, Donos N (2018) Maxillary sinus augmentation with leukocyte and platelet-rich fibrin and deproteinized bovine bone mineral: A split-mouth histological and histomorphometric study. Clin Oral Implants Res 29:67–75. https://doi.org/10.1111/clr.13044
32. Pichotano EC, de Molon RS, de Souza RV, et al (2019) Evaluation of L-PRF combined with deproteinized bovine bone mineral for early implant placement after maxillary sinus augmentation: A randomized clinical trial. Clin Implant Dent Relat Res 21:253–262. https://doi.org/10.1111/cid.12713
33. M. Lollobrigida, M. Maritato, G. Bozzuto, G. Formisano, A. Molinari, A. De Biase, Biomimetic Implant Surface Functionalization with Liquid L-PRF Products: In Vitro Study, Biomed Res Int, 2018. doi: 10.1155/2018/9031435.
34. C. Andrade, J. Camino, M. Nally, M. Quirynen, B. Martínez, N. Pinto, Combining autologous particulate dentin, L-PRF, and fibrinogen to create a matrix for predictable ridge preservation: a pilot clinical study, Clinical Oral Investigations, 24 (2020) 1151–1160.
35. J. E. Davies, Understanding peri-implant endosseous healing, Journal of Dental Education. 67 (2003) 932–949.
36. C. C. Villar, G. Huynh-Ba, M. P. Mills, D. L. Cochran, Wound healing around dental implants, Endodontic Topics, 25 (2011) 44–62.
37. J.W. Weisel, R.I. Litvinov, Mechanisms of fibrin polymerization and clinical implications, Blood, 121 (2013) 1712–1719. https://doi.org/10.1182/blood-2012-09-306639
38. M. Ting, S. R. Jefferies, W. Xia, H. Engqvist, J. B. Suzuki, Classification and effects of implant surface modification on the bone: human cell–based in vitro studies, The Journal of Oral Implantology, 43 (2017) 58–83.
39. X. Wang, Y. Zhang, J. Choukroun, S. Ghanaati, R.J. Miron, Behavior of Gingival Fibroblasts on Titanium Implant Surfaces in Combination with either Injectable-PRF or PRP, Int J Mol Sci, 18 (2017) 331.
40. F.J. Strauss, A. Stähli, R. Gruber, The use of platelet-rich fibrin to enhance the outcomes of implant therapy: A systematic review, Clin Oral Implants Res, 29 (2018) 6-19. doi: 10.1111/clr.13275.

CHAPTER II

1. Dahlin C, Obrecht M, Dard M, Donos N (2015) Bone tissue modelling and remodelling following guided bone regeneration in combination with biphasic calcium phosphate materials presenting different microporosity. Clin Oral Implants Res 26:814–822. https://doi.org/10.1111/clr.12361
2. Streckbein P, Kleis W, Buch RSR, et al (2014) Bone healing with or without platelet-rich plasma around four different dental implant surfaces in beagle dogs. Clin Implant Dent Relat Res 16:479–486. https://doi.org/10.1111/cid.12026
3. Lee J, Hurson S, Tadros H, et al (2012) Crestal remodelling and osseointegration at surface-modified commercially pure titanium and titanium alloy implants in a canine model. J Clin Periodontol 39:781–788. https://doi.org/10.1111/j.1600-051X.2012.01905.x
4. Barone A, Toti P, Quaranta A, et al (2016) Volumetric analysis of remodelling pattern after ridge preservation comparing use of two types of xenografts. A multicentre randomized clinical trial. Clin Oral Implants Res 27:e105–e115. https://doi.org/10.1111/clr.12572
5. Kämmerer PW, Schiegnitz E, Palarie V, et al (2017) Influence of platelet-derived growth factor on osseous remodeling properties of a variable-thread tapered dental implant in vivo. Clin Oral Implants Res 28:201–206. https://doi.org/10.1111/clr.12782
6. Urban IA, Nagursky H, Lozada JL (2011) Horizontal ridge augmentation with a resorbable membrane and particulated autogenous bone with or without anorganic bovine bone-derived mineral: a prospective case series in 22 patients. Int J Oral Maxillofac Implants 26:404–414
7. Hannink G, Arts JJC (2011) Bioresorbability, porosity and mechanical strength of bone substitutes: what is optimal for bone regeneration? Injury 42 Suppl 2:S22-5. https://doi.org/10.1016/j.injury.2011.06.008
8. Pradeep AR, Bajaj P, Rao NS, et al (2017) Platelet-Rich Fibrin Combined With a Porous Hydroxyapatite Graft for the Treatment of 3-Wall Intrabony Defects in Chronic Periodontitis: A Randomized Controlled Clinical Trial. J Periodontol 88:1288–1296. https://doi.org/10.1902/jop.2012.110722
9. Liu R, Yan M, Chen S, et al (2019) Effectiveness of Platelet-Rich Fibrin as an Adjunctive Material to Bone Graft in Maxillary Sinus Augmentation: A Meta-Analysis of Randomized Controlled Trails. Biomed Res Int 2019:7267062. https://doi.org/10.1155/2019/7267062
10. Degidi M, Perrotti V, Piattelli A, Iezzi G (2013) Eight-year results of site retention of anorganic bovine bone and anorganic bovine matrix. J Oral Implantol 39:727–732. https://doi.org/10.1563/AAID-JOI-D-11-00091
11. Comert Kilic S, Gungormus M, Parlak SN (2017) Histologic and histomorphometric assessment of sinus-floor augmentation with beta-tricalcium phosphate alone or in combination with pure-platelet-rich plasma or platelet-rich fibrin: A randomized clinical trial. Clin Implant Dent Relat Res 19:959–967. https://doi.org/10.1111/cid.12522
12. Schwarz F, Mihatovic I, Golubovic V, et al (2012) Influence of two barrier membranes on staged guided bone regeneration and osseointegration of titanium implants in dogs: part 1. Augmentation using bone graft substitutes and autogenous bone. Clin Oral Implants Res 23:83–89. https://doi.org/10.1111/j.1600-0501.2011.02238.x
13. Mendoza-Azpur G, de la Fuente A, Chavez E, et al (2019) Horizontal ridge augmentation with guided bone regeneration using particulate xenogenic bone

substitutes with or without autogenous block grafts: A randomized controlled trial. Clin Implant Dent Relat Res. https://doi.org/10.1111/cid.12740
14. Mathur A, Bains VK, Gupta V, et al (2015) Evaluation of intrabony defects treated with platelet-rich fibrin or autogenous bone graft: A comparative analysis. Eur J Dent 9:100–108. https://doi.org/10.4103/1305-7456.149653
15. Shawky H, Seifeldin SA (2016) Does Platelet-Rich Fibrin Enhance Bone Quality and Quantity of Alveolar Cleft Reconstruction? Cleft palate-craniofacial J Off Publ Am Cleft Palate-Craniofacial Assoc 53:597–606. https://doi.org/10.1597/14-290
16. Nizam N, Eren G, Akcali A, Donos N (2018) Maxillary sinus augmentation with leukocyte and platelet-rich fibrin and deproteinized bovine bone mineral: A split-mouth histological and histomorphometric study. Clin Oral Implants Res 29:67–75. https://doi.org/10.1111/clr.13044
17. Pichotano EC, de Molon RS, de Souza RV, et al (2019) Evaluation of L-PRF combined with deproteinized bovine bone mineral for early implant placement after maxillary sinus augmentation: A randomized clinical trial. Clin Implant Dent Relat Res 21:253–262. https://doi.org/10.1111/cid.12713
18. Tanaka H, Toyoshima T, Atsuta I, et al (2015) Additional Effects of Platelet-Rich Fibrin on Bone Regeneration in Sinus Augmentation With Deproteinized Bovine Bone Mineral: Preliminary Results. Implant Dent 24:669–674. https://doi.org/10.1097/ID.0000000000000306
19. Broggini N, Bosshardt DD, Jensen SS, et al (2015) Bone healing around nanocrystalline hydroxyapatite, deproteinized bovine bone mineral, biphasic calcium phosphate, and autogenous bone in mandibular bone defects. J Biomed Mater Res B Appl Biomater 103:1478–1487. https://doi.org/10.1002/jbm.b.33319
20. Hamzacebi B, Oduncuoglu B, Alaaddinoglu EE (2015) Treatment of Peri-implant Bone Defects with Platelet-Rich Fibrin. Int J Periodontics Restorative Dent 35:415–422
21. Pinto NR, Ubilla M, Zamora Y, et al (2018) Leucocyte- and platelet-rich fibrin (L-PRF) as a regenerative medicine strategy for the treatment of refractory leg ulcers: a prospective cohort study. Platelets 29:468–475. https://doi.org/10.1080/09537104.2017.1327654
22. Dohan DM, Choukroun J, Diss A, et al (2006) Platelet-rich fibrin (PRF): A second-generation platelet concentrate. Part I: Technological concepts and evolution. Oral Surgery, Oral Med Oral Pathol Oral Radiol Endodontology 101:. https://doi.org/10.1016/j.tripleo.2005.07.008
23. Dohan DM, Choukroun J, Diss A, et al (2006) Platelet-rich fibrin (PRF): A second-generation platelet concentrate. Part III: Leucocyte activation: A new feature for platelet concentrates? Oral Surgery, Oral Med Oral Pathol Oral Radiol Endodontology 101:. https://doi.org/10.1016/j.tripleo.2005.07.010
24. Choukroun J, Diss A, Simonpieri A, et al (2006) Platelet-rich fibrin (PRF): A second-generation platelet concentrate. Part IV: Clinical effects on tissue healing. Oral Surgery, Oral Med Oral Pathol Oral Radiol Endodontology 101:. https://doi.org/10.1016/j.tripleo.2005.07.011
25. Castro A, Cortellini S, Temmerman A, et al (2019) Characterization of the Leukocyte- and Platelet-Rich Fibrin Block: Release of Growth Factors, Cellular Content, and Structure. Int J Oral Maxillofac Implants. https://doi.org/10.11607/jomi.7275
26. Kawase T, Kamiya M, Kobayashi M, et al (2015) The heat-compression technique for the conversion of platelet-rich fibrin preparation to a barrier membrane with a reduced rate of biodegradation. J Biomed Mater Res - Part B Appl Biomater 103:825–831. https://doi.org/10.1002/jbm.b.33262

27. Dohan DM, Choukroun J, Diss A, et al (2006) Platelet-rich fibrin (PRF): a second-generation platelet concentrate. Part II: platelet-related biologic features. Oral Surgery, Oral Med Oral Pathol Oral Radiol Endodontology 101:e45–e50
28. Schär MO, Diaz-Romero J, Kohl S, et al (2015) Platelet-rich concentrates differentially release growth factors and induce cell migration in vitro. Clin Orthop Relat Res 473:1635–1643. https://doi.org/10.1007/s11999-015-4192-2
29. Yoon J-S, Lee S-H, Yoon H-J (2014) The influence of platelet-rich fibrin on angiogenesis in guided bone regeneration using xenogenic bone substitutes: a study of rabbit cranial defects. J Craniomaxillofac Surg 42:1071–1077. https://doi.org/10.1016/j.jcms.2014.01.034
30. Dohan Ehrenfest DM, Pinto NR, Pereda A, et al (2018) The impact of the centrifuge characteristics and centrifugation protocols on the cells, growth factors, and fibrin architecture of a leukocyte- and platelet-rich fibrin (L-PRF) clot and membrane. Platelets 29:171–184. https://doi.org/10.1080/09537104.2017.1293812
31. Varela HA, Souza JCM, Nascimento RM, et al (2019) Injectable platelet rich fibrin: cell content, morphological, and protein characterization. Clin Oral Investig 23:1309–1318. https://doi.org/10.1007/s00784-018-2555-2
32. Dohan Ehrenfest DM, Del Corso M, Diss A, et al (2010) Three-Dimensional Architecture and Cell Composition of a Choukroun's Platelet-Rich Fibrin Clot and Membrane. J Periodontol 81:546–555. https://doi.org/10.1902/jop.2009.090531
33. Pichotano EC, de Molon RS, Freitas de Paula LG, et al (2018) Early Placement of Dental Implants in Maxillary Sinus Grafted With Leukocyte and Platelet-Rich Fibrin and Deproteinized Bovine Bone Mineral. J Oral Implantol 44:199–206. https://doi.org/10.1563/aaid-joi-D-17-00220
34. Cortellini S, Castro AB, Temmerman A, et al (2018) Leucocyte- and platelet-rich fibrin block for bone augmentation procedure: A proof-of-concept study. J Clin Periodontol 45:624–634. https://doi.org/10.1111/jcpe.12877
35. Merli M, Moscatelli M, Mariotti G, et al (2015) Membranes and Bone Substitutes in a One-Stage Procedure for Horizontal Bone Augmentation: A Histologic Double-Blind Parallel Randomized Controlled Trial. Int J Periodontics Restorative Dent 35:463–471. https://doi.org/10.11607/prd.2418
36. Simion M, Rocchietta I, Dellavia C (2007) Three-dimensional ridge augmentation with xenograft and recombinant human platelet-derived growth factor-BB in humans: report of two cases. Int J Periodontics Restorative Dent 27:109–115
37. Block MS, Kelley B (2013) Horizontal posterior ridge augmentation: the use of a collagen membrane over a bovine particulate graft: technique note. J Oral Maxillofac Surg 71:1513–1519. https://doi.org/10.1016/j.joms.2013.05.015
38. Mahesh L, Salama MA, Kurtzman GM, Joachim FPC (2012) Socket grafting with calcium phosphosilicate alloplast putty: a histomorphometric evaluation. Compend Contin Educ Dent 33:e109-15
39. Alayan J, Vaquette C, Saifzadeh S, et al (2017) Comparison of early osseointegration of SLA®and SLActive®implants in maxillary sinus augmentation: a pilot study. Clin Oral Implants Res. https://doi.org/10.1111/clr.12988
40. De Santis E, Lang NP, Cesaretti G, et al (2013) Healing outcomes at implants installed in sites augmented with particulate autologous bone and xenografts. An experimental study in dogs. Clin Oral Implants Res 24:77–86. https://doi.org/10.1111/j.1600-0501.2012.02456.x
41. Schwarz F, Sahm N, Mihatovic I, et al (2011) Surgical therapy of advanced ligature-induced peri-implantitis defects: Cone-beam computed tomographic and histological

analysis. J Clin Periodontol 38:939–949. https://doi.org/10.1111/j.1600-051X.2011.01739.x
42. Kumarswamy A, Moretti A, Paquette D, et al (2012) In vivo assessment of osseous wound healing using a novel bone putty containing lidocaine in the surgical management of tooth extractions. Int J Dent 2012:894815. https://doi.org/10.1155/2012/894815
43. Miron RJ, Fujioka-Kobayashi M, Hernandez M, et al (2017) Injectable platelet rich fibrin (i-PRF): opportunities in regenerative dentistry? Clin. Oral Investig. 1–9
44. Chenchev IL, Ivanova V V, Neychev DZ, Cholakova RB (2017) Application of Platelet-Rich Fibrin and Injectable Platelet-Rich Fibrin in Combination of Bone Substitute Material for Alveolar Ridge Augmentation - a Case Report. Folia Med. (Plovdiv). 59:362–366
45. Choukroun J (2014) Advanced PRF, &i-PRF: platelet concentrates or blood concentrates. J Periodont Med Clin Pract 1:3
46. Scarano A, Inchingolo F, Murmura G, et al (2018) Three-dimensional architecture and mechanical properties of bovine bone mixed with autologous platelet liquid, blood, or physiological water: An in vitro study. Int J Mol Sci. https://doi.org/10.3390/ijms19041230
47. Souza JCM, Sordi MB, Kanazawa M, et al (2019) Nano-scale modification of titanium implant surfaces to enhance osseointegration. Acta Biomater. 94:112–131
48. Rodrigues YL, Mathew MT, Mercuri LG, et al (2018) Biomechanical simulation of temporomandibular joint replacement (TMJR) devices: a scoping review of the finite element method. Churchill Livingstone
49. Noronha Oliveira M, Schunemann WVH, Mathew MT, et al (2018) Can degradation products released from dental implants affect peri-implant tissues? J Periodontal Res 53:. https://doi.org/10.1111/jre.12479

CHAPTER III

1. Broggini N, Bosshardt DD, Jensen SS, Bornstein MM, Wang C-C, Buser D. Bone healing around nanocrystalline hydroxyapatite, deproteinized bovine bone mineral, biphasic calcium phosphate, and autogenous bone in mandibular bone defects. J Biomed Mater Res B Appl Biomater. 2015;103:1478–87.
2. Jung RE, Philipp A, Annen BM, Signorelli L, Thoma DS, Hämmerle CHF, Attin T, Schmidlin P. Radiographic evaluation of different techniques for ridge preservation after tooth extraction: a randomized controlled clinical trial. J Clin Periodontol. 2013;40:90–8.
3. Araujo MG, da Silva JCC, de Mendonca AF, Lindhe J. Ridge alterations following grafting of fresh extraction sockets in man. A randomized clinical trial. Clin Oral Implants Res. Denmark; 2015;26:407–12.
4. Kirchhoff M, Bienengräber V, Lenz S, Gerber T, Henkel KO. A new synthetic bone replacement material with osteoinductive properties–in vivo investigations. BIOmaterialien. 2006;7:78–96.
5. Best SM, Porter AE, Thian ES, Huang J. Bioceramics: Past, present and for the future. J Eur Ceram Soc. 2008;28:1319–27.
6. Oliveira MN, Rau LH, Marodin A, Corrêa M, Corrêa LR, Aragones A, De Souza Magini R. Ridge preservation after maxillary third molar extraction using 30% porosity PLGA/HA/β-TCP scaffolds with and without simvastatin: A pilot randomized controlled clinical trial. Implant Dent. 2017;
7. Jensen SS, Broggini N, Hjørting-Hansen E, Schenk R, Buser D. Bone healing and graft resorption of autograft, anorganic bovine bone and beta-tricalcium phosphate. A histologic and histomorphometric study in the mandibles of minipigs. Clin Oral Implants Res. 2006;17:237–43.
8. Carvalho AL, Faria PEP, Grisi MFM, Souza SLS, Taba MJ, Palioto DB, Novaes ABJ, Fraga AF, Ozyegin LS, Oktar FN, Salata LA. Effects of granule size on the osteoconductivity of bovine and synthetic hydroxyapatite: a histologic and histometric study in dogs. J Oral Implantol. 2007;33:267–76.
9. Oonishi H, Hench LL, Wilson J, Sugihara F, Tsuji E, Kushitani S, Iwaki H. Comparative bone growth behavior in granules of bioceramic materials of various sizes. J Biomed Mater Res. 1999;44:31–43.
10. Dahlin C, Obrecht M, Dard M, Donos N. Bone tissue modelling and remodelling following guided bone regeneration in combination with biphasic calcium phosphate materials presenting different microporosity. Clin Oral Implants Res. 2015;26:814–22.
11. Castro AB, Meschi N, Temmerman A, Pinto N, Lambrechts P, Teughels W, Quirynen M. Regenerative potential of leucocyte- and platelet-rich fibrin. Part B: sinus floor elevation, alveolar ridge preservation and implant therapy. A systematic review. J Clin Periodontol. 2017;44:225–34.
12. Dohan DM, Choukroun J, Diss A, Dohan SL, Dohan AJJ, Mouhyi J, Gogly B. Platelet-rich fibrin (PRF): A second-generation platelet concentrate. Part I: Technological concepts and evolution. Oral Surgery, Oral Med Oral Pathol Oral Radiol Endodontology. 2006;101.
13. Dohan DM, Choukroun J, Diss A, Dohan SL, Dohan AJJ, Mouhyi J, Gogly B. Platelet-rich fibrin (PRF): a second-generation platelet concentrate. Part II: platelet-related biologic features. Oral Surgery, Oral Med Oral Pathol Oral Radiol Endodontology. Elsevier; 2006;101:e45–50.

14. Mosesson MW, Siebenlist KR, Meh DA. The Structure and Biological Features of Fibrinogen and Fibrin. Ann N Y Acad Sci. 2006;936:11–30.
15. Guthold M, Liu W, Sparks EA, Jawerth LM, Peng L, Falvo M, Superfine R, Hantgan RR, Lord ST. A comparison of the mechanical and structural properties of fibrin fibers with other protein fibers. Cell Biochem Biophys. 2007.
16. Choukroun J. Advanced PRF, &i-PRF: platelet concentrates or blood concentrates. J Periodont Med Clin Pract. 2014;1:3.
17. Miron RJ, Fujioka-Kobayashi M, Hernandez M, Kandalam U, Zhang Y, Ghanaati S, Choukroun J. Injectable platelet rich fibrin (i-PRF): opportunities in regenerative dentistry? Clin Oral Investig. 2017;
18. Varela HA, Souza JCM, Nascimento RM, Araújo RF, Vasconcelos RC, Cavalcante RS, Guedes PM, Araújo AA. Injectable platelet rich fibrin: cell content, morphological, and protein characterization. Clin Oral Investig. Springer Verlag; 2019;23:1309–18.
19. Cortellini S, Castro AB, Temmerman A, Van Dessel J, Pinto N, Jacobs R, Quirynen M. Leucocyte- and platelet-rich fibrin block for bone augmentation procedure: A proof-of-concept study. J Clin Periodontol. United States; 2018;45:624–34.
20. Mir-Mari J, Wui H, Jung RE, Hammerle CHF, Benic GI. Influence of blinded wound closure on the volume stability of different GBR materials: an in vitro cone-beam computed tomographic examination. Clin Oral Implants Res. Denmark; 2016;27:258–65.
21. Del Corso M, Dohan Ehrenfest DM. Immediate implantation and peri-implant Natural Bone Regeneration (NBR) in the severely resorbed posterior mandible using Leukocyte-and Platelet-Rich Fibrin (L-PRF): a 4-year follow-up. 2013;
22. Simonpieri A, Del Corso M, Sammartino G, Dohan Ehrenfest DM. The Relevance of Choukroun's Platelet-Rich Fibrin and Metronidazole During Complex Maxillary Rehabilitations Using Bone Allograft. Part II: Implant Surgery, Prosthodontics, and Survival. Implant Dent. 2009;18:220–9.
23. Scarano A, Inchingolo F, Murmura G, Traini T, Piattelli A, Lorusso F. Three-dimensional architecture and mechanical properties of bovine bone mixed with autologous platelet liquid, blood, or physiological water: An in vitro study. Int J Mol Sci. 2018;
24. Gouveia PF, Mesquita-Guimarães J, Galárraga-Vinueza ME, Souza JCM, Silva FS, Fredel MC, Boccaccini AR, Detsch R, Henriques B. In-vitro mechanical and biological evaluation of novel zirconia reinforced bioglass scaffolds for bone repair. J Mech Behav Biomed Mater. Netherlands; 2021;114:104164.
25. Mesquita-Guimarães J, Detsch R, Souza AC, Henriques B, Silva FS, Boccaccini AR, Carvalho O. Cell adhesion evaluation of laser-sintered HAp and 45S5 bioactive glass coatings on micro-textured zirconia surfaces using MC3T3-E1 osteoblast-like cells. Mater Sci Eng C [Internet]. 2020;109:110492.
26. Faria D, Madeira S, Buciumeanu M, Silva FS, Carvalho O. Novel laser textured surface designs for improved zirconia implants performance. Mater Sci Eng C Mater Biol Appl. 2020;108:110390.
27. Castro AB, Meschi N, Temmerman A, Pinto N, Lambrechts P, Teughels W, Quirynen M. Regenerative potential of leucocyte- and platelet-rich fibrin. Part A: intra-bony defects, furcation defects and periodontal plastic surgery. A systematic review and meta-analysis. J Clin Periodontol. 2017;44:67–82.
28. Castro A, Cortellini S, Temmerman A, Li X, Pinto N, Teughels W, Quirynen M. Characterization of the Leukocyte- and Platelet-Rich Fibrin Block: Release of Growth Factors, Cellular Content, and Structure. Int J Oral Maxillofac Implants. 2019;

29. Kubesch A, Barbeck M, Al-Maawi S, Orlowska A, Booms PF, Sader RA, Miron RJ, Kirkpatrick CJ, Choukroun J, Ghanaati S. A low-speed centrifugation concept leads to cell accumulation and vascularization of solid platelet-rich fibrin: an experimental study in vivo. Platelets. 2019;
30. Bai MY, Chuang MH, Lin MF, Tang SL, Wong CC, Chan WP. Relationships of Age and Sex with Cytokine Content and Distribution in Human Platelet Fibrin Gels. Sci Rep. 2018;
31. Mamajiwala AS, Sethi KS, Raut CP, Karde PA, Mangle NM. Impact of different platelet-rich fibrin (PRF) procurement methods on the platelet count, antimicrobial efficacy, and fibrin network pattern in different age groups: an in vitro study. Clin Oral Investig. 2019;
32. Liu W. Fibrin Fibers Have Extraordinary Extensibility and Elasticity. Science (80-). 2006;313:634–634.
33. Ricci JL, Blumenthal NC, Spivak JM, Alexander H. Evaluation of a low-temperature calcium phosphate particulate implant material: Physical-chemical properties and in vivo bone response. J Oral Maxillofac Surg. 1992;
34. Mordenfeld A, Hallman M, Johansson CB, Albrektsson T. Histological and histomorphometrical analyses of biopsies harvested 11 years after maxillary sinus floor augmentation with deproteinized bovine and autogenous bone. Clin Oral Implants Res. 2010;21:961–70.
35. Jensen SS, Bosshardt DD, Gruber R, Buser D. Long-term stability of contour augmentation in the esthetic zone: histologic and histomorphometric evaluation of 12 human biopsies 14 to 80 months after augmentation. J Periodontol. 2014;85:1549–56.
36. Artzi Z, Tal H, Dayan D. Porous bovine bone mineral in healing of human extraction sockets. Part 1: histomorphometric evaluations at 9 months. J Periodontol. 2000;71:1015–23.
37. Kuroda T. [Bone formation and mechanical properties of the cancellous bone defect site filled with hydroxyapatite granules]. Nihon Seikeigeka Gakkai Zasshi. 1995;69:1037–49.
38. Ruano R, Jaeger RG, Jaeger MMM. Effect of a Ceramic and a Non-Ceramic Hydroxyapatite on Cell Growth and Procollagen Synthesis of Cultured Human Gingival Fibroblasts. J Periodontol. 2000;
39. Schwarz F, Bieling K, Latz T, Nuesry E, Becker J. Healing of intrabony peri-implantitis defects following application of a nanocrystalline hydroxyapatite (Ostim) or a bovine-derived xenograft (Bio-Oss) in combination with a collagen membrane (Bio-Gide). A case series. J Clin Periodontol. United States; 2006;33:491–9.
40. Vallet-Regí M, Ruiz-Hernández E. Bioceramics: From bone regeneration to cancer nanomedicine. Adv Mater. Departamento de Química Inorgánica y Bioinorgánica, Facultad de Farmacia, Universidad Complutense de Madrid, Plaza Ramón y Cajal s/n, 28040 Madrid, Spain; 2011;23:5177–218.
41. Werner J, Linner-Krcmar B, Friess W, Greil P. Mechanical properties and in vitro cell compatibility of hydroxyapatite ceramics with graded pore structure. Biomaterials. 2002;23:4285–94.
42. Elgendy E, Abo Shady T. Clinical and radiographic evaluation of nanocrystalline hydroxyapatite with or without platelet-rich fibrin membrane in the treatment of periodontal intrabony defects. J Indian Soc Periodontol. 2015;19:61.
43. Valen M. OsteoGen crystals coated with a biomimetic nano-crystalline fluorapatite surface technology to promote osteoblast cell differentiation, migration and proliferation. J Oral Implantol. United States; 2013.
44. Schünemann FH, Galárraga-Vinueza ME, Ricardo Magini, Fredel M, Silva F, Souza

JCM, Zhang Y, Henriques B. Zirconia surface modifications for implant dentistry. Mater Sci Eng C. 2019;98:1294-1305.
45. Lawrence J, Hao L, Chew HR. On the correlation between Nd:YAG laser- induced wettability characteristics modification and osteoblast cell bioactivity on a titanium alloy. Surf Coat Technol. 2006;200:5581–5589.
46. Hao L, Lawrence J, Chian KS, Osteoblast cell adhesion on a laser modified zirconia based bioceramic. J Mater Sci Mater Med. 2005;16:719–726.
47. Moura CG, Pereira R, Buciumeanu M, Carvalho O, Bartolomeu F, Nascimento R, Silva FS. Effect of laser surface texturing on primary stability and surface properties of zirconia implants. Ceram Int. 2017;43:15227–15236.
48. Liu Y, Liu L, Deng J, Meng R, Zou X, Wu F. Fabrication of micro-scale textured grooves on green ZrO2 ceramics by pulsed laser ablation. Ceram Int. 2017;43:6519–6531.
49. Han J, Zhang F, Van Meerbeek B, Vleugels J, Braem A, Castagne S. Laser surface texturing of zirconia-based ceramics for dental applications: A review. Mater Sci Eng C Mater Biol Appl. 2021;123:112034.
50. Henriques B, Fabris D, Souza JCM, Silva FS, Carvalho O, Fredel MC, Mesquita-Guimarães J. Bond strength enhancement of zirconia-porcelain interfaces via Nd:YAG laser surface structuring, J Mech Behav Biomed Mater. 2018;81:161–167.
51. Soon G, Pingguan-Murphy B, Lai KW, Akbar SA. Review of zirconia-based bioceramic: Surface modification and cellular response. Ceram Int. 2016;42:12543–12555.
52. Hao L, Lawrence J. Effects of Nd: YAG laser treatment on the wettability characteristics of a zirconia-based bioceramic. Opt Lasers Eng. 2006;44:803– 814.

CHAPTER IV

1. M.-S. Howe, W. Keys, D. Richards, Long-term (10-year) dental implant survival: a systematic review and sensitivity meta-analysis, Journal of Dentistry 84 (2019) 9–21.
2. A. Monje, A. Ravidà, H.L. Wang, J.A. Helms, J.B. Brunski, Relationship Between Primary/Mechanical and Secondary/Biological Implant Stability, Int J Oral Maxillofac Implants. 34 (2019) 7-23. doi: 10.11607/jomi.19suppl.g1.
3. J. E. Davies, Understanding peri-implant endosseous healing, Journal of Dental Education. 67 (2003) 932–949.
4. V. Iorio-Siciliano, R. Matarasso, R. Guarnieri, M. Nicolò, D. Farronato, and S. Matarasso, Soft tissue conditions and marginal bone levels of implants with a laser-microtextured collar: a 5-year, retrospective, controlled study, Clinical Oral Implants Research, 26 (2015) 257–262.
5. R. Guarnieri, R. Placella, L. Testarelli, V. Iorio-Siciliano, M. Grande, Clinical, radiographic, and esthetic evaluation of immediately loaded laser microtextured implants placed into fresh extraction sockets in the anterior Maxilla, Implant Den- tistry, 23 (2014) 144–154.
6. R. Smeets, B. Stadlinger, F. Schwarz et al., Impact of dental implant surface modifications on osseointegration, BioMed Research International, 2016.
7. B.D. Boyan, E.M. Lotz, Z. Schwartz, Roughness and hydrophilicity as osteogenic biomimetic surface properties, Tissue Engineering Parts A, 23 (2017) 1479–1489.
8. M. V. Olmedo-Gaya, F. J. Manzano-Moreno, E. Cañaveral- Cavero, J. De Dios Luna-Del Castillo, M. Vallecillo-Capilla, Risk factors associated with early implant failure: A 5-year retrospective clinical study, Journal of Prosthetic Dentistry, 115 (2016) 150–155.
9. L. Chambrone, J. Mandia, J. A. Shibli, G. A. Romito, M. Abrahao, Dental implants installed in irradiated jaws: A systematic review, Journal of Dental Research, 92 (2013).
10. N.-R. de-Freitas, L.-B. Lima, M.-B. de-Moura, C.-D. Veloso- Guedes, P.-C. Simamoto-Ju´nior, D. de-Magalhães, Bisphosphonate treatment and dental implants: A systematic review, Medicina Oral Patología Oral y Cirugía Bucal, 21 (2016) 644–651.
11. B. Stadlinger, M. Hennig, U. Eckelt, E. Kuhlisch, R. Mai, Comparison of zirconia and titanium implants after a short healing period. A pilot study in minipigs, Int. J. Oral Maxillofac. Surg. 39 (2010) 585–592, https://doi.org/10.1016/j.ijom.2010. 01.015.
12. R.J. Kohal, F.S. Schwindling, M. Bächle, B.C. Spies, Peri-implant bone response to retrieved human zirconia oral implants after a 4-year loading period: a histologic and histomorphometric evaluation of 22 cases, J. Biomed. Mater. Res. - Part B Appl. Biomater. 104 (2016) 1622–1631, https://doi.org/10.1002/jbm.b.33512.
13. S. Roehling, M. Astasov-Frauenhoffer, I. Hauser-Gerspach, O. Braissant, H. Woelfler, T. Waltimo, H. Kniha, M. Gahlert, In vitro biofilm formation on titanium and zirconia implant surfaces, J. Periodontol. 88 (2017) 298–307, https:// doi.org/10.1902/jop.2016.160245.
14. F.H. Schünemann, M.E. Galárraga-Vinueza, R. Magini, M. Fredel, F. Silva, J.C.M. Souza, Y. Zhang, B. Henriques, Zirconia surface modifications for implant dentistry, Mater Sci Eng C Mater Biol Appl. 98 (2019) 1294-1305.
15. N. Rohr, M. Balmer, R.E. Jung, R.J. Kohal, B.C. Spies, C.H.F. Hämmerle, J. Fischer, Influence of zirconia implant surface topography on first bone implant contact within a prospective cohort study, Clin Implant Dent Relat Res. 27 (2021), doi: 10.1111/cid.13013.

16. M.W. Mosesson, Fibrinogen and fibrin structure and functions, J Thromb Haemost, 3 (2005) 1894–904. https://doi.org/10.1111/j.1538-7836.2005.01365.x
17. J.W. Weisel, R.I. Litvinov, Mechanisms of fibrin polymerization and clinical implications, Blood, 121 (2013) 1712–1719. https://doi.org/10.1182/blood-2012-09-306639
18. C. C. Villar, G. Huynh-Ba, M. P. Mills, D. L. Cochran, Wound healing around dental implants, Endodontic Topics, 25 (2011) 44–62.
19. M. Ting, S. R. Jefferies, W. Xia, H. Engqvist, J. B. Suzuki, Classification and effects of implant surface modification on the bone: human cell–based in vitro studies, The Journal of Oral Implantology, 43 (2017) 58–83.
20. X. Wang, Y. Zhang, J. Choukroun, S. Ghanaati, R.J. Miron, Behavior of Gingival Fibroblasts on Titanium Implant Surfaces in Combination with either Injectable-PRF or PRP, Int J Mol Sci, 18 (2017) 331.
21. R. Shah, R. Thomas, T.M. Gowda, T.K.A. Baron, G.G. Vemanaradhya, S. Bhagat, *In Vitro* Evaluation of Osteoblast Response to the Effect of Injectable Platelet-rich Fibrin Coating on Titanium Disks, J Contemp Dent Pract, 22 (2021) 107-110.
22. Choukroun J, Advanced PRF, &i-PRF: platelet concentrates or blood concentrates, J Periodont Med Clin Pract, 1 (2014) 3.
23. A. Castro, S. Cortellini, A. Temmerman, X. Li, N. Pinto, W. Teughels, M. Quirynen. Characterization of the Leukocyte- and Platelet-Rich Fibrin Block: Release of Growth Factors, Cellular Content, and Structure, Int J Oral Maxillofac Implants, 34 (2019) 855-864.
24. A.B. Castro, E.R. Herrero, V. Slomka, N. Pinto, W. Teughels, M. Quirynen, Antimicrobial capacity of Leucocyte-and Platelet Rich Fibrin against periodontal pathogens, Sci Rep, 9 (2019) 8188. doi: 10.1038/s41598-019-44755-6.
25. L. Schuldt, L. Bi, G. Owen, Y. Shen, M. Haapasalo, L. Häkkinen, H. Larjava, Decontamination of rough implant surfaces colonized by multispecies oral biofilm by application of leukocyte- and platelet-rich fibrin, J Periodontol, 92 (2021) 875-885. doi: 10.1002/JPER.20-0205.
26. E. Öncü, B. Bayram, A. Kantarci, S. Gülsever, E.E. Alaaddinoğlu, Positive effect of platelet rich fibrin on osseointegration, Med Oral Patol Oral Cir Bucal, 21 (2016) 601-607. doi: 10.4317/medoral.21026.
27. P. Torkzaban, M. Khoshhal, A. Ghamari, L. Tapak, and E. Houshyar, Efficacy of application of platelet-rich fibrin for improvement of implant stability: a clinical trial, Journal of Long-Term Effects of Medical Implants, 28 (2018) 259–266.
28. H.A. Varela, J.C.M. Souza, R.M. Nascimento, R.F. Araújo, R.C. Vasconcelos, R.S. Cavalcante, P.M. Guedes, A.A. Araújo, Injectable platelet rich fibrin: cell content, morphological, and protein characterization, Clin Oral Investig, 23 (2019) 1309–1318.
29. S. Cortellini, A.B. Castro, A. Temmerman, J. Van Dessel, N. Pinto, R. Jacobs, M. Quirynen, Leucocyte- and platelet-rich fibrin block for bone augmentation procedure: A proof-of-concept study, J Clin Periodontol, 45 (2018) 624–634.
30. R.J. Miron, M. Fujioka-Kobayashi, M. Hernandez, U. Kandalam, Y. Zhang, S. Ghanaati, J. Choukroun, Injectable platelet rich fibrin (i-PRF): opportunities in regenerative dentistry?, Clin Oral Investig. 21 (2017) 2619-2627.
31. C. Andrade, J. Camino, M. Nally, M. Quirynen, B. Martínez, N. Pinto, Combining autologous particulate dentin, L-PRF, and fibrinogen to create a matrix for predictable ridge preservation: a pilot clinical study, Clinical Oral Investigations, 24 (2020) 1151–1160.

32. F.J. Strauss, A. Stähli, R. Gruber, The use of platelet-rich fibrin to enhance the outcomes of implant therapy: A systematic review, Clin Oral Implants Res, 29 (2018) 6-19. doi: 10.1111/clr.13275.
33. M. Lollobrigida, M. Maritato, G. Bozzuto, G. Formisano, A. Molinari, A. De Biase, Biomimetic Implant Surface Functionalization with Liquid L-PRF Products: In Vitro Study, Biomed Res Int, 2018. doi: 10.1155/2018/9031435.
34. C.X. Andrade, M. Quirynen, D.R. Rosenberg, N.R. Pinto, Interaction between Different Implant Surfaces and Liquid Fibrinogen: A Pilot In Vitro Experiment, BioMed Research International, 2021, https://doi.org/10.1155/2021/9996071
35. S.C. Sartoretto SC, J. Calasans-Maia, R. Resende, E. Câmara, B. Ghiraldini, F.J. Barbosa Bezerra, J.M. Granjeiro, M.D. Calasans-Maia, The Influence of Nanostructured Hydroxyapatite Surface in the Early Stages of Osseointegration: A Multiparameter Animal Study in Low-Density Bone, Int J Nanomedicine. 15 (2020) 8803-8817. doi: 10.2147/IJN.S280957.
36. D. Faria, S. Madeira, M. Buciumeanu, F.S. Silva, O. Carvalho, Novel laser textured surface designs for improved zirconia implants performance. Mater Sci Eng C Mater Biol Appl, 108 (2020). doi: 10.1016/j.msec.
37. L. Qian, M. Todo, Y. Matsushita, K. Koyano. Effects of implant diameter, insertion depth, and loading angle on stress/strain fields in implant/jawbone systems: finite element analysis. Int J Oral Maxillofac Implants, 24 (2009) 877-886.
38. X. Ding, S.H. Liao, X.H. Zhu, X.H. Zhang, L. Zhang. Effect of diameter and length on stress distribution of the alveolar crest around immediate loading implants. Clin Implant Dent Relat Res, 11 (2009) 279-287. doi: 10.1111/j.1708-8208.2008.00124.x.
39. J.C. Souza, M. Henriques, R. Oliveira, W. Teughels, J.P. Celis, L.A. Rocha. Biofilms inducing ultra-low friction on titanium. J Dent Res, 89 (2010) 1470-5. doi: 10.1177/0022034510378428.
40. R.F. Neiva, L.F. Gil, N. Tovar, M.N. Janal, H.F. Marao, E.A. Bonfante, N. Pinto, P.G. Coelho, The Synergistic Effect of Leukocyte Platelet-Rich Fibrin and Micrometer/Nanometer Surface Texturing on Bone Healing around Immediately Placed Implants: An Experimental Study in Dogs, Biomed Res Int. (2016). doi: 10.1155/2016/9507342.
41. T.A. Dantas, S. Roedel, J. Mesquita-Guimarães, P. Pinto, J.C.M. Souza, M.C. Fredel, F.S. Silva, B. Henriques, Sliding behavior of zirconia porous implant surfaces against bone, J Biomed Mater Res B Appl Biomater, 107 (2019) 1113-1121. doi: 10.1002/jbm.b.34204.
42. M. Buciumeanu, D. Faria, J. Mesquita-Guimarães, F.S. Silva, Tribological characterization of bioactive zirconia composite layers on zirconia structures, Ceramics International, 44 (2018) 18663-18671. https://doi.org/10.1016/j.ceramint.2018.07.094.
43. C.G. Moura, R. Pereira, M. Buciumeanu, O. Carvalho, F. Bartolomeu, R. Nascimento, F.S. Silva, Effect of laser surface texturing on primary stability and surface properties of zirconia implants, Ceram. Int. 43 (2017) 15227–15236. doi:10.1016/j.ceramint.2017.08.058.
44. M.A.A. Arakeeb, A.A. Zaky, T.A.-H. Harhash, W.S. Salem, M. El-Mofty, Effect of combined application of growth factors and diode laser bio-stimulation on the osseo integration of dental implants, Open Access Macedonian Journal of Medical Sciences, 7 (2019) 2520–2527.
45. F. Marco, F. Milena, G. Gianluca, O. Vittoria, Peri-implant osteogenesis in health and osteoporosis, Micron 36 (2005) 630–644.
46. M.B. da Cruz, J.F. Marques, B.F. Fernandes, P. Pinto, S. Madeira, O. Carvalho, F.S. Silva, J.M.M. Caramês, A.D.S.P. da Mata, Laser surface treatment on Yttria-stabilized

zirconia dental implants: Influence on cell behavior, J Biomed Mater Res B Appl Biomater, 2021. doi: 10.1002/jbm.b.34909.

47. T. Traini, S. Caputi, E. Gherlone, M. Degidi, A. Piattelli, Fibrin clot extension on zirconia surface for dental implants: a quantitative in vitro study, Clin Implant Dent Relat Res, 16 (2014) 718-727. doi: 10.1111/cid.12038.
48. T. Kitagawa, Y. Tanimoto, T. Iida, H. Murakami, Effects of material and coefficient of friction on taper joint dental implants, J Prosthodont ReS, 64 (2020) 359-367. doi: 10.1016/j.jpor.2019.10.003.
49. A. Ruggiero, R. D'Amato, L. Sbordone, F.B. Haro, A. Lanza, Experimental Comparison on Dental BioTribological Pairs Zirconia/Zirconia and Zirconia/Natural Tooth by Using a Reciprocating Tribometer, J Med Syst, 43 (2019) 97. doi: 10.1007/s10916-019-1230-8.
50. H. Teixeira, A.C. Branco, I. Rodrigues, D. Silva, S. Cardoso, R. Colaço, A.P. Serro, C.G. Figueiredo-Pina, Effect of albumin, urea, lysozyme and mucin on the triboactivity of Ti6Al4V/zirconia pair used in dental implants, J Mech Behav Biomed Mater, 118 (2021). doi: 10.1016/j.jmbbm.2021.104451.

APPENDIX A –UFSC ETHICS COMMITTEE

UNIVERSIDADE FEDERAL DE SANTA CATARINA - UFSC

Plataforma Brasil

PARECER CONSUBSTANCIADO DO CEP

DADOS DA EMENDA

Título da Pesquisa: Alterações dimensionais de cristas ósseas pós-extração após preservação com Fibrina Rica em Leucócitos e Plaquetas versus um xenoenxerto: um estudo clínico controlado randomizado de boca dividida.

Pesquisador: Miguel Alexandre Pereira Pinto Noronha de Oliveira

Área Temática:

Versão: 4

CAAE: 65391417.2.0000.0121

Instituição Proponente: Departamento de Odontologia

Patrocinador Principal: Financiamento Próprio

DADOS DO PARECER

Número do Parecer: 2.229.085

Apresentação do Projeto:

" Alterações dimensionais de cristas ósseas pós-extração após preservação com Fibrina Rica em Leucócitos e Plaquetas versus um xenoenxerto: um estudo clínico controlado randomizado de boca dividida". Projeto de pesquisa cujo objetivo é testar se a utilização da Fibrina Rica em Leucócitos e Plaquetas (L-PRF) resulta ou não em um ganho ótimo de tecido duro e na estabilização do tecido mole com o tempo, em alveólos de dentes mono-radiculares maxilares de 21 pacientes. Um estudo desenhado como um estudo clínico controlado randomizado de boca dividida, com um acompanhamento de 6 meses após instalação do implante dentário.

Objetivo da Pesquisa:

Objetivo Primário:

O objetivo primário deste estudo é determinar as diferenças nas alterações tridimensionais de alvéolos pós-extracionais preenchidos com L-PRF ou com um substituto ósseo xenógeno.

Objetivo Secundário:

O objetivo secundário é determinar se o ganho ósseo não impede a instalação e estabilidade dos implantes dentários. Também será avaliada a morbidade do paciente.

Endereço: Universidade Federal de Santa Catarina, Prédio Reitoria II, R: Desembargador Vitor Lima, nº 222, sala 401
Bairro: Trindade **CEP:** 88.040-400
UF: SC **Município:** FLORIANOPOLIS
Telefone: (48)3721-6094 **E-mail:** cep.propesq@contato.ufsc.br

Avaliação dos Riscos e Benefícios:

Riscos:

Não existem riscos relativos à utilização dos dois tipos de biomaterial. A única adversidade seria a não criação das condições necessárias para a instalação do implante dentário. Nesse caso, será abortada a instalação do implante nesse momento, permitindo a cicatrização do local por um período de tempo adicional (pelo menos 3 meses) para depois reentrar na área para nova tentativa de instalação do implante.

Benefícios:

Tanto a Fibrina rica em leucócitos e plaquetas (L-PRF) como o enxerto ósseo bovino mineral desproteinizado com 10% de colágeno (Bio-Oss® Collagen), já comercializados, promovem uma boa cicatrização óssea e produzem as condições necessárias para a instalação do implante dentário.

Comentários e Considerações sobre a Pesquisa:

Trata o presente da Primeira Emenda do Projeto de Pesquisa:"Alterações dimensionais de cristas ósseas pós-extração após preservação com Fibrina Rica em Leucócitos e Plaquetas versus um xenoenxerto: um estudo clínico controlado randomizado de boca dividida" , na qual o pesquisador responsável comunica as seguintes alterações:

• Alteração do número da amostra, passando de 21 para 30 pacientes.

• Alteração na tabela do orçamento do local onde será realizada a micro--CT e a análise das tomografias Micro-CT não terão custo pois serão realizadas gratuitamente na University of Illinois at Chicago. O Comitê tomou ciência da Emenda e recomenda a sua aprovação.

Considerações sobre os Termos de apresentação obrigatória:

Não se aplica.

Recomendações:

Não se aplica.

Conclusões ou Pendências e Lista de Inadequações:

Não se aplica.

Considerações Finais a critério do CEP:

Este parecer foi elaborado baseado nos documentos abaixo relacionados:

UNIVERSIDADE FEDERAL DE SANTA CATARINA - UFSC

Continuação do Parecer: 2.229.085

FLORIANOPOLIS, 20 de Agosto de 2017

Assinado por:
Ylmar Correa Neto
(Coordenador)

Endereço: Universidade Federal de Santa Catarina, Prédio Reitoria II, R: Desembargador Vitor Lima, nº 222, sala 401
Bairro: Trindade **CEP:** 88.040-400
UF: SC **Município:** FLORIANOPOLIS
Telefone: (48)3721-6094 **E-mail:** cep.propesq@contato.ufsc.br

APPENDIX B –BLOOD TEST OF THE TRIBOLOGY STUDY VOLUNTEER

UNIDADE LOCAL DE SAUDE MATOSINHOS, EPE
SERVIÇO DE PATOLOGIA CLINICA

Pág. 1 / 2

NC: 5978046

Nome : **MIGUEL ALEXANDRE FERREIRA PINTO NORONHA**
Utente :
S: M
Colheita : 23-10-2020
Nid :
Classe : Centros de Saúde
Id: 31 A
Abertura de ficha : 23-10-2020 9:52:43 AM
Serviço : USF Caravela
1ª Impressão :
Sala :
Cama :
Impressão actual : 03-12-2020 10:31
Médico : ANTONIO MACEDO

	Resultados / Unidades	V.Referência	Resultados Anteriores
QUIMICA CLINICA			
GLICOSE	71 mg/dL	70.0-105.0	
UREIA	37 mg/dL	19.0-44.0	
CREATININA / TFG (CKD-EPI)			
CREATININA	1.1 mg/dL	0.7-1.3	
TFG (CKD-EPI)	Não Aplicável	TFG: < 15 ml/min (estadio 5) TFG: 15 - 29 ml/min (estadio 4) TFG: 30 - 59 ml/min (estadio 3) TFG: 60 - 90 ml/min (estadio 2) TFG: > 90 ml/min - não aplicável	
COLESTEROL TOTAL	184 mg/dL	<200 Risco moderado : 200-239 Risco elevado : >=240	
COLESTEROL HDL	64 mg/dL	>=60 Risco moderado : 40-59 Risco elevado : <40	
COLESTEROL LDL			
COLESTEROL LDL (Calculado)	110 mg/dL	<100 Risco moderado : 100 - 129 Risco elevado : 130-189 Risco muito elevado >=189	
TRIGLICERIDOS	51 mg/dL	<150 Risco moderado : 150-199 Risco elevado : 200-500 Risco muito elevado : > 500	
LDH	160 U/L	125.0-220.0	
TGO (AST)	23 U/L	5.0-34.0	
TGP (ALT)	9 U/L	<55.0	

Validado por: Maria Jose Cupertino (Farmacêutica Especialista)

UNIDADE LOCAL DE SAUDE MATOSINHOS, EPE
SERVIÇO DE PATOLOGIA CLINICA

NC: 5978046 | Nome : MIGUEL ALEXANDRE FERREIRA PINTO NORONHA | S: M
Utente :
Colheita : 23-10-2020 | Nid : | Classe : Centros de Saúde | Id: 31 A
Abertura de ficha : 23-10-2020 9:52:43 AM | Serviço : USF Caravela
1ª Impressão : | Sala : | Cama :
Impressão actual : 03-12-2020 10:31 | Médico : ANTONIO MACEDO

	Resultados	/ Unidades	V.Referência	Resultados Anteriores

HEMATOLOGIA

HEMOGRAMA COM FORMULA

ERITROGRAMA

Eritrocitos		5.27	EXP6/uL	4.4-5.9
Hemoglobina		15.4	g/dL	13.0-18.0
Hematócrito		46.1	%	40-52
VGM		87.5	fL	80-100
HGM		29.2	pg	26-34
CHGM		33.4	g/dL	32-36
RDW-CV		12.5	%	11.5-14.5
Eritroblastos		0.0	/100wbc	

LEUCOGRAMA

Leucócitos		5.39	EXP3/uL	4.0-11.0
Neutrófilos	51.20 %	2.8		1.3-8.8 .
Eosinófilos	2.40 %	0.1		0.0-0.7
Basófilos	0.70 %	0.0		0.0-0.2
Linfócitos	38.60 %	2.1		1.0-4.8
Monócitos	6.90 %	0.4		0.2-1.0 .
Granulocitos Imaturos	0.20 %	0.0		<1

PLAQUETAS

	172	EXP3/uL	150-400
MPV (Volume plaquetário médio)	10.5	fL	8-12
PDW (Anisocitose plaquetária)	12.0	fL	9-15
P-LCR (Plaquetas gigantes)	29.2	%	17-40

IMUNOLOGIA / SEROLOGIA

ANTICORPO VIH 1 e 2

Resultado	Negativo		
Valor	0.24	UI/mL	< 1.0

Validado por: Maria Jose Cupertino (Farmacêutica Especialista)

ANNEX A – SCIENTIFIC PRODUCTION DURING THE DOCTORAL PROGRAM

1. PUBLISHED ARTICLES

- **NORONHA OLIVEIRA, M**; AGUILERA, VMR; RODRIGUEZ, JDS; BENFATTI, CAM; VOLPATO, CAM. Challenging replacement of a maxillary canine with an implant-supported restoration: A surgical and prosthetic approach. J Prosthet Dent. 2021 Feb 25:S0022-3913(21)00046-9. doi: 10.1016/j.prosdent.2020.09.061.

- SOUZA, JCM; CORREIA, MST; **NORONHA, OLIVEIRA, M**; SILVA, FS; HENRIQUES, B; NOVAES DE OLIVEIRA, AP; GOMES, JR. PEEK-matrix composites containing different content of natural silica fibers or particulate lithium-zirconium silicate glass fillers: Coefficient of friction and wear volume measurements. Biotribology. v. 24, 2020.

- MONTERO JD, SOUZA HC, MARTINS MS, **NORONHA OLIVEIRA MAPP**; BENFATTI CAM, MAGINI RS. Versatility and Importance of Bichat's Fat Pad in Dentistry: Case Reports of Its Use in Occlusal Trauma. J Contemp Dent Pract. v. 19, p. 888-894, 2018.

- **NORONHA OLIVEIRA M**; SCHUNEMANN WVH, MATHEW M, HENRIQUES B, MAGINI RS, TEUGHELS W, SOUZA JCM. Can debris released from degradation of dental implants affect peri-implant tissues?.J Periodontal Res. 2018 Feb;53(1):1-11. doi: 10.1111/jre.12479.

- **NORONHA OLIVEIRA M**, RAU LH, MARODIN A, CORRÊA M, CORRÊA LR, ARAGONES A, MAGINI RS. Ridge Preservation After Maxillary Third Molar Extraction

Using 30% Porosity PLGA/HA/β-TCP Scaffolds With and Without Simvastatin. Implant Dent, v. 26, p. 1, 2017.

2. ARTICLES ACCEPTED FOR PUBLICATION

- **NORONHA OLIVEIRA, M**; HOTZA, D; HENRIQUES, B; SILVA, FS; CARAMÊS, J; SOUZA, JCM. O efeito sinergístico da fibrina rica em plaquetas (PRF) e biomateriais cerâmicos para reparo ósseo. *RevSALUS* - Revista Científica Internacional da Rede Académica das Ciências da Saúde da Lusofonia.

3. ARTICLES SUBMITED FOR PUBLICATION

- **NORONHA OLIVEIRA, M**; VARELA, HA; CARAMÊS, J; HENRIQUES, B; TEUGHELS, W; QUIRYNEN, M; SOUZA, JCM. Synergistic benefits on combining injectable platelet-rich fibrin and bone graft porous materials: an integrative review.

- **NORONHA OLIVEIRA, M**, VARELA, HA; NASCIMENTO, RM; CARVALHO, O; HENRIQUES, B; CARAMÊS, J; SOUZA, JCM. Incorporation of injectable platelet rich fibrin (i-PRF) for coating and embedment of bone graft materials and implant surfaces: a detailed morphological analysis.

- REGA AGUILERA, V; **NORONHA OLIVEIRA, M**; PAULETTO, P; GALARRAGA-VINUEZA, ME; SCHWARZ F; BIANCHINI MA. Effect of Implantoplasty on Peri-implant Tissues: A Systematic Review.

.

4. BOOK CHAPTERS PUBLISHED

- VARELA, H; **NORONHA OLIVEIRA, MAPP**; PEREIRA, J; PINTO, N; QUIRYNEN, M; SOUZA, JCM. Chapter 7 - Platelet-rich fibrin to incorporate bioactive graft materials,

Editor(s): Júlio C.M. Souza, Dachamir Hotza, Bruno Henriques, Aldo R. Boccaccini, In Advanced Nanomaterials, Nanostructured Biomaterials for Cranio-Maxillofacial and Oral Applications, Elsevier, 2018, Pages 119-142, ISBN 9780128146217, https://doi.org/10.1016/B978-0-12-814621-7.00007-X.

- **NORONHA OLIVEIRA, M**; Gil, LF; MORATELLI PRADO, A; FARIA DE ALMEIDA, R; PEREIRA, J; CARAMÊS, J; SANDRO DA SILVA, S; SOUZA, JCM. Chapter 6 – Análises por Imagens, Editor(s): Júlio C.M. Souza, António Pedro Novaes de Oliveira, Bruno Henriques, Márcio C. Fredel, Filipe Samuel Silva, In Métodos de Pesquisa Laboratorial em Biomateriais Dentários, Brazil Publishing, 2021, ISBN 978655861446-3, https://doi.org/10.31012/978-65-5861-448-7.

5. ABSTRACTS FOR CONGRESSES

- SOUZA, JCM; **NORONHA OLIVEIRA, MAPP**; VARELA, H; GALARRAGA-VINUEZA, ME; ARAUJO, AA; HENRIQUES, B; SILVA, F. Interaction between biomaterials and platelet-rich fibrin: a microscopic evaluation. In: 2nd European Meeting on Enhanced Natural Healing in Dentistry, 2018, Leuven. Interaction between biomaterials and platelet-rich fibrin: a microscopic evaluation, 2018.
- SOUZA, JCM; SHAH, S; BEDOYA, KA; **NORONHA OLIVEIRA, MAPP**; MATHEW, M. Clinical Significance on the Degradation of Dental Implants. In: 22nd Annual Research Day, UIC Health Sciences Campus, 2017, Rockford. Clinical Significance on the Degradation of Dental Implants, 2017.
- **NORONHA OLIVEIRA, MAPP**; GALARRAGA-VINUEZA, ME; GUIMARAES, J; HENRIQUES, B; MAGINI, RS; FREDEL, M; TEUGHELS, W; SOUZA, JCM. Bioactive glass doped with calcium bromide to inhibit multi-species oral biofilm. In: 26th EAO

Congress, 2017, Madrid. Bioactive glass doped with calcium bromide to inhibit multi-species oral biofilm., 2017.

- TREVIZAN, L; GEREMIAS, TC; PEREIRA, MA; **NORONHA OLIVEIRA, MAPP**; ALECIO, ABW; MAGINI, RS; BIANCHINI, MA; MONTERO, JD. Relação entre perda óssea peri-implantar e o tempo em função de próteses sobre implantes. In: 34nd SBPqO Annual Meeting, 2017, Campinas. Relação entre perda óssea peri-implantar e o tempo em função de próteses sobre implantes, 2017.
- **NORONHA OLIVEIRA MAPP**; RAU, LH; MARODIN, A; CORREA, M; CORREA, LR; ARAGONES, A; MAGINI, RS. Ridge preservation following maxillary third molar extraction using PLGA/HA/β-TCP scaffolds with and without simvastatin: a pilot randomized controlled clinical trial. In: 25th EAO Congress, 2016, Paris. Ridge preservation following maxillary third molar extraction using PLGA/HA/β-TCP scaffolds with and without simvastatin: a pilot randomized controlled clinical trial, 2016.

6. PARTICIPATION ON EVENTS

- 25th Annual Congress of European Association for Osseointegration, Paris - France, 2016.
- 26th Annual Congress of European Association for Osseointegration, Madrid - Spain, 2017.

7. ORIENTATIONS

- Juliana Borges Muller. Efeito da medicação anti-inflamatória administrada pós-operatoriamente na preservação de alvéolos pós-extração tratados com Fibrina Rica em Plaquetas e Leucócitos: Revisão de Literatura. 2017. Trabalho de Conclusão de Curso. (Graduação em Odontologia) - Universidade Federal de Santa Catarina. Orientador: Miguel Alexandre Pereira Pinto Noronha de Oliveira.